THE SPATIOTEMPORAL DYNAMICS OF REGULATED CELL DEATH

by

Michelle M.E. Riegman

A Dissertation

Presented to the Faculty of the Louis V. Gerstner, Jr.

Graduate School of Biomedical Sciences,

Memorial Sloan Kettering Cancer Center

in Partial Fulfillment of the Requirements for the Degree of

Doctor of Philosophy

New York, NY

September 2020

Michael H. Overholtzer, PhD
Dissertation Mentor

Date

I dedicate this dissertation to my grandparents, Johannes and Elizabeth Wijnands, for their continued love and support, and Arie and Martha Riegman, in loving memory.

ABSTRACT

Cell death is a fundamental aspect of multicellular life and its dysregulation has been implicated in many diseases, from cancer to neurodegenerative disease. Most cell death research has focused on cell-intrinsic mechanisms of cell death execution. How different types of cell death affect populations of cells, on the other hand, is poorly understood, yet has profound implications for our understanding of the effects of cell death *in vivo*. Here we develop a quantitative method for the study of non-autonomous effects in cell death and apply it to ferroptosis, a form of regulated, iron-dependent necrosis that has previously been suggested to be able to spread from cell to cell. We show that ferroptosis occurs with non-random spatiotemporal dynamics when induced by some methods but not others, and that it is distinct from other forms of cell death in this respect. We also discover that the death-inducing signal spreads independently of cell rupture, as osmoprotectant molecules that block cell lysis do not prevent death wave propagation. The ability of large osmoprotectants to prevent lysis further implies that ferroptosis execution is mediated by the formation of nanoscale pores in the plasma membrane, in a similar manner to two known forms of programmed necrosis, pyroptosis and necroptosis. This is in contrast to the prevailing view that ferroptosis stems from the unregulated accumulation of cellular damage whereas pyroptosis and necroptosis are considered cellular suicide, and may mean ferroptosis has more of a programmed nature than previously thought.

BIOGRAPHICAL SKETCH

Michelle Riegman was born on September 3rd, 1991, to Ron Riegman and Wilma Wijnands in ‘s-Hertogenbosch, the Netherlands. She grew up in Haaren with her sister Renée and pet cat Teigetje, where she attended de Klim-op elementary school and later Maurick College in Vught. In 2005, the family moved to Bedminster, New Jersey, and Michelle continued secondary school at Bernards High School in Bernardsville. She graduated in 2008 and moved back to the Netherlands with her family to attend University College Utrecht. There she studied molecular biology and medical sciences while also completing a minor in economics, and performed research in the laboratory of Dr. Geert Kops at the University Medical Centre Utrecht investigating the molecular mechanisms of mitotic checkpoint silencing. Michelle then returned to the United States in 2012 to complete a master’s degree in Biotechnology at the University of Pennsylvania, where she continued to work on mitotic checkpoint regulation in the laboratory of Dr. Michael Lampson. In 2014, she began her PhD at the Louis V. Gerstner, Jr. Graduate School of Biomedical Sciences and joined the Overholtzer lab, where she studied the population dynamics and mechanisms of regulated cell death.

ACKNOWLEDGEMENTS

First and foremost, I would like to thank my PhD advisor, Michael Overholtzer, for his mentorship and support during my time in the lab. Thank you for instilling in me the confidence to believe in my own ideas, to take risks, and to pursue challenging problems. I have enjoyed an extraordinary degree of independence during my dissertation research, and I am very grateful to have had the freedom to set my own research directions and tackle the questions that interested me.

A heartfelt thank you goes out to my friends and colleagues in the Overholtzer lab, past and present – Sung Eun Kim, Shefali Krishna, Jens Hamann, Yongchan Lee, Urmi Bandyopadhyay, Chan Lee, Ruoyao Chen, and Lilian Lamech. Working alongside a group of such talented scientists and all-around stellar human beings every day has been an honor and a privilege and I will miss you all dearly. I am also extremely grateful to Maria Chui, whose hard work and extensive knowledge of MSK's inner workings keep our experiments going. And thank you to Noah Steinberg, whom I had the pleasure of mentoring for a summer, for your enthusiasm, dedication, and early contributions to this project.

I would be remiss if I did not acknowledge the many collaborators with whom I've had the pleasure of working, and who've taught me so much. First of all, thank you to Dr. Assaf Zaritsky and members of his lab, Chen Galed, Liran Sagie, and Tom Levin, for your help, insight, and enthusiasm in embarking on this spatiotemporal death quantification journey with us – we truly could not have done it without you. Thank you also to Dr. Philipp Niethammer and Dr. Scott Dixon for all the helpful discussions and the

reagents you have so generously shared with us, and Dr. Michelle Bradbury for your insights on the more clinically relevant aspects of this project. I'm also grateful to everyone in the Cell Biology Program, especially the Jiang and Niethammer labs, for all the great discussions and experimental help.

Thank you to my thesis committee members, Dr. Philipp Niethammer and Dr. Daniel Bachovchin, for their critical evaluation of my work and helpful suggestions over the years. Your valuable insights contributed greatly to shaping my research trajectory. I'd also like to extend my thanks to Dr. Richard White for chairing my dissertation defense, and to Dr. Carol Prives for agreeing to serve as my external examiner. A further thank you goes out to all my previous scientific mentors, Dr. Geert Kops, Dr. Mathijs Vleugel, Dr. Michael Lampson, Dr. Lukas Chmatal, and especially Dr. Edward Ballister, whose example I am continuing to fail to live up to. It was a pleasure learning from you and I cannot thank you enough for the generosity and support you have shown me throughout my scientific journey.

Next, I'd like to thank everyone in the GSK office for their hard work and support – your dedication makes this school special. Thank you to Linda Burnley, Dr. Tom Magaldi, David McDonagh, Stacy de la Cruz, Julie Masen, and Raphaelle Chassagne. I'd also like to thank the past members of the GSK administration who had such a large part impact on my early years in the program – Maria Torres, Ivan Gerena, Alexandria Woodside, Iwona Abramek, Katherine Gentile, and of course Dr. Ken Marians. Thank you for making GSK such a welcoming place and always being ready to help its students in any way you could.

Thank you to my classmates, Steven Albanese, Jake Boyer, Chris Hulton, Nayan Jain, Nick Kuhn, Xiaoyi Li, Ben Tischler, and Yuchen Xie, for making the first few years of grad school amazing. I also want to express my gratitude to the entire GSK student body for the warm and supportive community you have created, and for all the feedback, ideas, advice, and encouragement throughout the years.

To my friends, far and near, old and new – THANK YOU! Your friendship means the world to me and I could not have done this without you. I wish I could list each and every one of you here, but alas, space does not allow. Just know that you have all had a profound impact on my life and I love you dearly. I would like to especially thank Corry and Theo van Lith for welcoming my sister and me into your home and being like second parents to us. My childhood would have been unimaginably different without you.

To my partner, Timo McGregor, thank you for your constant love and support through all the ups and much more frequent downs of grad school. I am so grateful to have you in my life and I can confidently say I would not have made it through this PhD without you. I would like to thank my grandparents, Johannes and Elizabeth Wijnands, for instilling in me a deep sense of curiosity and a love of travel and the natural world, and for teaching me to think critically and question everything from a very young age. Finally, I am deeply grateful to my parents and my sister for all the love, encouragement, guidance, and advice you have given me over the years. Thank you for your stubbornness and persistence in believing in me, even in the face of all evidence, and occasionally convincing me to do the same. I could not wish for a more supportive family.

TABLE OF CONTENTS

LIST OF FIGURES

LIST OF ABBREVIATIONS

AA: arachidonic acid

ACSL4: acyl-CoA synthetase long chain family member 4

ALOX: lipoxygenase

AML: acute myeloid leukemia

AMPK: AMP-activated protein kinase

Apaf-1: apoptotic protease activating factor 1

ASC: apoptosis-associated speck-like protein containing a CARD

BAP1: BRCA1-associated protein 1

BSO: buthionine sulfoximine

CoQ_{10}: Coenzyme Q_{10}

COX-2: cyclooxygenase 2

cPLA2: cytosolic phospholipase 2

Cx43: connexin-43

DAMP: damage-associated molecular pattern

DFO: deferoxamine

DIC: differential interference contrast

DISC: death-inducing signaling complex

EMT: epithelial-mesenchymal transition

FAC: ferric ammonium citrate

Fer-1: ferrostatin-1

FIN: ferroptosis inducer

FSP1: ferroptosis suppressor protein 1

GCL: glutamate cysteine ligase

GPX4: glutathione peroxidase 4

GSDMD: gasdermin D

GSH: glutathione

H_2O_2: hydrogen peroxide

H2B: histone 2B

IFN: interferon

IL: interleukin

I/R: ischemia-reperfusion

JNK: c-Jun N-terminal kinase

KO: knockout

LDH: lactate dehydrogenase

Lip-1: liproxstatin-1

LPCAT3: lysophosphatidylcholine acyltransferase 3

LPS: lipopolysaccharide

MLKL: mixed lineage kinase domain like pseudokinase

MPT: mitochondrial permeability transition

MUFA: monounsaturated fatty acid

NAD(P): nicotinamide adenine dinucleotide (phosphate)

PAMP: pathogen-associated molecular pattern

PCD: programmed cell death

PE: phosphatidylethanolamine

PEG: polyethylene glycol

PRR: pattern recognition receptor

PS: phosphatidylserine

PTGS2: prostaglandin-endoperoxide synthase 2

PUFA: polyunsaturated fatty acid

RCD: regulated cell death

RIBE: radiation-induced bystander effect

ROS: reactive oxygen species

RSL3: RAS-selective lethal 3

SPI: spatial propagation index

SSMD: Sedaghatian type spondylometaphyseal dysplasia

tBH: tert-butyl hydroperoxide

TLR: toll-like receptor

TNFR: tumor necrosis factor receptor

TNFα: tumor necrosis factor α

TRAIL: TNF-related apoptosis-inducing ligand

XIAP: X-linked inhibitor of apoptosis protein

α-MSH: alpha-melanocyte-stimulating hormone

CHAPTER 1: Introduction

Death is the inevitable fate of every somatic cell in a multicellular organism. In the adult human body, three hundred million cells are estimated to undergo cell death every minute.[1] Some types of cell, such as intestinal epithelial cells, leukocytes, and red blood cells, are turned over at a high rate as part of their normal lifecycle, whereas others, such as neurons, are long-lived and undergo death only when they become aged, damaged or infected. Death plays important roles in embryonic development, for example to eliminate supernumerary cells and to sculpt tissue structures,[2] as well as organismal homeostasis in adults, while dysfunctional regulation of cell death is known to contribute to the development of disease. Cell death is therefore involved in nearly every aspect of physiology, and is a highly regulated and coordinated activity.

A Brief History of Cell Death Research

The history of scientific study of cell death dates back to 1842, when Carl Vogt described the 'resorption' and 'destruction' of notochord and cartilage cells in developing midwife toads.[3,4] It would not be until over a hundred years later, however, that scientists began to appreciate that death was not always merely accidental.[5] In 1964 Lockshin and Williams coined the term "programmed cell death" when they showed that muscle breakdown during silkworm transformation was controlled by endocrine signaling,[6] concluding that this death event was somehow predetermined by the developmental program of the organism. In a seminal paper published in 1972, Kerr, Wyllie, and Currie used electron microscopy to carefully investigate the morphological features of cell

death occurring during vertebrate development and homeostasis.[7] They proposed the name apoptosis (lit. “falling-off”) in order to distinguish these naturally occurring deaths from necrosis caused by stress and injury. Around the same time, John Sulston and H. Robert Horvitz conducted their groundbreaking work in the nematode *Caenorhabditis elegans*, mapping out the lineage of every cell in the adult organism to reveal that the exact same 131 cells die in each worm during development,[8] many with morphological features similar to those described by Kerr *et al*. This demonstrated that tight control was exerted over programmed cell death in invertebrates as well, and that apoptosis was likely conserved across metazoan species. A spate of research followed over the next two decades, and by the early 1990s the genetic basis of apoptosis had been largely elucidated in *C. elegans*,[9–12] paving the way for the further discovery of the more complex mechanisms of apoptotic cell death in vertebrates.[13–16]

Based on some of the early research described here, Schweichel and Merker in 1973 proposed the classification of cell death events occurring during development into three types based on their morphological characteristics.[17] These were later recognized to correspond to apoptosis (type I), autophagy (type II), and necrosis (type III), characterized by cell fragmentation and nuclear condensation, cytosolic vacuolization, and loss of plasma membrane integrity, respectively. Over time, the meaning of “programmed cell death” evolved to denote any death whose mechanism of execution was genetically encoded, rather than cell death occurring as part of a developmental program. For several decades, apoptosis and programmed cell death were seen as synonymous terms, while necrosis was thought to be purely accidental, caused by direct

physical damage to the cell. Since then, however, the number of known types of cell death has expanded considerably (Figure 1.1),[18] and many newly characterized forms of cell death do not fit neatly into one of these three categories. Indeed, with the discovery of necroptosis[19] and pyroptosis,[20] both cellular suicides that involve plasma membrane permeabilization and the release of cellular contents, it has become clear that necrosis, too, can be programmed. As mechanistic insight into different cell death pathways increases, a perhaps more meaningful distinction is emerging between programmed, regulated, and accidental cell death.[21]

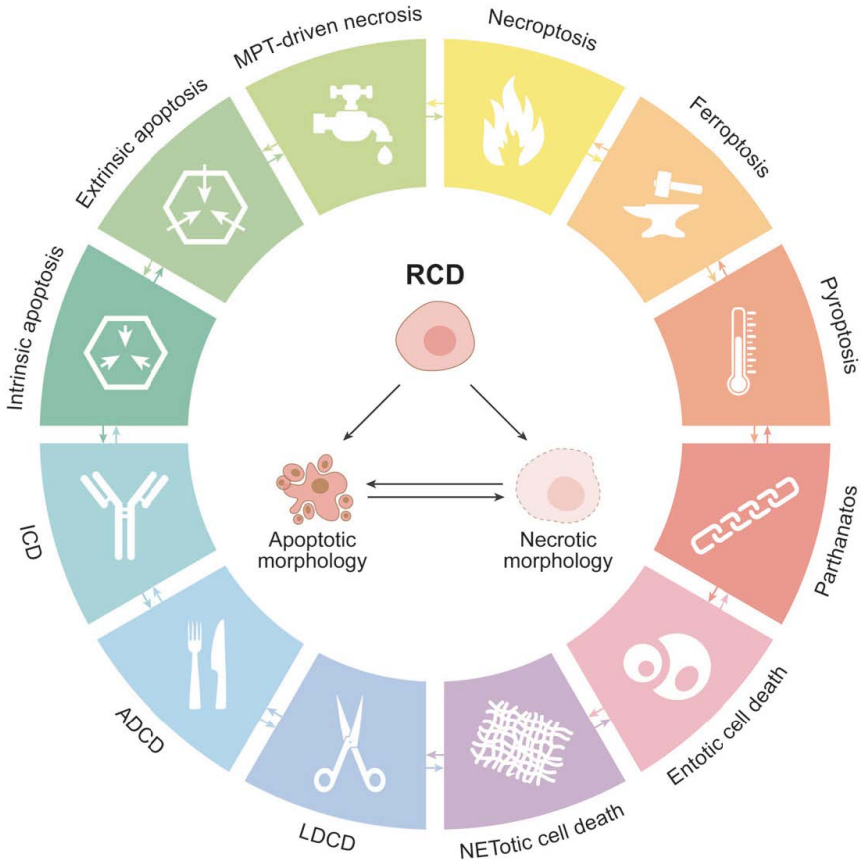

Figure 1.1 Known forms of Regulated Cell Death.
Many different mechanisms of cell death have been identified in mammalian cells exposed to lethal stimuli. These can manifest with a range of different morphologies. While each type of death has defined molecular features, there is also substantial crosstalk between different death modalities. MPT: mitochondrial permeability transition. ICD: immunogenic cell death. ADCD: autophagy-dependent cell death. LDCD: lysosome-dependent cell death. NET: neutrophil extracellular trap. Figure reproduced from Galluzzi *et al.*, 2018.[18]

Programmed Cell Death

Apoptosis

Apoptosis is the earliest recognized form of programmed cell death and was initially defined as a set of morphological characteristics, including nuclear and cytoplasmic condensation, plasma membrane blebbing, and the fragmentation of the cell into so-called "apoptotic bodies".[7] Under normal conditions these cell fragments are rapidly phagocytosed by macrophages or surrounding cells,[1,22] and as plasma membrane integrity is maintained during apoptosis this type of death was long thought to be immunogenically silent, though this is now known to not always be the case.[22–25] It is clear, however, that the lack of release of dangerous intracellular molecules such as proteases and nucleases during apoptosis protects the cell environment from injury. Apoptosis can be triggered by a wide variety of internal and external factors, and seems to be the predominant mode of cell elimination both in development and during homeostasis, most likely due to its relatively safe nature. However, it is also involved in the response to infection, the elimination of malignant cells, and a range of other pathological conditions.[26]

Apoptosis is executed by a family of cysteine-dependent aspartate-directed proteases, or caspases.[27] There are seven known apoptotic caspases in humans, which can be subdivided into initiator (2, 8, 9, and 10) and executioner (3, 6, and 7) caspases that together form a proteolytic cascade.[28,29] All caspases are synthesized as inactive proenzymes that need to undergo cleavage to be activated. Upstream apoptosis-inducing signals trigger the dimerization of initiator caspases, enabling them to cleave

and activate each other. These active enzymes then go on to cleave effector caspases, thereby amplifying the pro-apoptotic signal. Executioner caspases cleave a large variety of intracellular substrates, such as regulators of the cell cytoskeleton including ROCK1 and vimentin, antiapoptotic transcription factors like NF-κB, as well as a large number of proteins involved in transcription and translation,[30] thereby causing apoptotic death.

The activation of apoptotic caspases can occur through either of two pathways (Figure 1.2). Intrinsic apoptosis is generally triggered by intracellular signals, such as DNA damage, nutrient withdrawal, or endoplasmic reticulum (ER) stress. The extrinsic pathway, on the other hand, is initiated in response to extracellular ligands, through the activation of so-called death receptors. Many death receptors are part of the Tumor Necrosis Factor Receptor (TNFR) superfamily and bind to cytokines in the Tumor Necrosis Factor (TNF) family, which includes TNFα, Fas ligand, and TNF-related apoptosis-inducing ligand (TRAIL).[31] Ligand binding causes the clustering of these receptors, triggering a conformational change in their intracellular domains that allows the recruitment and assembly of a protein complex termed the death-inducing signaling complex (DISC).[32,33] This complex promotes the homodimerization and subsequent activation of caspase 8, which then goes on to directly cleave executioner caspases. In so-called type I cells this is sufficient to induce the full execution of apoptosis.[34] However, in cells that express high levels of the caspase 3 and 7 inhibitor X-linked Inhibitor of Apoptosis Protein (XIAP), known as type II cells,[35] caspase 8 also has to cleave Bid,[36] which then activates the intrinsic apoptotic pathway, in order to trigger cell death.

The intrinsic pathway of apoptosis is controlled by a group of proteins called the Bcl-2 family, after its founding member.[16] Several of its members, including Bcl-2, Bcl-x_L, Bax, and Bak, have transmembrane domains that insert into the mitochondrial outer membrane. When activated, Bax and Bak (and, in some circumstances, the related protein Bok[37]) oligomerize and form large membrane pores that allow the release of pro-apoptotic mitochondrial contents,[26,38] a process called mitochondrial outer membrane permeabilization (MOMP).[39] Anti-apoptotic Bcl-2 family members such as Bcl-2, Bcl-x_L, and Mcl-1 inhibit apoptosis by sequestering Bax and Bak and preventing their activation.[26] Pro-apoptotic members, which include Bim, Bid, Bad, Puma, and others, either directly activate Bax and Bak or prevent their interaction with the anti-apoptotic Bcl-2 proteins.[26,38] This intricate system is largely regulated through the control of protein levels by transcription factors such as p53, which can be activated in response to a large variety of intercellular stressors, and upregulate the transcription of pro-apoptotic Bcl-2 family genes.[40,41] However, posttranslational modification of Bcl-2 proteins can also play a large role.[36,42]

MOMP promotes apoptosis mainly by allowing the release of cytochrome c, which is normally localized to the mitochondrial intermembrane space, enabling its interaction with the cytosolic protein apoptotic protease activating factor 1 (Apaf-1).[13,39] Together, cytochrome c and Apaf-1 assemble into a large, heptameric protein complex named the apoptosome, which then binds caspase 9 and promotes its dimerization and autoactivation.[43,44] Caspase 9 then cleaves and activates the downstream executioner caspases, thereby triggering apoptosis. MOMP also controls the release of other

mitochondrial factors including Smac/Diablo[45,46] and Htra2/Omi,[47] which inhibit the activity of XIAP, thus allowing cell death execution in type II cells undergoing extrinsic apoptosis.

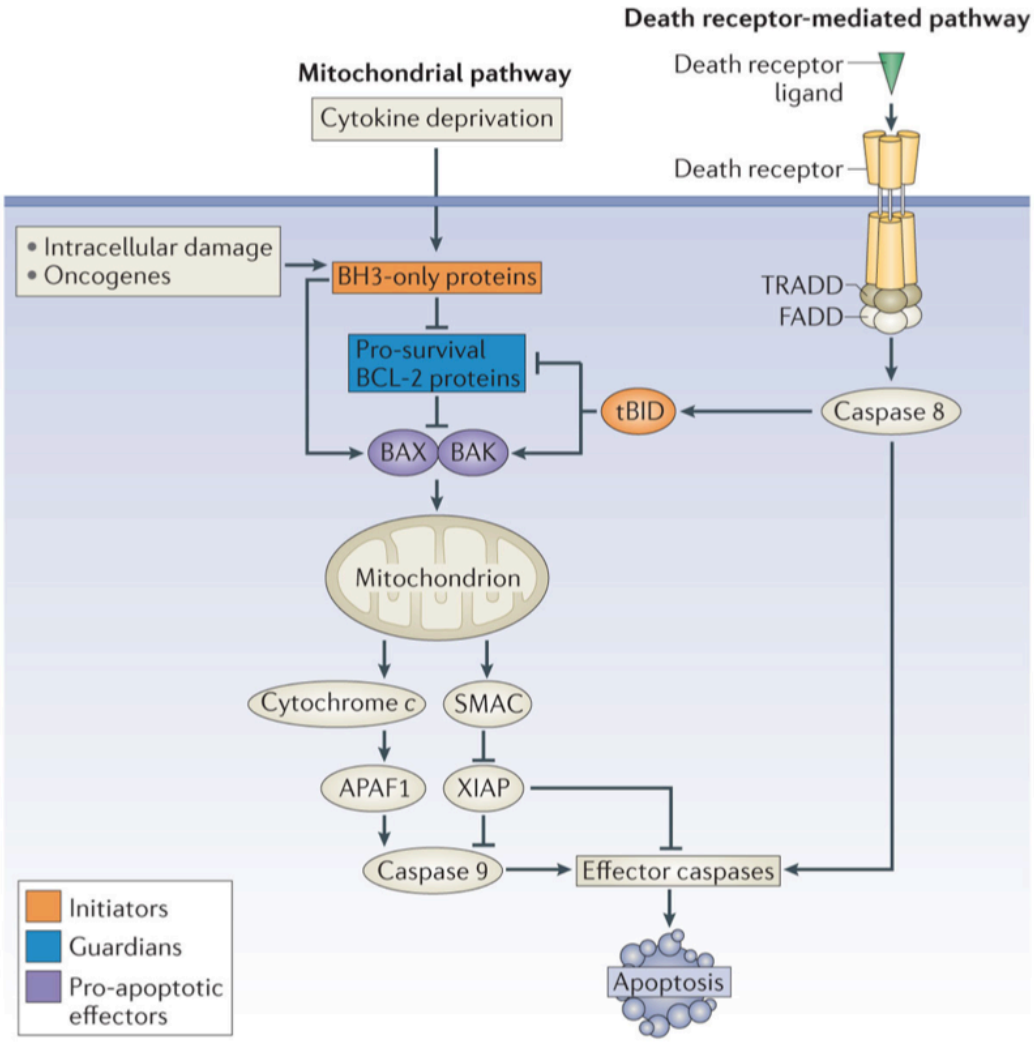

Figure 1.2 The intrinsic and extrinsic pathways of apoptosis.
The intrinsic or mitochondrial pathway can be activated by a variety of stimuli. These factors influence the levels and activity of pro-apoptotic Bcl-2 family proteins, which either inhibit anti-apoptotic members or directly activate the pore-forming proteins Bax and Bak. Once activated, Bax and Bak trigger MOMP, resulting in the release of pro-apoptotic factors. Among these, cytochrome c binds to Apaf-1 to form the apoptosome and activate the initiator caspase 9, while SMAC contributes to caspase activation by binding and inactivating cellular caspase inhibitors such as XIAP. Extrinsic apoptosis is triggered by signaling through death receptors, which recruit death domain-containing proteins, including TRADD and FADD, to their cytosolic tails upon ligand binding. These interactions promote the activation of caspase 8, enabling it to activate downstream executioner caspases and trigger apoptosis in type I cells. In type II cells, which express high levels of XIAP, caspase 8 is also required to cleave Bid into its truncated form (tBid), which is then able to engage the intrinsic pathway. Both pathways end in the cleavage of cellular substrates by executioner caspases, which together cause apoptosis. Figure reproduced from Czabotar *et al.*, 2014.[38]

Necroptosis

Necroptosis is similar to extrinsic apoptosis in that it too can be activated by death receptor signaling, but it generally manifests with a necrotic morphology and occurs only when caspase 8 function is inhibited. Furthermore, this cell death type can also be induced by Toll-like receptor (TLR) activation in response to pathogens.[48] Necroptosis may be specific to vertebrates[49] and is thought to have evolved in response to virally encoded caspase inhibitors in order to provide a backup mechanism for infected cells unable to undergo apoptosis.[50] Because necroptosis involves plasma membrane permeabilization and the release of damage-associated molecular patterns (DAMPs) and other inflammatory mediators, it induces a potent immune response.[23]

Upon ligand binding to TNFR family receptors the kinase RIPK1 is recruited to the cytosolic domain of the receptor and forms part of the so-called "complex I", which also comprises TRADD and several ubiquitin ligases and scaffold proteins. RIPK1 is ubiquitinated, which results in the activation of pro-survival NF-κB signaling.[51] However, if RIPK1 is subsequently deubiquitinated by CYLD (cylindromatosis) the complex dissociates from the receptor and recruits capase 8, c-FLIP, and RIPK3 to form the DISC. If caspase 8 is able to dimerize as part of this complex, it is activated, cleaves several of the other complex components including RIPK1, RIPK3, and CYLD, and triggers apoptosis. If, on the other hand, caspase 8 is absent or inactivated pharmacologically or by viral proteins, RIPK1 and RIPK3 are able to associate and auto- and trans-phosphorylate each other,[52–54] forming yet another complex called the necrosome. This complex then recruits MLKL, which is subsequently phosphorylated at several sites by

RIPK3.[55] Phosphorylated MLKL is able to translocate to and insert into the plasma membrane, causing pore formation[56] and the exposure of phosphatidylserine (PS) on the outer plasma membrane.[57,58] MLKL activation additionally triggers the processing and release of the pro-inflammatory cytokine interleukin-1β (IL-1β),[59] and necroptotic cells are known to also release IL-6, CXCL1, and other molecules that contribute to inflammation.[60]

Pyroptosis

Pyroptosis is another recently discovered form of inflammatory programmed cell death that was initially described in macrophages infected with intracellular pathogens such as *Salmonella typhimurium* and *Shigella flexneri*.[20,61,62] Pyroptotic cell death can be triggered by pathogen-associated molecular patterns (PAMPs) such as flagellin, cytosolic double-stranded DNA, and components of the bacterial type III secretion system, which are recognized by so-called Pattern Recognition Receptors (PRRs).[63] During canonical pyroptosis, activation of these receptors triggers the formation of the inflammasome,[64] a large, multimeric complex composed of a sensor protein/PRR bound to its cognate ligand, and an adaptor protein, most commonly ASC (apoptosis-associated speck-like protein containing a CARD). This complex then recruits inactive caspase 1, one of several inflammatory caspases that are not involved in apoptosis. Upon binding to the inflammasome, caspase 1 is able to dimerize and become activated, enabling it to cleave the inflammatory cytokines IL-1β and IL-18 into their active forms.[65–69] It also cleaves Gasdermin D (GSDMD),[70,71] releasing its pore-forming N-terminal domain and allowing it

to permeabilize the plasma membrane.[72,73] GSDMD pores mediate the release of IL-1β and IL-18 into the extracellular environment to incite an inflammatory response, and can also trigger the swelling and lysis of pyroptotic cells by allowing ion and water influx.

Many different stimuli can induce pyroptosis, and the inflammasome can be composed of different sensor and adaptor proteins whose combinations regulate the strength of the resulting inflammatory response.[63,74] In addition, bacterial lipopolysaccharides (LPS) are known to bind directly to human caspases 4 and 5 (caspase 11 in mice) and trigger their activation and subsequent pyroptosis induction while bypassing inflammasome formation.[75] Pyroptosis has been shown to play an important role in the defense against invading pathogens,[76–78] but its activation can also result in deleterious effects under some circumstances. For example, it has been suggested that the death of T cells due to HIV infection is mediated by pyroptosis,[79] possibly resulting in the recruitment of additional T cells that are then also killed, giving rise to the profound T cell deficiency usually seen in AIDS patients. LPS-mediated pyroptosis is also thought to contribute to some of the serious, potentially lethal symptoms seen during severe sepsis.[77]

Ferroptosis

The Mechanism of Ferroptosis

Ferroptosis is a regulated form of necrosis that depends on the presence of cellular iron. It was first defined as the type of death occurring in response to treatment with the small molecule erastin, which was discovered to inhibit the cystine-glutamate antiporter system x_c^-.[80] The abrogation of cystine import into the cell inhibits the synthesis of the critical cellular antioxidant glutathione (GSH), thereby disrupting cellular redox homeostasis. Ferroptosis involves the accumulation of lethal levels of lipid reactive oxygen species (ROS),[80] which was later found to be due to the inactivation of the enzyme glutathione peroxidase 4 (GPX4).[81] GPX4 is part of a family of enzymes that use GSH as a cofactor to combat cellular ROS, but it is unique in that it is the only member that is able to act on lipids that are esterified into phospholipids.[82,83]

Thus, the central pathway of ferroptosis is that the inactivation of GPX4, either through direct inhibition or the depletion of GSH, allows the accumulation of phospholipid peroxides and cell damage and thereby triggers cell death (Figure 1.3). Accordingly, ferroptosis can be induced by agents that inhibit the import of cystine, so-called class I ferroptosis inducers (FINs), or by molecules that bind and inactivate GPX4 (class II FINs, e.g. RSL3 and ML162). Other drugs that are thought to act as FINs are FIN56, which triggers the depletion of both GPX4 and the lipophilic antioxidant coenzyme Q10 (CoQ10, known as ubiquinol in its reduced form),[84] and $FINO_2$, which indirectly reduces GPX4 activity and causes iron oxidation.[85] Conversely, ferroptosis can be inhibited by the chelation of iron with e.g. deferoxamine (DFO) or ciclopirox olamine

(CPX), or through the application of lipophilic antioxidants such as liproxstatin, ferrostatin, or vitamin E (Figure 1.3). Intriguingly, recent work has uncovered an additional ferroptosis-preventing pathway controlled by Ferroptosis Suppressor Protein 1 (FSP1), which uses NAD(P)H to catalyze the reduction of CoQ10, acting in parallel to GPX4.[86,87] The pharmacological inhibition of FSP1 was shown to sensitize cells to ferroptosis inducers,[86] raising the possibility that other ferroptosis-inducing mechanisms are yet to be discovered.

The sensitivity of cells to ferroptosis can be modulated by a variety of different factors. One of the first to be identified was the level of cellular NADPH. NADPH is used for the reduction of both GSH and CoQ10, and accordingly higher relative NADPH levels confer resistance to ferroptosis.[88] Ferroptosis sensitivity is also influenced by proteins involved in lipid metabolism. One study identified the enzymes ACSL4 and LPCAT3, which act successively to acylate the polyunsaturated fatty acid (PUFA) arachidonic acid (AA) and catalyze its insertion into phospholipids, as positive regulators of ferroptosis.[89] PUFAs are much more sensitive to oxidation than saturated or monounsaturated fatty acids (MUFAs), due to the presence of an easily oxidized bis-allylic hydrogen atom, and are therefore especially affected by the lipid peroxidation that occurs during ferroptosis. Indeed, ferroptosis can be suppressed by supplying cells with deuterated PUFAs[90] or the MUFA oleic acid,[91] whereas addition of AA sensitizes cells to ferroptotic cell death.[92] Lipidomics studies confirmed that ferroptosis involves the preferential oxidation of PUFA-containing phosphatidylethanolamine (PE) phospholipids.[90,92] The source of oxidized lipids during ferroptosis has been a matter of some debate, with various

reports proposing the mitochondria,[93] endoplasmic reticulum,[92] or lysosomes[94] as the cellular site of oxidation. Many studies have highlighted a potential role for lipoxygenases,[90,92,95–97] iron-dependent enzymes that catalyze the dioxygenation of PUFAs in order to generate lipid signaling molecules. The current consensus is that while lipoxygenases may be able to contribute to lipid peroxidation under some circumstances, their activity is not necessary for cell death to occur.[98,99]

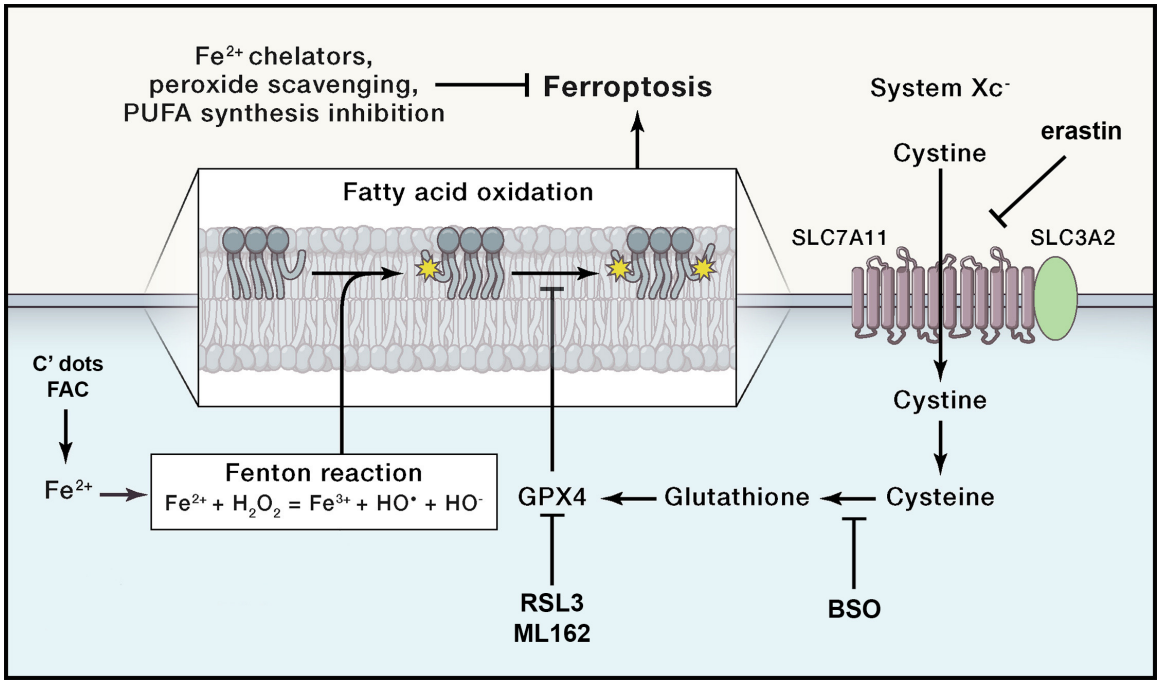

Figure 1.3 The mechanism of ferroptotic cell death.
Ferroptosis results from the oxidation of membrane phospholipids. Free redox-active iron (Fe^{2+}) engages in Fenton chemistry with hydrogen peroxide (H_2O_2) to generate free radicals that react with PUFAs in cellular membranes, forming lipid radicals. In the presence of oxygen, this sets off a chain reaction that results in widespread lipid peroxidation. GPX4 uses GSH as a cofactor to reduce lipid peroxides to their corresponding alcohols, thus limiting membrane damage. When GPX4 is inactivated and the accumulation of lipid peroxides goes unchecked, ferroptosis occurs. GSH synthesis is dependent on cystine import by system x_c^-, which consists of SLC7A11 and SLC3A2. Cystine is reduced to cysteine in the cytosol and incorporated into glutathione by glutamate-cysteine ligase (GCL), which can be inhibited by buthionine sulfoximine (BSO). Molecules that prevent cystine import through inhibition of system x_c^-, such as erastin, are known as class I ferroptosis inducers (FINs). Ferroptosis can also be induced by direct (class II FINs) or indirect inactivation of GPX4. C' dots are ultrasmall silica nanoparticles that induce ferroptosis when combined with amino acid starvation, most likely by increasing cellular iron content. Ferric ammonium citrate (FAC) can also be used as an iron source to sensitize cells to ferroptosis. By contrast, ferroptosis can be inhibited by treatment with iron chelators such as deferoxamine (DFO), lipophilic antioxidants such as liproxstatin-1 that act as lipid peroxide scavengers, or molecules that inhibit enzymes that contribute to the incorporation of PUFAs into phospholipids, such as ACSL4. Figure adapted from Green, 2019.[100]

One remaining question in ferroptosis research is how the accumulation of lipid peroxides leads to necrotic cell death. Lipid peroxidation is known to cause the formation of reactive products such as malondialdehyde (MDA) and 4-hydroxy-2-nonenal (4-HNE), which can result in damage to proteins and DNA.[101] A recent study profiled the extent of one such type of damage, protein carbonylation, in ferroptotic cells, and found that over 400 different proteins were modified by reactive aldehyde or ketone groups.[102] It has been hypothesized that this extensive protein damage might be directly responsible for cell death. However, there is much evidence to suggest that lipid peroxidation also directly alters the structure and properties of lipid membranes. Modeling studies have shown that oxidized fatty acid chains may protrude from the membrane into the aqueous environment,[103] resulting in membrane thinning and increased membrane curvature[104] and water permeability.[105] More dramatically, extensive oxidation and/or aldehyde accumulation may enable the formation of lipid-based hydrophilic pores in the membrane.[106–108] However, many of these studies simulate much higher levels of lipid peroxidation than are observed during ferroptosis, and experimental evidence demonstrating the mechanism of ferroptotic membrane permeabilization is currently lacking.

Physiological and Clinical Relevance of Ferroptosis

In mice, homozygous deletion of GPX4 is embryonic lethal,[109,110] suggesting that ferroptosis must be continuously prevented in order for normal development to occur. In adult animals inducible GPX4 knockout was shown to predominantly affect the

kidneys, resulting in lethal renal failure,[111] indicating that this organ is especially sensitive to this type of cell death. GPX4 is also expressed at high levels in the developing brain and heart.[112] In humans, GPX4 mutations have been suggested to contribute to an ultra-rare pediatric disease called Sedaghatian-type Spondylometaphyseal Displasia (SSMD).[113] Due to its rarity and rapid progression this disorder is little studied, with only around 20 published case studies.[114] SSMD presents with skeletal abnormalities and decreased muscle tone, and most infants suffering from the disease die within the first few weeks of life due to respiratory failure and cardiac arrhythmia.[115] Other issues that have been identified at autopsy are kidney necrosis, cardiac abnormalities, pulmonary hemorrhage, and severe central nervous system malformations including frontotemporal pachygyria and absence of the corpus collosum.[116] Whether excessive ferroptosis is responsible for some or all of the symptoms seen in SSMD remains to be determined, but if so the development of ferroptosis inhibitors appropriate for therapeutic use could represent a promising strategy to mitigate some of the effects of this debilitating disease.

Ferroptosis is still challenging to study *in vivo* due to the lack of easily measurable, high-fidelity biomarkers and the difficulty of genetic modulation, but it has been suggested to participate in several physiological conditions. As mentioned previously, GPX4 knockout in adult mice triggers acute kidney injury and rapid death.[111] Inducible knockout of GPX4 in various other organs and cell types, including neurons,[95] hepatocytes,[117] and T cells,[118] also causes widespread cell death, indicating that prevention of ferroptosis is essential for cell survival in a range of different contexts.

Furthermore, inhibitors of ferroptosis were shown to have protective effects in several *in vivo* and *ex vivo* models of ischemia-reperfusion injury, including in the kidney,[119] heart,[120,121] and brain.[122] Ferroptosis is also hypothesized to play a role in neurodegenerative conditions such as Alzheimer's and Huntington's disease, many of which involve the accumulation of iron and lipid peroxidation in particular regions of the brain.[123] For example, iron chelation reduced disease progression in patients with Parkinson's disease,[124] and ferroptosis has been implicated in dopaminergic neuron cell death in a Parkinson's mouse model.[125] Although more work is needed, these studies suggest that ferroptosis could play important roles in human disease.

While ferroptosis is almost certainly involved in the promotion of pathophysiology, it may also be able to suppress it in certain contexts. It is thought that several tumor suppressor proteins are able to induce ferroptosis upon activation in order to prevent the development of cancer. Both p53[126] and BAP1[127] have been suggested to repress the transcription of SLC7A11, which encodes a subunit of system x_c^-, thereby not only restricting cystine import but also releasing 12-lypoxygenase (ALOX12) from SLC7A11-mediated inhibition.[128] However, stabilization of p53 using nutlin-3 has also been shown to suppress ferroptosis through a mechanism dependent on its transcriptional target p21,[129] so these results require further validation. Intriguingly, a recent study reported a potential function for ferroptosis in immune-mediated tumor suppression, demonstrating that the secretion of interferon-γ (IFNγ) by activated $CD8^+$ T cells also induced the downregulation of SLC7A11 and SLC3A2 (the other system x_c^- subunit) expression in tumor cells, thereby triggering ferroptosis.[130]

Thus, it is possible that ferroptosis may have an important physiological role in tumor suppression.

Several reports have suggested that cancer cells may be particularly vulnerable to ferroptosis, making ferroptosis-inducing compounds potentially attractive chemotherapeutic agents. For example, work by Viswanathan *et al.* showed ferroptosis sensitivity in a panel of cancer cell lines correlated with a ZEB1-dependent mesenchymal state, which has previously been linked to lipid remodeling and resistance to commonly used cancer therapies.[131] As epithelial-mesenchymal transition (EMT) commonly occurs in cancer and has been linked to both metastasis and therapy resistance, ferroptosis sensitivity may be an important exploitable vulnerability of difficult-to-treat cancers. Indeed, another study by Hangauer *et al.* lent credence to this theory by confirming that drug-resistant persistor cells are far more sensitive to GPX4 inhibitors than the parental population they are derived from due to the disruption of the cells' antioxidant program.[132] Additionally, iron levels, redox homeostasis, and other metabolic pathways are often disrupted in cancer cells, potentially increasing their sensitivity to ferroptosis compared to untransformed cells. In clear cell renal carcinoma, for example, ferroptosis sensitivity is linked to metabolic alterations arising from inactivation of the VHL tumor suppressor,[133] whereas triple-negative breast cancer may be more susceptible due to elevated levels of PUFA-containing phospholipids.[134] The reduced ferroportin expression seen in acute myeloid leukemia (AML) results in elevated levels of intracellular iron that also predispose cells to ferroptosis.[135] In previous work, we showed that iron-carrying nanoparticles called C' dots induce ferroptosis when combined with amino acid

starvation.[136] As cancer cells at the center of a solid tumor are often deprived of key nutrients, including amino acids, C' dots may be able to selectively induce ferroptosis in these starved cells. However, a recent study demonstrated that glucose withdrawal impedes ferroptosis through the activity of the energy sensor AMPK.[137] Thus, the exact effect of nutrient deprivation on ferroptosis sensitivity in cancer cells is likely context-dependent and remains to be elucidated.

Interestingly, ferroptosis was recently shown to spread through cell populations, resulting in spatiotemporal patterns of cell death with a wave-like appearance not previously observed in other forms of cell death.[119,136] Given emerging links between ferroptosis and degenerative diseases and injuries that involve large, often continuous areas of necrotic tissue,[138] the propagative nature of ferroptosis is important to understand. However, the mechanism underlying this phenomenon and whether death propagation is a consistent feature of ferroptosis are still unknown. In the next section, I will discuss the population dynamics and non-autonomous properties of different forms of cell death in more detail.

The Population Dynamics of Cell Death*

The distinct mechanisms and inflammatory effects of different cell death programs are becoming increasingly well-characterized. A less studied feature is the effects that different types of cell death may have on the dynamics of the cell populations in which they occur. The demise of an individual cell can be a completely autonomous event, having no effect on neighboring cells; but death can also affect neighboring cell viability, either negatively, through what is sometimes called a bystander effect, or positively, by promoting the survival of surrounding cells. Among the known forms of cell death, three examples best illustrate these extremes (Figure 1.4). First, apoptosis is generally thought to be a neutral, cell-autonomous suicide that has a minimal impact on neighboring cells, although in some contexts the execution of apoptotic cell death can be associated with secreted factors that either induce death or support survival in neighboring cells.[139] Entosis, by contrast, is competitive by nature, as death execution requires the ingestion and killing of one cell by its neighbor,[140] providing the engulfing cell with a survival advantage.[141] And at the other end of the spectrum, several groups have shown that ferroptosis has the ability to spread between cells in a wave-like manner, suggesting potent non-cell-autonomous killing activity.[119,136] Induction of each of these different mechanisms has very different effects on cell populations (Figure 1.4). Entosis can support the long-term survival of stressed populations, thereby potentially promoting cancer progression,[141] while ferroptosis can eliminate large groups of cells, which is predicted to be of therapeutic benefit for cancer treatment.

* This section is adapted from Riegman *et al.*, 2019.[138]

The death of cells in large groups is a widespread occurrence in biological systems[139] (Figure 1.5). From bacterial populations, where large numbers of individual cells die in biofilms,[142] to the slime mold *Dictyostelium*, where a significant proportion of cells undergoes death to form a spore-supporting stalk structure,[143] and plants, where thousands of cells die synchronously to form the water and nutrient channeling vasculature,[144] population-scale cell death is a shared feature across evolutionary kingdoms. In metazoans, entire organs are eliminated by cell death to remove developmental structures, such as the salivary gland in *Drosophila,* or the tails of developing tadpoles,[2] and in mammals, groups of cells die to hollow the amniotic cavity in early development,[145] to sculpt digits during the development of the limbs,[146] and to hollow luminal structures in ducts of the developing mammary gland.[147]

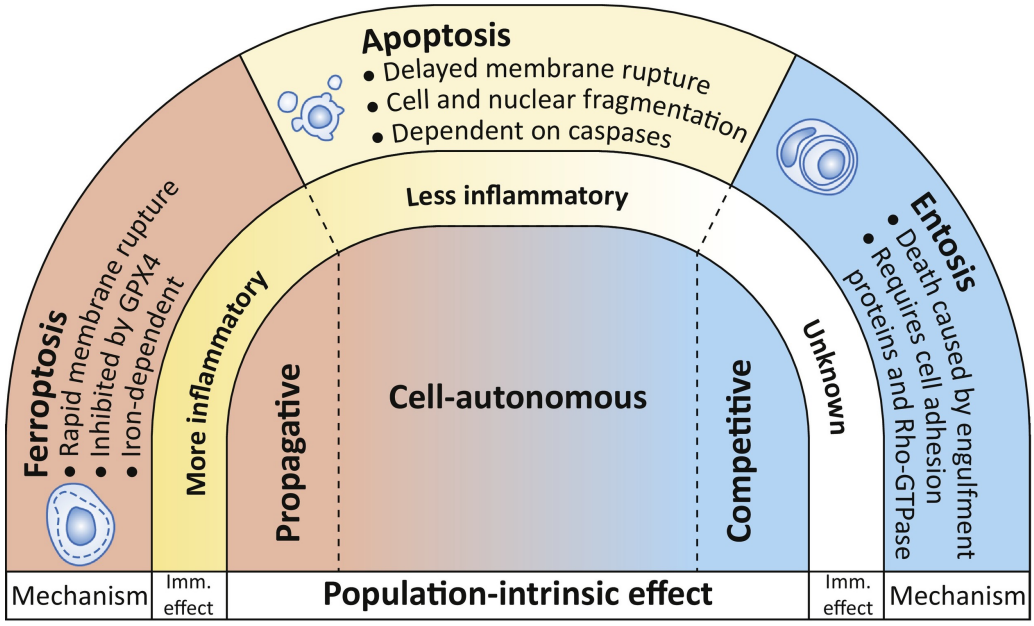

Figure 1.4 Cell death mechanisms have different population-intrinsic effects.
Three regulated forms of cell death are shown with their molecular mechanisms, effects on inflammation, and population-intrinsic effects. Apoptosis is mostly cell autonomous in its execution, but can be involved in cell competition or propagation in a context-dependent manner. Entosis involves the killing of one cell by its neighbor and is an inherently competitive process. Ferroptosis has the ability to spread through populations and may be intrinsically propagative. Imm. effect: immune effect. Figure reproduced from Riegman *et al.*, 2019.[138]

How are deaths that occur in large groups of cells coordinated? In some contexts, population-scale death is systemically controlled by signaling events that cause individual cell deaths to occur in a synchronous manner – for example, tail resorption in amphibians is induced by signaling from increased levels of thyroid hormone in the blood stream that induces individual cells to undergo apoptosis. In other cases, the death of individual cells can trigger the spreading of trans factors that affect neighboring cells. Deaths in this context often occur in a successive manner, with an expanding, wave-like appearance. In plants for example, the spreading of death signals between cells is a common activity that synchronizes differentiation of the vasculature,[148] or promotes expansion of cell death zones as part of an innate immune response that limits pathogen infection (Figure 1.5A).[149,150] In metazoan organisms, too, some mechanisms of cell death exhibit context-specific or even intrinsic abilities to spread between cells and synchronize death across cell populations. Despite the prevalence of population-scale deaths across biological systems, little is known about how different forms of cell death affect population dynamics in this manner. This section discusses mechanisms of death synchronization and propagation in cell populations, and the potential influence of cell death population dynamics on cancer therapy.

Mechanisms of Cell Death Propagation in Metazoan Organisms

Apoptosis

Programmed cell death occurring in metazoan organisms is not generally thought to spread between cells. Apoptosis, for example, typically eliminates small numbers of individual cells in normal tissues, and is usually not observed to affect the viability of surrounding cells.[151] In *C. elegans* development, the majority of developmental cell deaths occur as isolated apoptotic events, and dying cells are engulfed by healthy adjacent cells. The fact that neighboring cells can function in the clearance of apoptotic cells through phagocytosis provides evidence that proximity to an apoptotic cell does not intrinsically inhibit viability. Epithelial cells also mediate engulfment of their apoptotic neighbors in mammalian tissues, for example in the hair follicle,[152] lung,[153] and mammary gland.[154]

In certain cases, however, the execution of apoptosis may be linked to diffusible signals that can lead to the death of adjacent cells. In *Drosophila*, apoptotic cell death during adult wing development occurs as a massive synchronous wave that successively kills the dorsal and ventral cuticle layers of epithelium, shortly after adults emerge from the puparium[155,156] (Figure 1.5B). Apoptosis in this context is initiated by upregulation of the pro-apoptotic gene *hid* in the wing epithelium, a common mechanism of apoptosis induction in *Drosophila*, and also requires the peptide hormone Bursicon, secreted by the nervous system, to eliminate cells primed by *hid* expression.[156] That *hid* expression can induce a propagative mechanism in flies has been shown experimentally in the wing imaginal disc, where enforced *hid* overexpression in cells in the posterior portion

induces the spread of cell death to anterior disc cells. This effect, called "apoptotis-induced-apoptosis", results from the secretion of the death receptor ligand Eiger (a TNFα ortholog) by dying cells, which activates pro-apoptotic signaling in neighboring cells through activation of Jun-Kinase (JNK).[157] While the execution of apoptosis may not have intrinsic spreadable properties, the additional secretion of paracrine factors can therefore endow apoptosis with propagative features that could play specialized roles in normal development. Intriguingly, TNFα secretion by apoptotic cells may also coordinate collective cell death in mammalian tissues, as epithelial cell death in the hair follicle in mice, which also involves groups of synchronously dying epithelial cells, was shown to involve a similar mechanism (Figure 1.6).[157]

In developmental systems, communication between dying cells to coordinate the clearance of large structures may be a more commonly utilized strategy than is currently appreciated. Another example was recently discovered in the *Drosophila* salivary gland, which is removed during metamorphosis by simultaneous induction of apoptosis and the lysosomal degradative pathway autophagy.[158] The execution of death is timed by systemic signaling through the steroid hormone ecdysone, which controls upregulation of *hid*[159] and the autophagy-initiating kinase *atg1*,[158,160,161] thereby activating both pathways. Intriguingly, autophagy induction in this system is also synchronized between neighboring cells by the release of Macroglobulin complement-related (Mcr), a ligand that binds to the receptor Draper.[162,163] Draper activation is required cell-autonomously for autophagy induction and the death of salivary gland cells,[162] suggesting that the

synchronous removal of an organ structure in this context may be partially enhanced by coordination of a death program between neighboring cells.

Necrosis

Necrotic forms of cell death are often considered to be dangerous to surrounding tissue because they result in the release of toxic intracellular contents. Yet necrosis, like apoptosis, can also eliminate individual cells within tissues,[151] and may spread to neighboring cells only under certain circumstances. In *Drosophila*, waves of death can be initiated by the expression of an activated glutamate receptor cation channel in a subset of developing neurons in the eye. This leads to necrotic death initiated by calcium influx, known as excitotoxicity, that spreads to neighboring cells through secretion of Eiger and activation of JNK (Figure 1.6).[164] Waves of necrosis are also observed in response to excitotoxicity in mice, during neuronal cell death resulting from excessive stimulation of neurotransmitter receptors upon ischemic stroke or accumulation of extracellular glutamate. Receptor overstimulation leads to the pathological influx of calcium and causes necrosis that spreads from cell to cell through the transfer of calcium, or potentially other death-inducing signals, via gap junctions.[165] Interestingly, the propagation of calcium signals through gap junctions is also implicated in waves of necrotic cell death that occur in the gut epithelium of *C. elegans* upon aging-induced organismal death (Figure 1.6).[166]

One recently identified form of regulated necrosis, ferroptosis, has been proposed to mediate a spreading effect that may be intrinsic to its execution. Certain

cell types, such as kidney epithelium, have been shown to be particularly sensitive to ferroptosis induction, and indeed this mechanism may underlie the pathological cell death associated with renal ischemia reperfusion injury and acute kidney failure, during which renal tubules are observed to undergo extensive necrosis.[167] Intriguingly, treatment of renal tubules with erastin *ex vivo* was shown to lead to the elimination of entire tubules by a necrotic death that appeared to spread from cell to cell, suggesting that ferroptosis might have the ability to propagate.[119,168] Cell death resulting from ischemia-reperfusion injury in other tissues including intestinal epithelium,[169] heart tissue,[120] and excitotoxicity in brain,[170,171] which can also result in the necrotic death of large regions of cells, has also been linked to ferroptosis. Indeed, two recent publications have shown ischemia-reperfusion injury following myocardial infarction is at least partially mediated by ferroptosis.[121,172] Intriguingly, this process often results in the formation of large contiguous areas of necrotic cells, a phenomenon referred to as contraction band necrosis, which has been hypothesized to be due to the cell-to-cell spreading of death. Together, these findings suggest that ferroptosis contributes to pathological necrosis in multiple contexts and may have the ability to spread through tissues (Figure 1.5C). It remains to be established whether other forms of necrotic cell death can also spread between cells. Interestingly, macrophages undergoing pyroptosis can release prion-like structures called ASC specks, which can then be taken up by neighboring cells and induce activation of the inflammasome. It is unclear, however, whether this activity is sufficient to induce cell death in neighboring macrophages.[173,174]

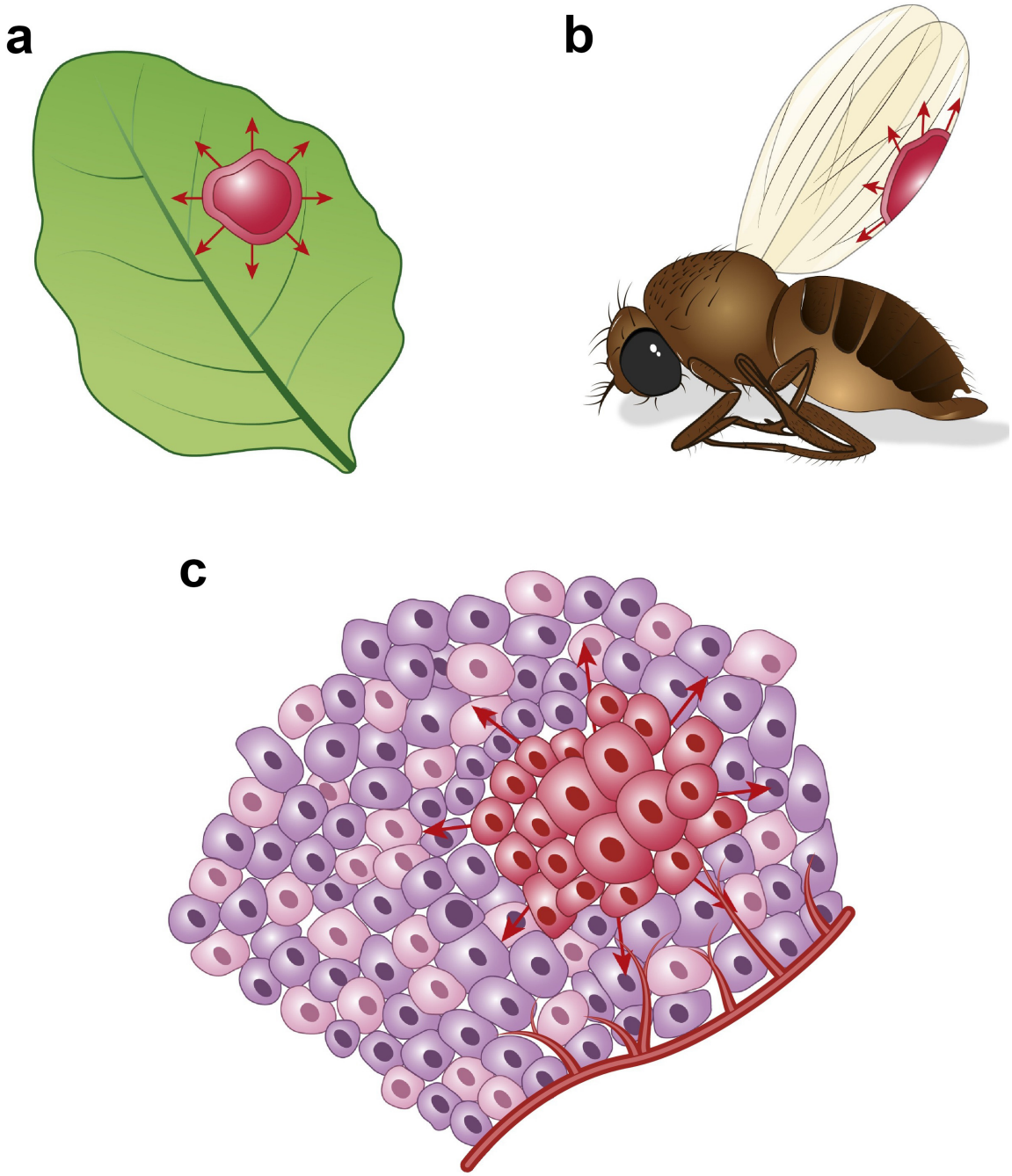

Figure 1.5 Cell death spreading occurs in a variety of biological systems.
(A) Plants exhibit cell death that can propagate between cells, forming expanding zones of dead tissue in response to oxidative damage or pathogen infection (red indicates zone of dead tissue, arrows indicate spreading).
(B) A wave of apoptosis is observed in developing flies that eliminates entire epithelial cell sheets to promote wing development.
(C) Ferroptosis may be able to propagate from cell to cell, potentially resulting in the large necrotic zones observed during ischemia-reperfusion injury in various organs. In cancerous tissues, propagating forms of cell death such as ferroptosis might be effective mechanisms to eliminate large groups of malignant cells.
Figure reproduced from Riegman *et al.*, 2019.[138]

Death Propagation in Cancer

Intrinsic Mechanisms

Although the development of cancer is generally linked to lowered levels of cell death, in some contexts tumors are found to contain large regions of dead cells, an observation commonly referred to as tumor necrosis. Tumor necrosis is a poor prognostic factor,[175] and is thought to result from reduced nutrient availability due to tumor expansion or high interstitial pressure that outpaces or disrupts the available vasculature, leading to chronic ischemia. One type of tumor necrosis called comedo necrosis is characterized by large regions of dead cells within the interior of cancer lesions, where cells fail to survive beyond the diffusion limit of key nutrients from blood vessels. Necrosis of large cell populations in this context may result from the apoptotic death of individual cells[176,177] and a lack of phagocytic clearance, which allows apoptotic cells to eventually lyse.[1] Alternatively, apoptosis-inhibited cancer cells may undergo necrosis due to energy deprivation,[178] or due to induction of a regulated necrotic mechanism called necroptosis, which has also been shown to be induced by ischemic conditions,[179–181] but is not known to exhibit propagative activity. Whether ferroptosis could contribute to spreadable necrosis in this context is not clear, but the links between ferroptosis induction and ischemia are suggestive of this possibility.[182] In a recent report, the detachment of breast epithelial cells from extracellular matrix, a condition that also affects cells in the interior regions of carcinomas,[183] was observed to lead to ferroptotic death.[184] Moreover, the emerging connection between p53-mediated tumor suppression and ferroptosis[126] suggests that this type of cell death could therefore

conceivably be induced during cancer initiation or progression, and contribute to tumor necrosis by inducing the propagation of death across large regions of cells. Further studies are needed to examine whether ferroptosis occurs during carcinogenesis in model systems and clinical specimens.

The Radiation-Induced Bystander Effect

In a therapeutic context, mechanisms that could induce or promote the propagation of cell death through solid tumors may be of particular interest, as cancer recurrence typically results from a failure of therapy to target all of the cells in a lesion, known as "fractional killing", or from the intrinsic resistance of a minority of cells. In either case, the propagation of cell death may contribute to the elimination of cells that escape treatment or are resistant to cell-autonomous induction of death but may be sensitive to propagative mechanisms. Death propagation is a known contributor to the effects of radiation therapy, where the irradiation of individual cells can lead to the death of non-irradiated neighboring cells *in trans*, through what is called the radiation-induced bystander effect (RIBE).[185] The bystander effect is thought to promote the propagation of cell death through two parallel mechanisms, involving the secretion of death-promoting factors and direct cell-to-cell signaling through cell junctions, respectively, leading to both long- and short-range effects. Conditioned medium from irradiated human fibroblasts or keratinocytes, for example, has been shown to induce death in 15-25% of non-irradiated cells,[186,187] and to inhibit clonogenic survival by up to 40%.[187] Furthermore, in 3-dimensional models of skin tissue, apoptotic events were observed at

a distance of up to 1mm from alpha particle-irradiated cells, leading to cell death in 4% of cells in non-irradiated neighboring tissue.[188] Gap junctions have been suggested to mediate RIBEs directly between neighboring cells (Figure 1.6). For example, in cultured human fibroblasts and epithelial cells, low confluency or treatment with gap junction inhibitors was shown to block a bystander effect that led to the induction of p53 in neighboring, non-irradiated cells.[189,190]

Interestingly, cancer cell death following irradiation was recently shown to be partially attributable to induction of ferroptosis,[191] suggesting a possible link between RIBEs and ferroptosis propagation. Radiation and ferroptosis are both known to damage cells through the generation of (lipid) ROS that are normally buffered by glutathione and may lead to lipid peroxidation.[192,193] In addition, both the RIBE and ferroptosis induction in tumors have been linked to increased expression of prostaglandin-endoperoxide synthase 2 (*PTGS2*),[81,186] the gene encoding cyclooxygenase-2 (COX-2). COX-2 dioxygenates and subsequently reduces arachidonic acid to generate inflammatory lipid signaling molecules called prostanoids, and its inhibition can block bystander effects following irradiation[186,194] (Figure 1.6). COX-2 inhibition did not affect ferroptotic cell death induced by treatment with erastin or the GPX4 inhibitor RSL3, but spatiotemporal patterns of cell death were not examined.[81] Together, these results suggest that irradiation and ferroptosis may share some regulatory features that could impinge upon propagation.

Therapeutic Induction of Ferroptosis

Like erastin-induced ferroptosis in kidney tubules, the induction of ferroptosis in cancer cells by treatment with specialized nanoparticles was recently shown to occur with wave-like spatiotemporal patterns that resulted in the elimination of all cells in a culture. Ferroptosis induction by intravenous nanoparticle administration in mice also resulted in the regression of xenograft tumors, suggesting that this form of cell death may have potent tumor suppressive activity.[136] Whereas the radiation-induced bystander effect leads to the death of a relatively small percentage of surrounding cells, ferroptosis may be able to eliminate all neighboring cells in a propagating wave. Thus, the induction of ferroptosis may represent a new strategy to trigger propagation of death through cancer tissues.

In addition to treatment with ferroptosis-inducing nanoparticles, which mediate the delivery of iron into cells following particle endocytosis, ferroptosis induction through other mechanisms may also hold therapeutic potential. For example, erastin has been found to enhance the efficacy of treatment with various chemotherapeutic agents, such as the DNA damaging agents cisplatin in head and neck cancers,[195] doxorubicin in AML,[196] and temozolomide in glioblastoma,[197] while treatment with sorafenib, a tyrosine kinase inhibitor, can induce ferroptosis as a monotherapy.[198] As an increasing number of ferroptosis-inducing therapeutic options are now being developed, it is important to know whether wave-like propagation is a consistent feature of this type of cell death, and whether such waves can eliminate untreated cells *in trans,* similar to the RIBE. In future studies, it will become increasingly important to

consider the intrinsic population-level properties of different forms of cell death and their potential consequences for human health and disease.

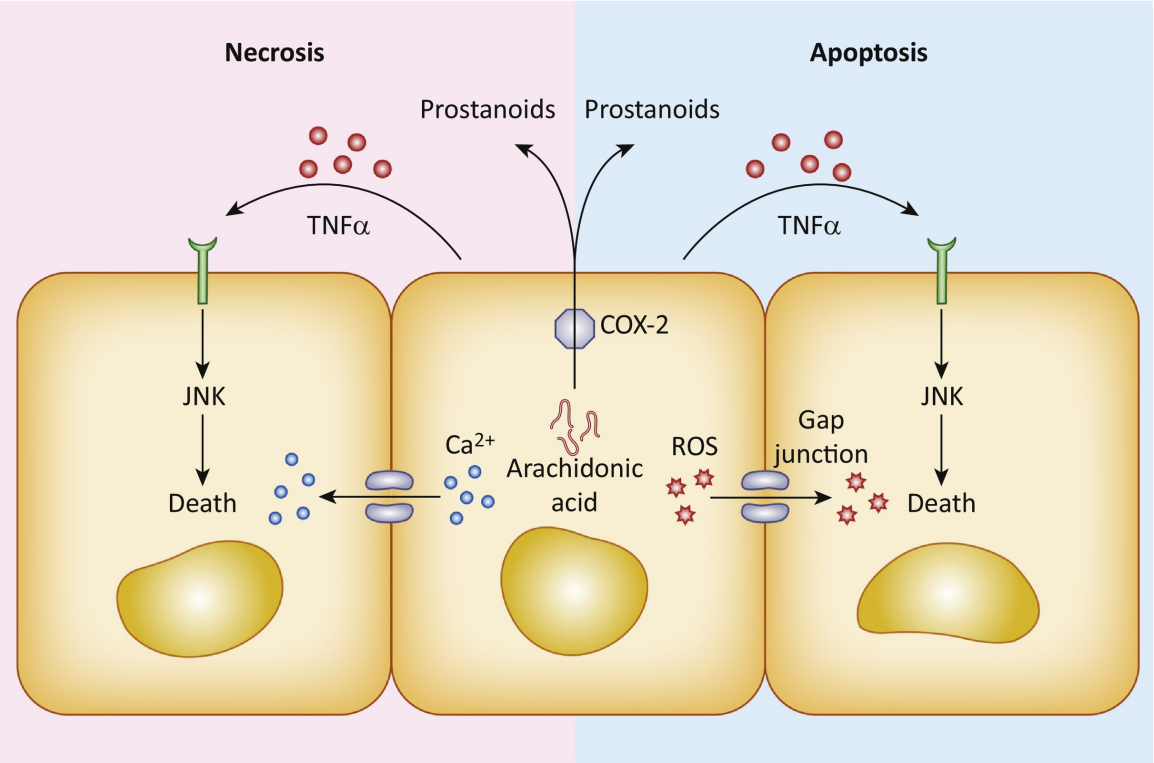

Figure 1.6 Mechanisms of cell death propagation.
Apoptotic and necrotic forms of cell death can propagate between cells by direct cell-to-cell transfer of death-inducing stimuli, such as calcium or reactive oxygen species, through gap junctions. Secreted factors such as TNFα or arachidonic acid-derived prostanoids can also play a role in killing neighboring cells or cells at larger distances. COX-2: Cyclooxygenase-2. JNK: Jun-Kinase. ROS: reactive oxygen species. Figure reproduced from Riegman *et al.*, 2019.[138]

Thesis Aims

Over the last fifteen years numerous new mechanisms of regulated cell death have been discovered that participate, along with apoptosis, in normal physiology or in cell responses to stress and infection. While the distinct regulatory features of different forms of cell death are becoming clear, death at the population scale is much less well understood. One form of regulated necrosis called ferroptosis may have the ability to spread through cell populations in a wave-like manner, and has also been shown to have therapeutic potential for the treatment of cancer. However, it is still unclear whether ferroptosis induction is invariably linked to propagative activity, and little is know about the mechanism of ferroptosis execution downstream of lipid peroxidation. In the following chapters I will address these questions.

In Chapter 3, we develop a quantitative method for the analysis of spatiotemporal cell death patterns. We employ this method to investigate the propagative features of ferroptosis induced by different stimuli, and compare ferroptosis to other forms of cell death. We further investigate some of the potential requirements for propagation to occur.

In Chapter 4, we explore the mechanism of ferroptotic cell lysis and discover that ferroptosis is an osmotic process that is mediated by the formation of plasma membrane pores. We examine the ability of different inducers of ferroptosis to stimulate pore formation, and lastly investigate the connection between pore formation and propagative death.

In Chapter 5, I discuss the questions raised by this work, including potential mechanisms of ferroptosis propagation and pore formation. I also touch on the therapeutic implications of cell death spreading for treatment of degenerative diseases and cancer therapy.

CHAPTER 2: Materials and Methods

Cell Culture

HT1080 cells (ATCC), HeLa cells (ATCC), HAP1 chronic myelogenous leukemia cells (the kind gift of Dr. Jan Carette, Stanford School of Medicine), and MCF7 breast cancer cells (Lombardi Cancer Center, Georgetown University) were cultured in high-glucose Dulbecco's Modified Eagle's Medium (DMEM) (MSKCC Media Preparation Facility) supplemented with 10% heat-inactivated fetal bovine serum (FBS) (F2442; Sigma-Aldrich) and penicillin/streptomycin (30-002-CI; Mediatech). B16F10 melanoma cells (ATCC), Jurkat T cells (ATCC), and U937 promonocytic leukemia cells (ATCC) were grown in RPMI-1640 (11875-093; ThermoFisher) containing 10% heat-inactivated FBS and penicillin/streptomycin, and MCF10A mammary epithelium cells (ATCC) were cultured in DMEM/F12 (11320-033; ThermoFisher) supplemented with 5% horse serum (HS) (S12150; Atlanta Biologicals), 20ng/mL epidermal growth factor (EGF) (AF-100-15; Peprotech), 10µg/mL insulin (I9278; Sigma-Aldrich), 0.5µg/mL hydrocortisone (H-0888; Sigma-Aldrich), 100ng/mL cholera toxin (C-8052; Sigma-Aldrich), and penicillin/streptomycin. HeLa cells expressing *Danio rerio* cytosolic phospholipase A2 (cPLA2)-mKate have been described previously.[199] Cx43 knockout cells were generated by lentiviral transduction of MCF10A cells using lentiCRISPRv2 plasmid encoding Cas9 and an sgRNA designed using the Zhang lab CRISPR tool at http://crispr.mit.edu. Transduced cells were selected using puromycin and single clones were validated using DNA sequencing and immunoblotting. HAP1 cells expressing GCaMP6-NLS were generated using the Sleeping Beauty transposase system. HAP1 cells were transfected

with pSB-CMV-MCS-Puro GCaMP6-NLS and pSB-cag-100x-Transposase, using Lipofectamine 3000 (L3000-015; ThermoFisher) as recommended by the manufacturer. Amino acid-free culture medium was prepared by dialyzing FBS or HS in PBS (MSKCC Media Preparation Facility) using MWCO 3500 dialysis tubing (21-152-9; Fisherbrand) and adding it to amino acid-free base media (MSKCC Media Preparation Facility). These media were used in combination with FAC and BSO to induce ferroptosis in MCF10A and MCF7 cells, and with αMSH-tagged C' dots to induce ferroptosis in B16F10 cells.

Reagents

Ferric ammonium citrate (FAC) (F5879; Sigma-Aldrich), L-buthionine sulfoximine (BSO) (B2515; Sigma-Aldrich), and deferoxamine (DFO) (D9533; Sigma-Aldrich) were dissolved in water and stock solutions were stored at -20°C. FAC and BSO were used at 400µM and DFO at 200µM. SuperKillerTRAIL (ALX-201-115-C010; Enzo) stock solution was diluted to 100µg/mL in KillerTRAIL dilution buffer (20mM HEPES, 300mM NaCl, 0.01% Tween-20, 1% sucrose, 1mM DTT), aliquotted, and stored at -80°C. It was used at a final concentration of 50ng/mL. Hydrogen peroxide (216763; Sigma-Aldrich) and tert-butyl hydroperoxide (458139; Sigma-Aldrich) were first diluted in water and then added to cell culture media at a final concentration of 1mM for hydrogen peroxide and 50µM for tert-butyl hydroperoxide. C11-BODIPY$^{581/591}$ (D3861; Molecular Probes) was dissolved in DMSO, stored at -20°C, and diluted to a final concentration of 5µM prior to use. Sucrose (S7903; Sigma-Aldrich), raffinose (R0514; Sigma-Aldrich), polyethylene glycol (PEG) 1450 (P7181; Sigma-Aldrich), and PEG3350 (P3640; Sigma-Aldrich) were dissolved directly

into cell culture media at a concentration of 20mM. All other compounds were prepared as stock solutions in DMSO and stored at -20°C. Erastin (E7781, used at 7.5μM with HAP1s and 2μM with HT1080s), ferrostatin-1 (SML0583, used at 4μM), Trolox (238813, used at 100μM), and z-VAD-fmk (V116, used at 20 μM) were from Sigma-Aldrich; RSL3 (S8155, used at 1μM) and liproxstatin-1 (S7699, used at 200nM) were from SelleckChem. Necrosulfonamide (20844; Cayman Chemicals) was used at 1μM. ML162 was a kind gift from Dr. Scott Dixon and was used at 4μM. αMSH-tagged C' dots were synthesized as described previously[136,200] in water, stored at 4°C, and used at a concentration of 15μM. SYTOX Green (S7020; Molecular Probes) was used at a concentration of 10nM and SYTOX Orange (S11368; Molecular Probes) at a concentration of 50nM for all experiments.

Microscopy

Live-Cell Imaging

Cells were seeded on glass-bottom plates (P24G-1.5-13-F; Mattek) and treated in fresh culture media the next day. For amino acid-free conditions, cells were washed with PBS twice prior to treatment. Imaging was performed in live-cell incubation chambers maintained at 37°C and 5% CO_2. Images were acquired every 5 to 30 min for 24-48 hours using a Nikon Ti-E inverted microscope attached to a CoolSNAP charge-coupled device camera (Photometrics) and NIS Elements AR software (Nikon, 3.22.15). For experiments with ML162, time-lapse imaging was performed on plastic tissue culture plates (3527; Corning) on a Zeiss Observer.Z1 microscope coupled to an Axiocam 506 mono camera

(Zeiss) using ZEN software (Zeiss). Images were quantified manually in NIS Elements AR (Nikon) or ZEN (Zeiss) and processed using ImageJ (2.0.0) and Adobe Photoshop (CS6 13.0.5).

Confocal Imaging

Cells were plated on glass-bottom dishes and treated the next day. For C11-BODIPY$^{581/591}$ imaging, cells were washed twice with Hank's Balanced Salt Solution (HBSS) (14025-092; ThermoFisher) 24 hours after treatment, stained in 5μM C11-BODIPY$^{581/591}$ in HBSS for 10 minutes at 37°C and 5% CO_2, and again washed twice in HBSS. Cells were imaged at 37°C and 5% CO_2 using the Ultraview Vox spinning-disk confocal system (PerkinElmer) equipped with 488nm and 568nm lasers and an electron-multiplying charge-coupled device camera (Hamamatsu C9100-13), and attached to a Nikon Ti-E microscope. For cPLA2 imaging in HeLa cells, a single confocal plane is shown from the indicated time points. For C11-BODIPY$^{581/591}$ imaging, maximum projections are shown. Images were acquired and processed using Volocity software (Perkin Elmer, version 5.2.0).

Analysis of Live-Cell Imaging

Single-Cell Time of Death Annotation

We used a custom MATLAB (R2016A) script to record the xy position and time of death (for Sytox) or time of calcium influx (for GCaMP) of each cell. For each frame of a given timelapse movie, every new event was manually clicked and its position and frame

number recorded and saved. The resulting files were then used for further analysis as detailed below.

Measuring Propagation

We used Voronoi tessellation,[201] a computational geometry method to divide a plane into regions given a set of loci where each locus corresponds to a cell nucleus's xy location. Each point on the plane belongs to a single region and each region consists of all the closest points to the associated nuclear locus. Neighbors were defined as regions sharing a border, which allowed us to identify all pairs of neighboring cells. Note that neighboring cells in the tessellation do not necessarily share cell-cell junctions in the experiment. For each field of view we calculated the mean difference in time of death between all neighboring cell pairs as a measure for propagation speed, marked with $\mu_{exp\Delta t}$. This analysis was performed using custom Python 3 scripts.

Permutation Testing

We devised a statistical test to determine the statistical significance of the hypothesis that there is a relationship between a cell's and its neighbors' times of death. This was achieved by using a non-parametric permutation test to reject the null hypothesis that the cells' time of death is independent of their neighbors' time of death. For every field of view, the following procedure was repeated for 1000 iterations. The recorded time of death was randomly permuted between the cells (i.e., each cell was assigned a random time of death, with the same number of deaths at each time point as in the

experimental data) and the mean difference in time of death between all neighboring cell pairs was recorded. The p-value was calculated as the fraction of iterations in which the mean time difference between neighbors using the permuted ("random") cell death was faster than the experimental measurement. We considered a p-value of 0.05 as statistically significant. This analysis was performed using custom Python 3 scripts.

Spatial Propagation Index

We devised the spatial propagation index to quantify the contribution of the spatial component to the observed experimental cell-cell propagation. This measure was defined as the deviation of the experimental mean propagation ($\mu_{exp\Delta t}$) from the 95th percentile of the mean randomly permuted death times ($\mu_{perm95\Delta t}$) normalized to $\mu_{perm95\Delta t}$: $\frac{\mu_{perm95\Delta t} - \mu_{exp\Delta t}}{\mu_{perm95\Delta t}}$. This measure can be interpreted as the fraction of the $\mu_{perm95\Delta t}$ needed to reconstruct back the spatial information in the experimental data.

Quantifying Ferroptosis Propagation from DIC

To quantify the distance covered by the ferroptosis wave in each field of view, lines delineating live and dead cell regions were drawn manually in NIS elements AR (Nikon, 3.22.15) at one-hour intervals, starting from a timepoint at which smaller initiation points, if present, had converged into larger waves. For each interval, the area between two lines was measured and divided by their average length to obtain the mean distance travelled during a given interval in a given field of view. Information from different fields of view in the same condition was then combined to plot the mean

distance covered in each condition, and a linear regression performed to calculate the speed of the corresponding ferroptosis wave.

Western Blotting

Western blotting was performed as described previously.[136] Briefly, cells were placed on ice, washed twice with cold PBS, then lysed in radioimmunoprecipitation assay (RIPA) buffer (50 mM Tris at pH 7.4, 150 mM NaCl, 2 mM EDTA, 1% NP40, 0.1% SDS) containing protease and phosphatase inhibitors. Cell lysates were centrifuged at 4°C for 20 min. and protein content of supernatants was quantified using BCA assay (23225; ThermoFisher). Samples were separated using SDS-PAGE and transferred to PVDF membranes. Membranes were blocked for 1h in 5% BSA in TBS-T, followed by overnight incubation with primary antibody at 4°C. After washing with TBS-T, secondary antibody incubation was performed in 5% BSA in TBS-T for 1h at room temperature. Blots were incubated with ECL reagent (32106; ThermoFisher) and exposed to film to detect protein levels. Antibodies used: anti-Connexin43 (3512S; Cell Signaling), anti-tubulin (3873; Cell Signaling), anti-rabbit IgG HRP-linked antibody (7074; Cell Signaling), and anti-mouse IgG HRP-linked antibody (7076; Cell Signaling).

LDH Assay

LDH assays were performed using the Pierce LDH Cytotoxicity Assay Kit (88954; ThermoFisher) following the manufacturer's instructions. Briefly, cells were seeded on 96 well plates and treated in triplicate the next day. At the indicated time, 50µL media

was transferred from each well to a well containing 50µL assay buffer, and plates were incubated at room temperature for 30 mins. At this point 50µL stop solution was added to each well, bubbles were removed using a syringe, and the absorbance was read on a BioTek Synergy H1 Hybrid Reader at 490nm and 680nm wavelengths. The 490nm absorbance was subtracted from the 680nm absorbance, and background from cell culture medium was subtracted from all values. Data were averaged across technical replicates and normalized to the indicated treatment without osmoprotectants to calculate percent LDH release. For suspension cells, cells were treated in 24 well tissue culture plates containing 1mL media per well. At the indicated time, 200µL media was taken from each well, spun down to remove dead cells, and supernatant was used to perform the assay as described.

Crystal Violet Assay

Cells were seeded on 24-well tissue culture plates (3527; Corning) and treated in triplicate the next day. After 24 hours, when most control cells had died, wells were washed twice with PBS, then fixed in 4% paraformaldehyde (15710-S; Electron Microscopy Sciences) in PBS for 15 minutes. After washing with water, cells were stained with 0.1% crystal violet (61135; Sigma-Aldrich) in 10% ethanol for 20 minutes, then washed again with water until clear and allowed to air dry. After drying, crystal violet stain was dissolved in 10% acetic acid by shaking plate at room temperature for 30 minutes. This solution was diluted 1:4 with water and absorbance measured at 590nm on a BioTek Synergy H1 Hybrid Reader. Background absorbance from wells

containing only tissue culture medium was subtracted from all readings, and values were averaged across technical replicates and normalized to the untreated controls to obtain percent viability.

Quantification and Statistics

Data were analyzed in Microsoft Excel (Office 2011) and GraphPad Prism 7 and are represented as mean with individual data points or mean ± SD. P values were obtained using two-sided Dunnett's multiple comparisons test unless otherwise indicated. * = $p<0.05$, ** = $p<0.01$, *** = $p<0.001$, **** = $p<0.0001$. All data presented here are from at least three technical or biological replicates; exact n are reported in the figure legends.

CHAPTER 3: Quantifying the spatiotemporal dynamics of cell death*

Introduction

While the molecular mechanisms of different forms of cell death have been studied in great detail, comparatively little is known about the population-level effects of different types of cell death. Researchers have traditionally focused on the cell-intrinsic properties of cell death, but it is now becoming clear that dying cells can affect their neighbors in unexpected and interesting ways. For example, the irradiation of some cells in a population has been shown to result in DNA damage, elevation of reactive oxygen species (ROS), and death even in non-irradiated cells, a phenomenon termed the Radiation-Induced Bystander Effect (RIBE).[186,202] While RIBE was first described over two decades ago, the underlying causes are still an active area of investigation. Numerous factors, including gap junctions, TNF-α, and COX-2, have been proposed to play a role in this process, but the exact mechanisms and importance remain unclear.

One type of cell death whose population-level effects have been studied in more detail is entosis, which involves the engulfment of one live cell by another and its subsequent lysosome-mediated degradation.[183] Interestingly, this process appears to be driven mechanically by the engulfed "loser" cell and may represent an instance of altruistic suicide. Indeed, recent work has shown that entosis can be induced by glucose starvation and provides a survival advantage to engulfing "winner" cells in nutrient-depleted environments.[141] Thus, in the case of entosis, the death of some cells enables the survival of neighboring cells for the benefit of the population.

* This chapter is adapted from Riegman *et al.*, 2020.[206]

The population-level effects of different types of cell death have profound implications for our understanding and treatment of disease, as many human health conditions are caused by inappropriate levels of cell death. In the case of too much death, e.g. in neurodegenerative disease, it is important to understand any potential non-autonomous properties of the death type in question in order to prevent excessive amounts of it. When there is too little death, as occurs during tumorigenesis, understanding the population-level properties of different forms of cell death may help inform future therapeutic efforts seeking to maximize cell death induction. For example, inducing entosis as a cancer treatment would be suboptimal as this may actually aid the survival and proliferation of the remaining cells.

Ferroptosis is a recently discovered form of iron-dependent necrosis that involves the accumulation of lipid peroxidation products within the plasma membrane.[80] It has been implicated in several pathological processes, such as ischemia-reperfusion injury and traumatic brain injury.[182] In a previous study, *ex vivo* treatment of mouse renal tubules with the ferroptosis inducer erastin was shown to result in a wave of tissue deformation, progressing from one end of the tubule to the other.[119] Interestingly, we observed a similar phenomenon in cultured cells upon treatment with ultra-small ferroptosis-inducing nanoparticles called C' dots.[136] However, whether wave-like ferroptosis occurs in other contexts is still unknown. In this chapter, we systematically investigate and quantify the spatiotemporal dynamics of ferroptosis and compare them to other forms of cell death.

Results

A novel method of ferroptosis induction

We previously observed wave-like spreading of ferroptosis when cells were treated with specialized ferroptosis-inducing nanoparticles called C' dots,[136] and a similar phenomenon was reported in mouse renal tubules treated with the ferroptosis-inducing agent erastin.[119] While waves of ferroptotic death have been observed in these contexts, propagation of cell death during ferroptosis has not been systematically investigated. In order to do so, we first developed a novel method of ferroptosis induction that is effective in multiple different systems. We previously showed that C' dots are able to induce ferroptosis in a wide variety of cell lines when combined with amino acid starvation, but their synthesis is a labor- and time-intensive process. Published ferroptosis inducers such as erastin and RSL3 are commercially available, but their efficacy varies widely between cell lines.[81,203] Since ferroptosis depends on the presence of iron and can be induced through the inactivation of the glutathione-dependent enzyme GPX4, we reasoned that supplying cells with excess iron while preventing glutathione (GSH) synthesis might be sufficient to induce cell death. We therefore treated cells with a combination of ferric ammonium citrate (FAC), a soluble iron-containing compound, and buthionine sulfoximine (BSO), which inhibits Glutamate Cysteine Ligase (GCL),[204] the enzyme that catalyzes the first step of GSH synthesis. In many of the cell lines we tested, this combination treatment indeed resulted in extensive cell death. Since C' dots generally have to be combined with amino acid starvation to induce ferroptosis, we also tested FAC and BSO in amino acid-free media.

This combination enabled us to induce cell death in the remaining cell lines, including MCF7 breast cancer cells and MCF10A mammary epithelial cells.

While ferroptosis has few validated biomarkers, it is known to be inhibited by the chelation of iron or treatment with lipophilic antioxidants.[80] To confirm that the form of cell death induced by FAC&BSO was indeed ferroptosis, we co-treated HAP1 cells with FAC&BSO and the known ferroptosis inhibitors liproxstatin-1 (Lip-1), ferrostatin-1 (Fer-1), and Trolox. These lipophilic antioxidants rescued viability (Figure 3.1A), confirming that the type of cell death we observed was indeed ferroptosis. As the treatment involved iron supplementation through FAC, we did not test the effect of iron chelation. Additionally, we performed C11-BODIPY$^{581/591}$ staining in HAP1 cells treated with FAC&BSO. C11-BODIPY$^{581/591}$ is a ratiometric, lipophilic dye that shifts its emission wavelength from ~590nm (red) to ~510nm (green) upon oxidation, and thus allows for the imaging of lipid peroxidation.[205] FAC&BSO-treated cells indeed displayed increased green fluorescence prior to death (Figure 3.1B), indicating that this treatment induced lipid peroxidation within cells. Taken together, these results demonstrate that combination treatment with FAC and BSO is a new way to induce ferroptosis that is effective in a variety of cell lines.

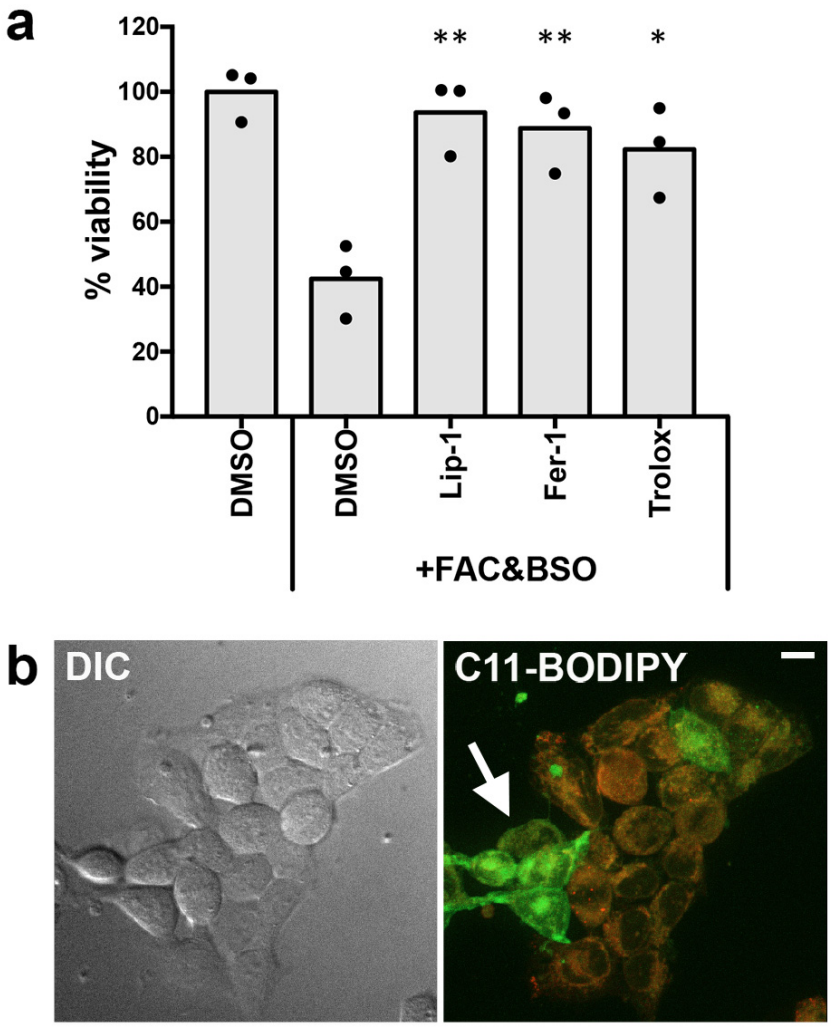

Figure 3.1 Treatment of HAP1 cells with FAC and BSO induces ferroptosis.
(A) Viability of HAP1 cells after treatment with FAC and BSO and either DMSO or ferroptosis inhibitors as measured by crystal violet staining. N = three independent experiments. Dunnett's test; **p=0.0024 for Lip-1; **p=0.0045 for Fer-1; *p=0.0107 for Trolox.
(B) Confocal images of HAP1 cells treated with FAC and BSO and stained with C11-BODIPY$^{581/591}$. Non-oxidized probe is shown in red, oxidized probe is shown in green (arrow). Scale bar = 10mm. Images are representative of three independent experiments.
Figure adapted from Riegman *et al.*, 2020.[206]

Quantifying the spatiotemporal patterns of cell death

To systematically study cell death propagation, we devised a method to do so quantitatively using live cell imaging. For this analysis we used movies of cells undergoing death in the presence of SYTOX Green, a cell-impermeable death indicator that becomes fluorescent upon interaction with nucleic acids (Figure 3.2A, B). First, using a custom Matlab script, we recorded the time and position of each cell death event in a given movie. Using this information, we identified every pair of neighboring cells in each field of view through Voronoi tessellation[201] (Figure 3.2C). This technique, given a set of loci (in this case, the positions of dead cells' nuclei), divides the plane into a number of separate regions, each containing one locus and the set of points closest to that locus. Two cells were considered neighbors if the two regions containing their corresponding loci shared a border. For each cell death movie, we were thus able to calculate the mean time difference between neighboring cell deaths in the experiment, which we termed $\mu_{exp\Delta t}$.

We then used a bootstrapping approach to quantify intercellular propagation of cell death. For each field of view, we generated 1000 permutations of cell death order, with each cell assigned a random time of death but keeping the total number of deaths per timepoint the same as in the experiment (Figure 3.2C). An example analysis showing the distribution of time differences between neighboring deaths in the experiment and the simulation is shown in Figure 3.2D. We then calculated the mean time difference between neighboring deaths for each of these random simulations, thus generating a distribution of means that we would expect to observe assuming no relationship

between neighboring deaths, with each distribution specific to one particular field of view. Next, we compared the experimentally observed $\mu_{exp\Delta t}$ to the 95th percentile of the randomly generated distribution, $\mu_{perm95\Delta t}$, to determine whether the observed death pattern was statistically non-random. If $\mu_{exp\Delta t}$ is smaller than $\mu_{perm95\Delta t}$ and therefore falls into the bottom 5% of random means, we can conclude that the difference is statistically significant with $p<0.05$, consistent with wave-like propagation.

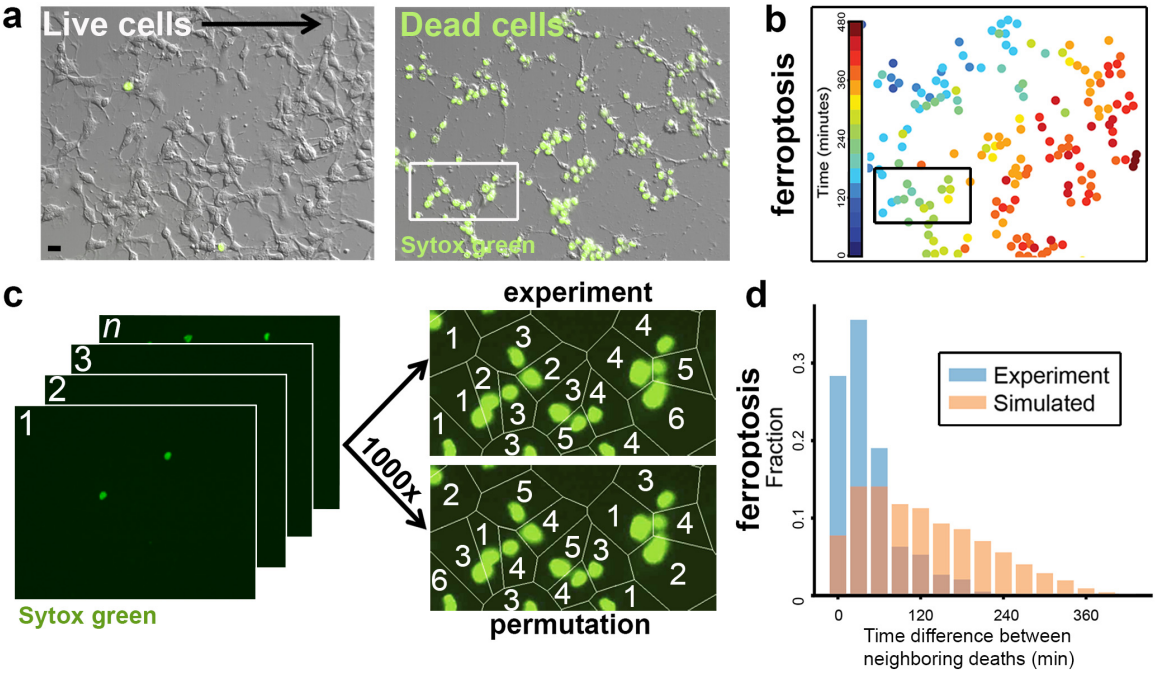

Figure 3.2 Quantitative analysis of spatiotemporal death patterns.
(A) B16F10 cells treated with C' dot nanoparticles in amino acid-free (-AA) media to induce ferroptosis. Images show DIC and SYTOX Green; SYTOX-positive cells are dead. Scale bar = 20µm. Images are representative of five movies from one experiment.
(B) Nuclei of ferroptotic cells in panel a, pseudocolored to indicate relative timing of cell death, as determined by time-lapse microscopy. See Supplementary Video 1.
(C) Schematic summarizing our method to quantify cell death patterns. Images from time-lapse microscopy (left) are processed to determine relative timing of neighboring cell deaths (top right image, "experiment") versus permuted trials (bottom right image, "permutation") to detect potential non-random patterns. Images match insets in panels a and b. Scale bar = 10µm
(D) Distribution of time differences between neighboring deaths (Δt) from experiment in panels a-c shown in blue, versus averaged distribution of the set of random permutations shown in orange. Graph shows fraction of total deaths with given time differences.
Figure adapted from Riegman *et al.*, 2020.[206]

This statistical test can determine whether spatiotemporal death patterns are non-random or not, but in itself does not give any information regarding the strength of the relationship between neighboring death times. We therefore devised a new measure termed the *spatial propagation index* (SPI) to quantify the contribution of the spatial component to the observed $\mu_{exp\Delta t}$. When intercellular death propagation is not the major determinant of the spatiotemporal distribution of cell death across a population, we expect $\mu_{exp\Delta t}$ to have a value similar to or larger than $\mu_{perm95\Delta t}$, as death occurs independently of neighboring cell deaths in the vicinity. However, when propagation does play a major role, i.e. cells are affected by the death of other nearby cells, we expect $\mu_{exp\Delta t}$ to be much smaller than $\mu_{perm95\Delta t}$ due to the non-random spatial order of death. Thus we defined the $SPI = \frac{\mu_{perm95\Delta t} - \mu_{exp\,\Delta t}}{\mu_{perm95\Delta t}}$, the spatial contribution to the experimentally observed death patterns as a fraction of the neighboring death times expected under the assumption that the death order is spatially random, as a way to directly compare the non-autonomous properties of different cell death types.

Comparing the spatiotemporal dynamics of different forms of cell death

To measure intercellular death propagation in different forms of cell death, we examined the spatiotemporal death patterns of ferroptosis induced by various stimuli (C' dots, erastin, FAC&BSO, or the GPX4 inhibitor ML162), as well as necrosis induced by treatment with hydrogen peroxide (H_2O_2), and apoptosis induced with TNF-related apoptosis-inducing ligand (TRAIL). We performed these experiments in several different cultured cell lines (MCF-10A mammary epithelial cells, MCF-7 breast cancer cells, U937

promonocytic leukemia cells, HAP1 chronic myelogenous leukemia-derived cells, and B16F10 melanoma cells). When we analyzed the resulting movies and compared the experimental mean from each experiment, $\mu_{exp\Delta t}$, to the corresponding randomly generated distribution, we found that all treatment conditions resulted in death with significantly non-random spatiotemporal patterns (Figure 3.3A). This indicates that in all the death types we studied (ferroptosis, apoptosis, and necrosis), two neighboring cells are more likely to die at similar times than two randomly selected cells. However, the cell death movies for apoptosis, H_2O_2-induced necrosis, and ML162-induced ferroptosis did not visibly display wave-like propagation of death, and closer examination revealed that the distribution of time differences between neighboring deaths was much more similar to that of the computationally generated simulations in these experiments (Figure 3.3C-F). Similarly, the experimental mean was much closer to the 95^{th} percentile of the random permutations. We therefore calculated the Spatial Propagation Index for each xy position, and observed it to be much lower in these three conditions than when ferroptosis was induced by C' dots, erastin, or FAC&BSO (Figure 3.3B). Thus, while the spatiotemporal patterns of TRAIL-induced apoptosis, H_2O_2-induced necrosis, and ferroptosis are all statistically non-random, cell death propagation only plays a dominant role in ferroptosis induced with erastin, C' dots, or FAC&BSO, but not when induced by ML162. These results demonstrate that the ability to spread in wave-like patterns by propagating between neighboring cells is a feature of particular forms of ferroptosis.

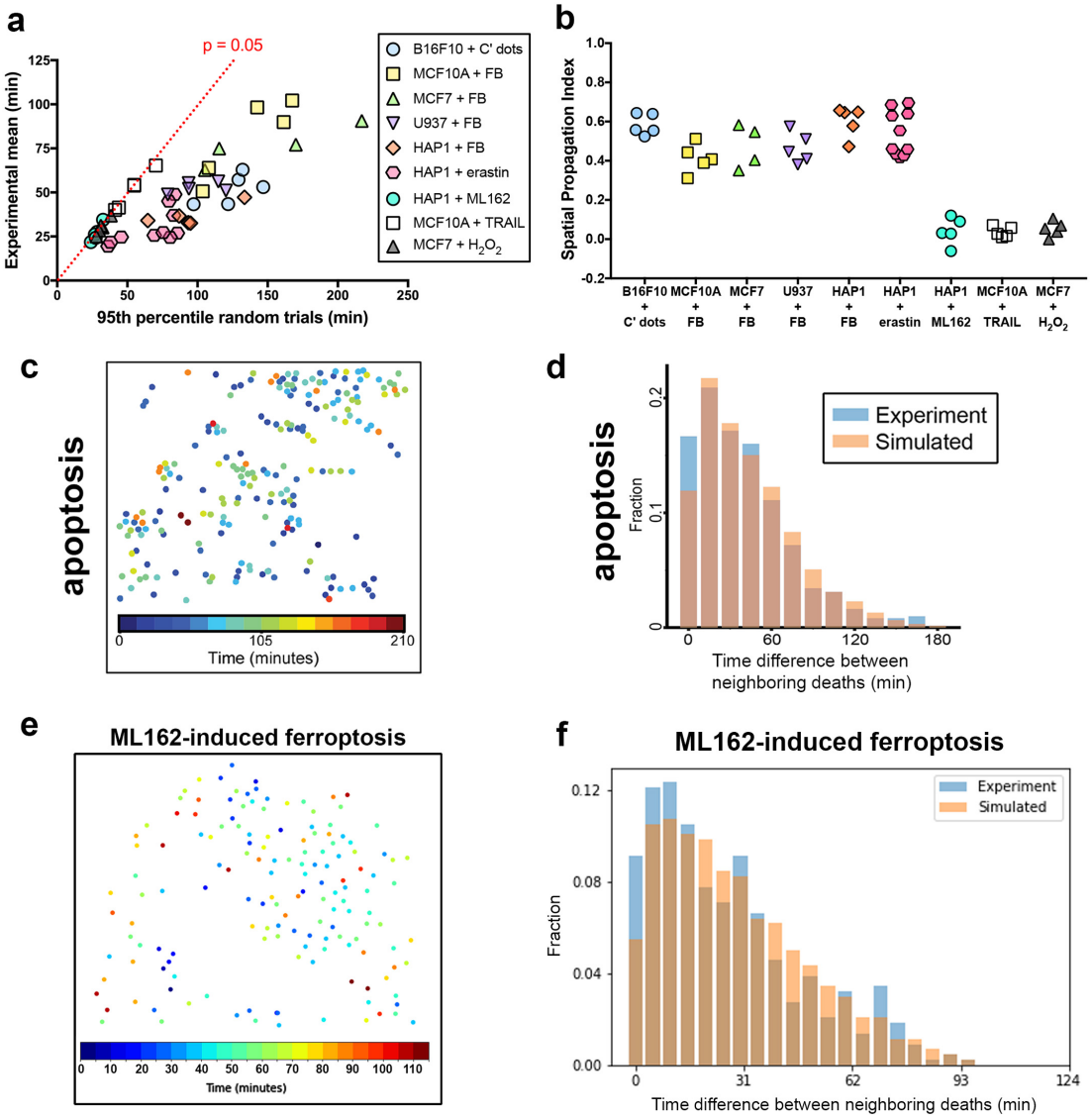

Figure 3.3 Ferroptosis exhibits propagative features when induced by C' dots, erastin, or FAC and BSO.
(A) Ferroptosis, apoptosis, and H_2O_2-induced necrosis show significantly non-random spatiotemporal patterns. Graph shows $\mu_{exp\Delta t}$ vs. $\mu_{perm95\Delta t}$ of different cell lines undergoing ferroptosis induced by the indicated treatment (FB = FAC+BSO), apoptosis induced with TRAIL, or necrosis induced with H_2O_2. Dashed line indicates $\mu_{exp\Delta t} = \mu_{perm95\Delta t}$; experimental means below the line are significant with $p<0.05$ as determined using a non-parametric permutation test. Each data point represents one movie.
(B) Spatial Propagation Index generated from data in panel A.
(C) Spatiotemporal distribution of apoptosis in MCF10A cells treated with TRAIL. Each dot represents a cell; colors indicate relative times of cell death as determined by cell morphology.
(D) Distribution of experimental time differences between neighboring deaths (Δt) in blue and averaged distribution of Δts from the corresponding permuted data in orange. Data belong to the experiment in panel C.
(E) Spatiotemporal distribution of cell death in HAP1 cells treated with ML162 to induce ferroptosis. Each dot represents a cell; colors indicate relative times of cell death as determined by SYTOX Green staining.
(F) Distribution of experimental time differences between neighboring deaths in blue and averaged distribution of the corresponding permuted data in orange. Data belong to the experiment in panel E.
Figure adapted from Riegman *et al.*, 2020.[206]

Investigating the mechanism of ferroptotic propagation

The fact that ferroptosis has strong non-autonomous properties raises the possibility that there may be a signal that emanates from ferroptotic cells and triggers death in their neighbors. However, it is also possible that the wave-like propagation we observe may be the result of anti-ferroptotic resource sharing between neighboring cells. One could imagine a scenario in which an antioxidant such as glutathione can move between cells. As cells move closer to ferroptosis, the GSH concentration across the population declines, until one cell reaches a critically low level and dies. This would in turn make the next cell over more vulnerable, causing it to be the next to die, and so on and so forth, creating a domino effect. This hypothesis could also explain why wave-like ferroptosis is induced only by treatments that lower cellular GSH levels and not by those that directly inhibit GPX4. GSH cannot cross the cell membrane, but is small enough to fit through gap junctions, channels that directly connect the cytoplasms of neighboring cells formed by a family of proteins called connexins. To test whether gap junctions are involved in ferroptosis propagation, we knocked out the main gap junction-forming protein, connexin-43 (Cx43), in MCF10A cells (Figure 3.4A). Cx43 knockout (KO) cells treated with FAC&BSO in amino acid-free media displayed the same wave-like cell death patterns as control cells (Figure 3.4B), and upon quantitative analysis we found them to be significantly non-random with a similar SPI to controls (Figure 3.4C). This suggests that the transfer of pro- or anti-ferroptotic molecules through gap junctions is not involved in ferroptosis propagation, which is further corroborated by the fact that U937

cells, which are suspension cells that do not form cell junctions, still display wave-like death upon ferroptosis induction.

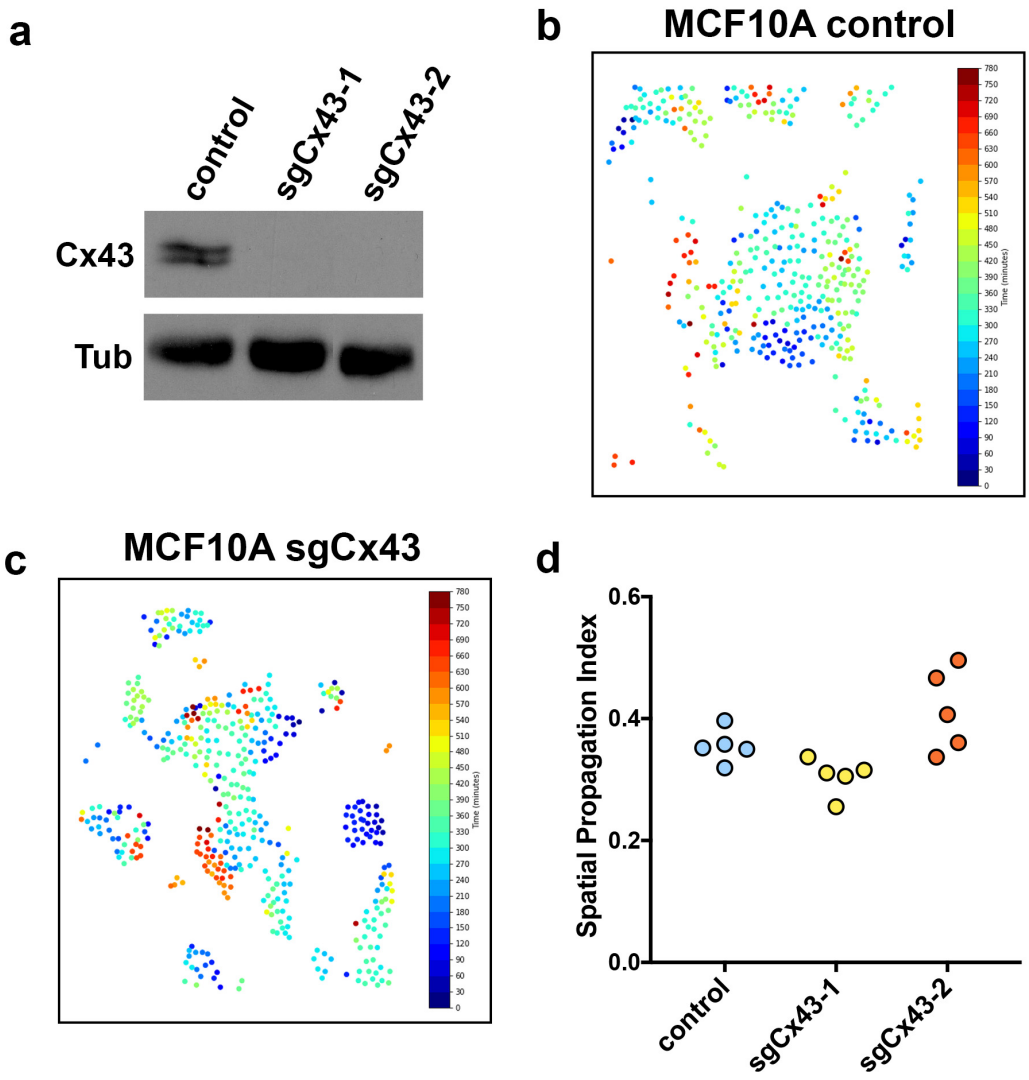

Figure 3.4 Ferroptosis propagation in MCF10A cells does not depend on connexin 43.
(A) Immunoblot of wild-type (wt) and CRISPR-generated connexin-43 (Cx43) knockout cells (sgCx43) using anti-Cx43 antibody and anti-tubulin as a loading control.
(B, C) Spatiotemporal cell death maps from MCF10A wt and sgCx43 cells undergoing ferroptosis after treatment with FAC and BSO in amino acid-free media. Each dot represents one cell; colors indicate relative times of death in minutes.
(D) Spatial Propagation Index calculated for movies of MCF10A wt and sgCx43 cells undergoing ferroptosis after treatment with FAC and BSO in amino acid-free media.

If there is indeed a ferroptosis-inducing signal that acts *in trans*, we wondered if it might be able to kill less sensitive bystander cells. We therefore performed mixing experiments using two suspension cell lines, U937 cells and Jurkat cells, that die at similar times when ferroptosis is induced using FAC&BSO. We treated Jurkat cells with FAC&BSO, then added U937 cells expressing an mCherry-tagged version of histone 2B (H2B-mCherry) to the same wells six hours later and performed timelapse imaging of the mixed cultures. As expected, Jurkat cells died first in a wave-like manner. Soon after, another wave of death started in the surrounding U937 cells. Interestingly, the wave starting point was located at the border between the two cell types, while death normally starts from the edge of a colony, and occurred before the death of control U937s that were treated at the same time. Thus, mixing U937s with pretreated Jurkat cells appeared to accelerate their death, although the delay between the occurrence of the two waves implies that the hypothetical signal emanating from dead cells is not sufficient to induce death, and only triggers ferroptosis when cells have been pre-conditioned. This is supported by the fact that when we increased the amount of time for which the Jurkats were pre-treated before addition of the U937 cells to 20 hours, the dying Jurkat cells were unable to induce death in surrounding U937 cells. Since in this case the U937 cells did not have a protective effect and delay death in the colony of Jurkat cells this result also argues against the 'local depletion' model in which an anti-ferroptotic resource such as glutathione is locally exhausted, thereby accounting for the wave-like dynamics of death.

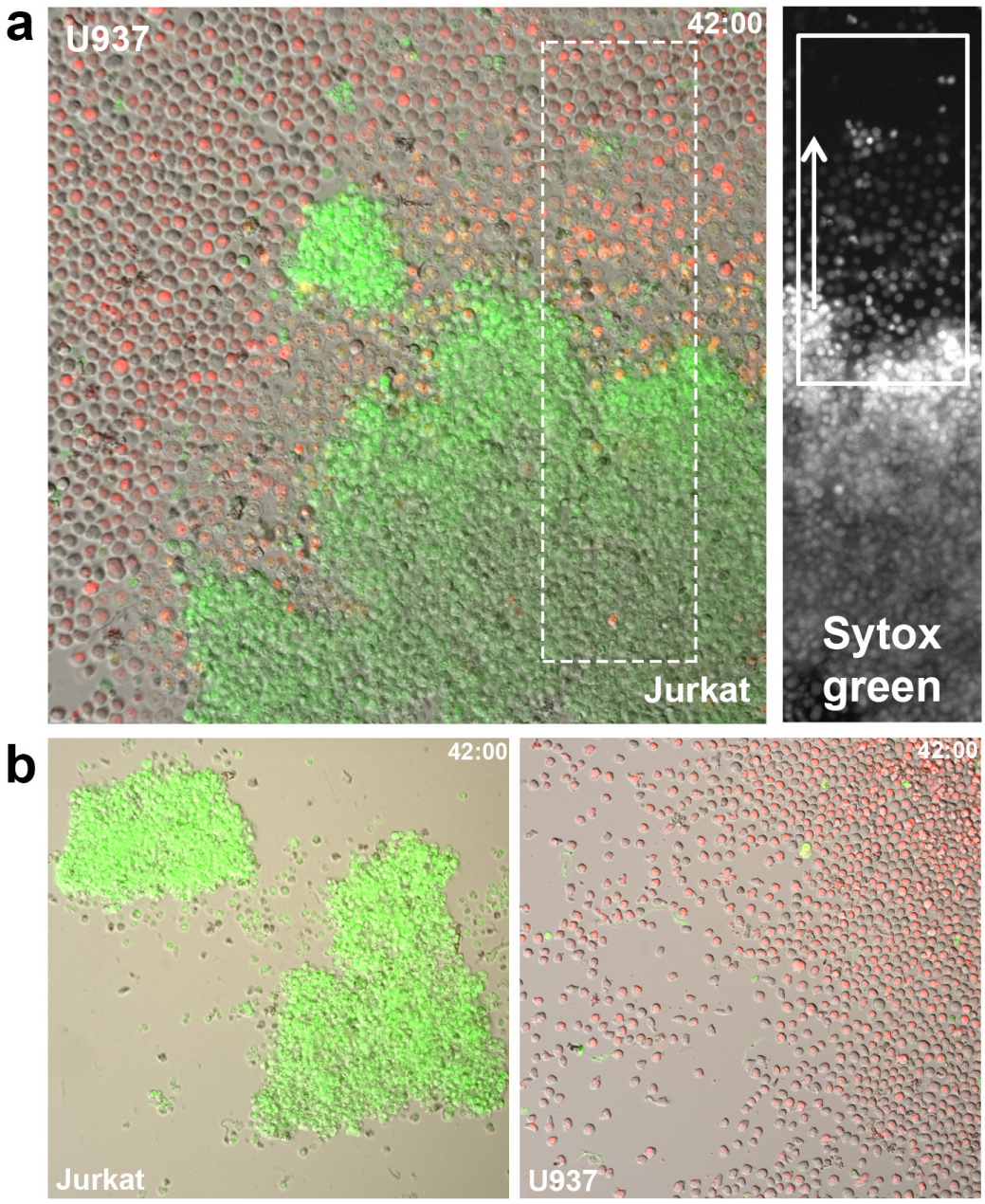

Figure 3.5 Ferroptosis can propagate to pre-conditioned cells in trans.
(A) U937-H2BmCh (red) cells were mixed with Jurkat cells that had been treated 6h prior and followed by timelapse imaging. Image shows cluster of dead Jurkat cells (marked by Sytox Green) surrounded by an expanding circle of dead U937 cells at 42h. Inset (indicated by dashed line) shows Sytox Green fluorescence; arrow indicates direction of death spreading.
(B) Left image shows dead (Sytox Green-positive) Jurkat cells treated at the same time as in A but without mixing with U937 cells. Right image shows U937-H2BmCh cells (red) treated at the same time U937 cells were added to mixed condition.

Together, these results suggested that there is a pro-ferroptotic signal that propagates between pre-conditioned cells to induce death. To further examine the nature of this signal, we asked whether iron and lipid peroxidation, two known drivers of ferroptosis, are required for propagation. We treated HAP1 cells with FAC&BSO and, upon initiation of wave-like ferroptosis, added media containing either liproxstatin-1 or the iron chelator deferoxamine (DFO) to cell cultures. Addition of these inhibitors indeed stopped death from spreading while media containing DMSO did not (Figure 3.6A-D), demonstrating that iron and lipid peroxidation are both required for continuous ferroptosis propagation. This shows that there is no signal that is generated downstream of lipid peroxidation that is sufficient to induce ferroptosis propagation. Because iron and lipid peroxidation are also necessary for ferroptosis to occur in individual cells, these results suggested that the full execution of ferroptosis, including cell lysis, may be required for the spreading of death between cells.

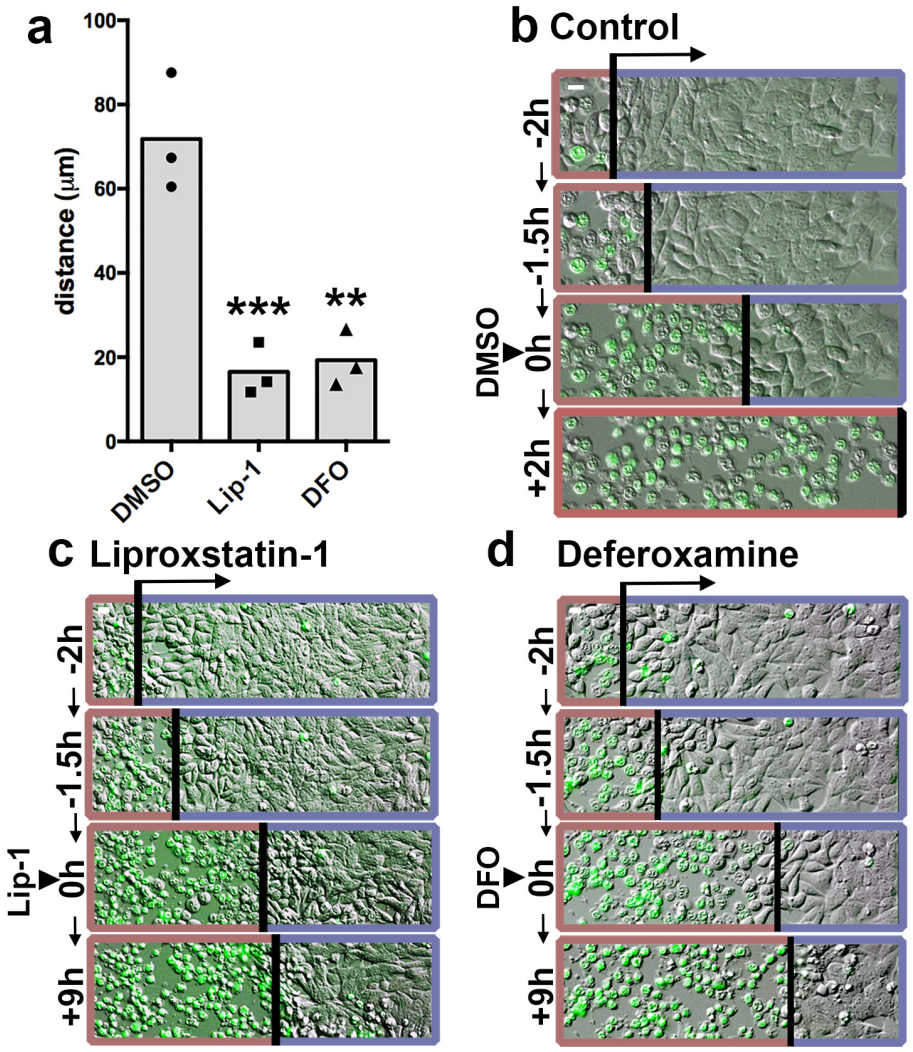

Figure 3.6 Ferroptosis spreading requires lipid peroxidation and iron.

(A) Distance of ferroptosis spreading in HAP1 cells incubated with FAC and BSO, and treated with Liproxstatin-1 (Lip-1), Deferoxamine (DFO), or DMSO control after wave initiation. Distance was quantified 2h after drug addition. N = three independent experiments, averaged across three or four microscopic fields of view per replicate. Dunnett's test; ***p=0.0008, **p=0.001.

(B-D) Representative images from experiments quantified in panel a. Timing of treatment with DMSO (b), Lip-1 (c), or DFO (d) is indicated as 0h. Images show DIC and SYTOX Green fluorescence. Death waves are indicated by an arrow and a red border, live cells are indicated with a blue border on each image. Note Lip-1 and DFO-treated cells are shown 9 hours after treatment (+9h), versus 2 hours after treatment for DMSO (+2h). All scale bars = 10μm.

Figure adapted from Riegman *et al.*, 2020.[206]

Discussion

In this chapter we develop a quantitative method for the analysis of spatiotemporal patterns of cell death from live cell imaging, allowing us to determine whether or not a given pattern of cell death is non-random, as well as how strong the relationship between neighboring cell death events is. This method relies on computationally generated permutations to simulate random death for a given configuration of cells, letting each field of view serve as its own control. This allows us to determine where that experiment falls with respect to the randomly generated distribution of mean time differences between neighboring deaths. When we performed this analysis for several different death-inducing stimuli, we found that almost every treatment we tested resulted in significantly non-random patterns of death in every field of view, the only exceptions being one movie each for HAP1 + ML162 and MCF7 + H_2O_2. This indicates that even in forms of death like TRAIL-induced apoptosis, where we did not expect to see any non-autonomous effects, there is a correlation between the times at which neighboring death events occur. It is possible that all these death types do possess weak non-autonomous properties, with the death of one cell ever so slightly increasing the likelihood of its neighbor dying. A more attractive hypothesis, however, is that as cells that are physically closer to one another also tend to be more closely related, they are more likely to respond to a given death stimulus in a similar manner and timeframe. Support is lent to this model by the work of Spencer et al., who previously showed that sister cells treated with TRAIL have a highly correlated time of death for a period of time after division due to the transient heritability of differences in protein levels.[207] We did

not perform lineage tracing to determine whether correlations in neighboring cell death times are explained by relatedness, but the degree to which genetic and non-genetic heritable factors affect the similarity of cell behavior in response to various cell death stimuli would be an interesting area for further study.

We observed from our spatiotemporal analysis that, while all forms of death tested were largely non-random, this effect appeared much stronger in several types of ferroptosis. In fact, for many of the movies of ferroptosis induced by C' dots, erastin, or FAC and BSO, the experimental mean was smaller than in any of the simulations. In order to more closely compare the spatiotemporal dynamics of these different forms of death, we developed the Spatiotemporal Propagation Index, the difference between $\mu_{perm95\Delta t}$ and $\mu_{exp\Delta t}$ normalized to $\mu_{perm95\Delta t}$. This measure allowed us to assess the degree to which a cell's location relative to its neighbors affected its time of death. The SPI was much higher in most forms of ferroptosis compared to TRAIL-induced apoptosis and H_2O_2-induced necrosis, demonstrating that ferroptotic cells affect each other to a much greater degree. Interestingly, the SPIs of ML162-treated cells were similar to those of apoptotic and necrotic cells, suggesting that direct GPX4 inhibition does not result in ferroptosis propagation. Thus, our method allowed us to distinguish two types of ferroptosis: cell-autonomous or "single-cell ferroptosis" observed in response to GPX4 inhibition, and propagative or "multicellular ferroptosis" that is induced by treatments that inhibit the generation of glutathione (erastin, BSO) and/or increase cellular iron concentrations (FAC, C' dots). Why ferroptosis induced by GPX4 inhibition does not result in death with non-autonomous properties is still unclear. One possibility is that

this difference is due to other functions of glutathione. Glutathione is a major cellular antioxidant and regulates many other processes besides the activity of GPX4 and the detoxification of lipid peroxide species.[208] When glutathione is depleted upon induction of multicellular ferroptosis, the cellular redox balance is completely altered and other glutathione-dependent enzymes are also inactivated, potentially allowing for the unchecked accumulation of many different types of ROS. When GPX4 is chemically inhibited, by contrast, lipid peroxidation is known to occur but glutathione can still perform its other functions. The fact that the addition of liproxstatin-1 interrupts death spreading indicates that lipid peroxidation is continuously required for the propagation of ferroptosis, but the fact that GPX4 inhibition does not trigger propagative death suggests that it is not sufficient. We also investigated the possibility that glutathione sharing between cells might be responsible for the wave-like patterns of death observed during ferroptosis, but this appears not to be the case based on our mixing experiments with suspension cell lines and the fact that elimination of gap junctions does not abrogate wave-like ferroptosis. The nature of the signal responsible for ferroptosis propagation thus remains elusive, and will be an important subject for future studies.

Ferroptosis spreading has previously been suggested to occur in isolated murine renal tubules, which displayed a progressive wave of deformation moving through the tissue upon treatment with erastin.[119] However, whether ferroptosis can also propagate *in vivo* remains unclear. Recent work has linked ferroptosis to cell death in a wide variety of human diseases, from stroke to acute kidney injury. Many of these conditions result in the formation of large continuous zones of necrotic tissue, possibly indicating a

role for ferroptosis propagation in these diseases. Intriguingly, a recent study by Katikaneni *et al.* shows large waves of cellular deformation occurring in intact zebrafish larvae following microperfusion of arachidonic acid (AA).[209] As AA is a known driver of ferroptosis, this paper may provide the first evidence that wave-like propagation of ferroptosis can also occur *in vivo*, causing widespread tissue damage. Interestingly, in both this case and the erastin-treated renal tubules, waves moved much faster than what we have observed in cell culture. This could be due to the much smaller extracellular volume present in these experiments, which could potentially limit the dispersion of a diffusible factor.

Ferroptosis has also been studied quite extensively in the context of tumor suppression. Induction of ferroptosis may be an effective strategy for cancer treatment, as the initiation of a wave of cell death within a tumor may enable the elimination of less sensitive cells that would not die in a cell-autonomous manner. The phenomenon of "fractional killing", in which only a certain fraction of a cell population exposed to a chemotherapeutic agent dies irrespective of the absolute number of cells, is a major obstacle in cancer therapy as a proportion of cells is able to survive the treatment and potentially regrow. In our experiments using *in vitro* cancer models, ferroptosis is remarkable in that it is able to eliminate nearly all cells in a population, reducing the probability of cells surviving long enough to develop resistance. Our results also suggest, however, that GPX4 inhibitors are of limited efficacy in inducing propagation of ferroptosis, and may therefore be less attractive as cancer therapies. Further study is needed to determine whether wave-like death can be induced in solid tumors and how

different ferroptosis-inducing compounds compare as tumor treatments. Uncovering the molecular mechanisms that regulate ferroptosis execution and propagation through cell populations will ultimately further our understanding of how modulators of ferroptosis may be leveraged for therapeutic benefit.

CHAPTER 4: Investigating the mechanism of ferroptotic cell rupture*

Introduction

Ferroptosis is known to require the peroxidation of cell membrane phospholipids, but exactly how this leads to necrotic cell death is still unclear. A recent study showed that oleic acid, a mono-unsaturated lipid that inhibits ferroptosis, suppresses lipid peroxidation in the plasma membrane but not the perinuclear region,[91] raising the possibility that direct membrane damage mediated by lipid ROS might be responsible for ferroptotic cell lysis. One widely accepted hypothesis is that the destruction of phospholipids leads to slight increases in plasma membrane permeability, allowing the influx of ions and water molecules and thereby triggering cell rupture, but there is currently no experimental evidence supporting this model. In addition, computational modeling studies of oxidized membranes have suggested that lipid peroxidation causes membrane deformation and micellization,[104–106,108] leading to eventual plasma membrane destruction, but these studies necessarily rely on a simplified simulation of membrane architecture and composition.

The most well-studied forms of regulated necrosis are pyroptosis and necroptosis, both inflammatory cell death types that occur in response to infection. While ferroptosis is thought to result from the accumulation of cell damage, these death forms are considered cellular suicides and have been shown to be executed by dedicated machinery. Pyroptosis involves the caspase-mediated cleavage of GSDMD,[70,71] resulting in its oligomerization and assembly into pores that permeabilize the plasma

* This chapter is adapted from Riegman *et al.*, 2020.[206]

membrane.[72,73] Similarly, necroptosis has been suggested to involve pore formation mediated by MLKL.[56] In both of these cases, the formation of plasma membrane pores is thought to result in the rapid flux of ions and small molecules into the cell, followed by water, which then triggers cell swelling and lysis. How plasma membrane rupture occurs during other forms of necrosis is still unclear. In this chapter we investigate the mechanism of cell lysis during ferroptosis, and the relationship between cell rupture and cell death propagation.

Results

Ferroptotic cell death is an osmotic process

How ferroptosis is executed downstream of lipid peroxidation is not clearly defined. We noted from time-lapse imaging that ferroptotic cells appeared to round and swell prior to cell death (Figure 4.1A). Like death, cell rounding also spread through cell populations in a manner that was blocked by treatment with liproxstatin-1 or DFO. To further examine this process, we performed confocal imaging on HeLa cells expressing an mKate-tagged version of the zebrafish Cytosolic Phospholipase 2 (cPLA2) enzyme. This protein normally localizes to the nucleoplasm, but translocates to the nuclear envelope upon calcium influx and nuclear membrane stretch caused by osmotic swelling.[199] When we induced ferroptosis using FAC and BSO, cPLA2-mKate indeed formed nuclear rings, indicating that ferroptotic cell death involves osmotic swelling. Furthermore, cPLA2 translocation tended to occur 30 to 60 minutes prior to the appearance of a SYTOX Green signal, demonstrating that swelling and possibly calcium influx occur well before cell rupture (Figure 4.1B).

Osmoprotectants inhibit cell rupture during ferroptosis

Cell swelling is also known to occur during the execution of pyroptosis and necroptosis, both of which involve the formation of pores in the plasma membrane, leading to the influx of extracellular ions and water molecules. Pore formation and size has been studied in many systems through the use of osmoprotectants, large carbohydrates that are added to the cell media to osmotically balance out intracellular contents.[210–213]

When a pore opens up in the plasma membrane, ions and molecules small enough to fit through the pore will diffuse across the membrane along their concentration gradients and thus achieve equilibrium between the intra- and extracellular space. Because the cytosol contains more large molecules than the extracellular environment, this results in a net influx of solvents and water into the cell, eventually causing rupture. Osmoprotectants with a diameter larger than the pore prevent this by increasing the concentration of large molecules outside the cell. Thus, while osmoprotectants of sufficient size do not block plasma membrane permeabilization, pore-mediated ion exchange, or cell death, they prevent osmotic cell lysis and release of large intracellular molecules caused by pore formation.

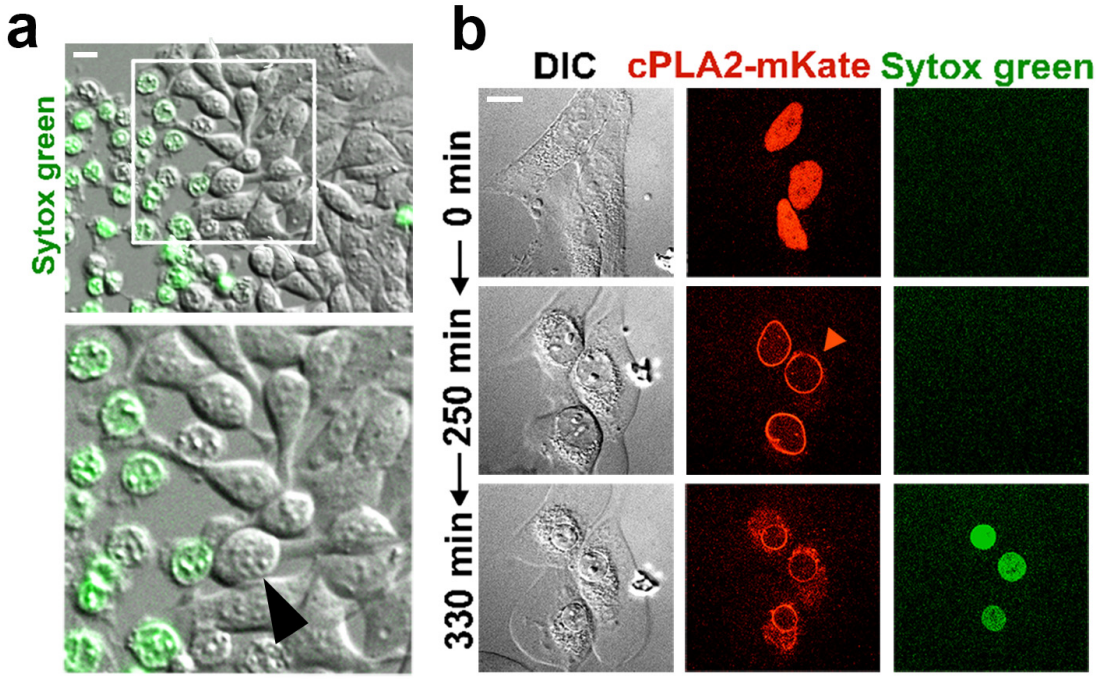

Figure 4.1 Ferroptosis involves osmotic cell swelling.
(A) HAP1 cells treated with FAC and BSO round prior to ferroptotic cell rupture (arrowhead). Images are representative of four independent experiments.
(B) The cell swelling marker cPLA2-mKate translocates to the nuclear envelope (arrowhead) prior to SYTOX Green labeling in HeLa cells treated with FAC and BSO. All scale bars = 10µm.
Figure adapted from Riegman *et al.*, 2020.[206]

To test whether ferroptosis might involve the formation of plasma membrane pores, we treated HeLa cells with FAC and BSO in the presence of 20mM sucrose, raffinose, or polyethylene glycols (PEGs) with molecular weights of 1450 or 3350 Da, and assessed the extent of cell lysis by measuring the release of lactate dehydrogenase (LDH). LDH release was inhibited by the addition of PEG1450 and PEG3350, but not by the smaller molecules sucrose and raffinose (Figure 4.2A). PEG1450 and PEG3350 also reduced the translocation of cPLA2-mKate to the nuclear envelope (Figure 4.2B), suggesting that swelling and cell rupture during ferroptosis may be caused by the opening of nano-scale pores in the plasma membrane. By contrast, none of the four tested osmoprotectants affected LDH release by HeLa cells treated with hydrogen peroxide, demonstrating that pore formation is not a general feature of necrotic cell death (Figure 4.2C).

We then asked whether pore formation occurs in other contexts, and treated HAP1 and HT1080 cells with several different ferroptosis inducers. Induction of ferroptosis with erastin or the GPX4 inhibitors RSL3 and ML162 likewise resulted in cell rupture that was inhibited by treatment with PEG1450 and PEG3350 but not sucrose and raffinose (Figure 4.2D,E). As we observed in HeLa cells, H_2O_2-induced LDH release was not affected by osmoprotectant treatment in HT1080 cells. These results suggest that pore formation occurs downstream of GPX4 inactivation, as direct inhibition of GPX4 resulted in rupture that could be inhibited with large osmoprotectants.

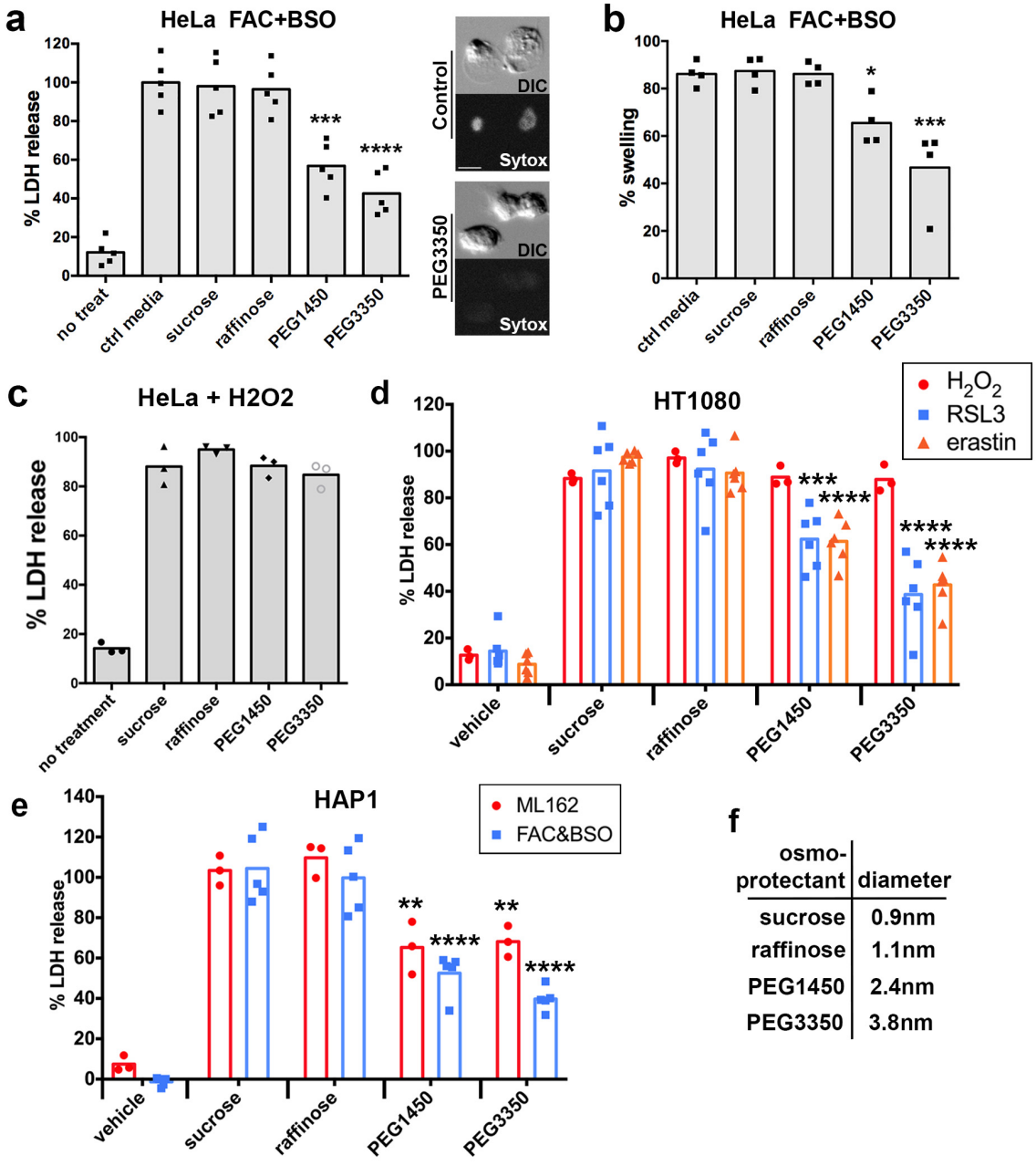

Figure 4.2 Ferroptotic cell rupture is inhibited by osmoprotectants.

(A) Percent LDH released from HeLa cells treated with FAC and BSO and the indicated osmoprotectants. Images show DIC and Sytox Green for Hela cells treated with FAC + BSO with or without PEG3350. Scale bar = 10μm. N=5 biologically independent experiments. Dunnett's test; ***p=0.0001, ****p=0.0001.

(B) Swelling of ferroptotic HeLa cells treated with FAC and BSO as measured by recruitment of cPLA2-mKate to the nuclear envelope, determined by time-lapse microscopy. N=4 biologically independent experiments. Dunnett's test; *p=0.0318, ***p=0.0002.

(C) LDH release by HeLa cells treated with H_2O_2 and the indicated osmoprotectants, relative to HeLa cells treated with H_2O_2 only. N=3 biologically independent experiments.

(D, E) LDH release in HT1080 cells treated with H_2O_2, RSL3, or erastin and HAP1 cells treated with ML162 or FAC and BSO and osmoprotectants, relative to treatment alone. N=6 (RSL3, erastin), 3 (H_2O_2, ML162), or 5 (FAC + BSO) independent experiments. Dunnett's test; **p<0.01, ***p<0.001, ****p<0.0001.

(F) Diameters of osmoprotectants. Figure adapted from Riegman *et al.*, 2020.[206]

Investigating the mechanism of ferroptotic pore formation

Given the similarity between our results and those previously seen in pyroptosis,[214] and as there is known to be substantial crosstalk between cell death pathways, we wanted to ascertain whether known pore-forming proteins are activated during ferroptosis. During pyroptosis, activated caspase-1 cleaves Gasdermin D and releases its N-terminal domain, allowing it to form pores in the plasma membrane. In necroptosis, phosphorylation of MLKL enables its insertion into the membrane. To test the involvement of these two pathways we induced ferroptosis with FAC and BSO in the presence of the pan-caspase inhibitor z-VAD-fmk or the MLKL blocker necrosulfonamide. Neither of these compounds affected LDH release by ferroptotic cells (Figure 4.3A), indicating that caspase and MLKL activity are not required for cell lysis during ferroptosis. While this experiment does not completely rule out a role for GSDMD in ferroptosis, as it may be cleaved by enzymes other than caspases, it suggests that it is unlikely ferroptotic pores are formed by these proteins. It is conceivable that ferroptotic pores may not be protein-based at all, as a modeling study previously suggested that lipid peroxidation and subsequent breakdown of peroxides to aldehydes may be able to generate lipid membrane pores.[108] To test whether lipid peroxidation is sufficient to induce pore formation, we used tert-butyl hydroperoxide (tBH), an organic peroxide that has been reported to induce lipid peroxidation and ferroptosis.[215] We confirmed that tBH treatment resulted in ferroptosis in HT1080 cells by co-treating cells with tBH and several different ferroptosis inhibitors (Figure 4.3B). Similar to our results with other ferroptosis inducers, LDH release by tBH-treated cells was inhibited by

incubation with PEG1450 and PEG3350, but not by sucrose and raffinose (Figure 4.3C). This indicates that direct induction of lipid peroxidation is sufficient to cause pore formation during ferroptosis.

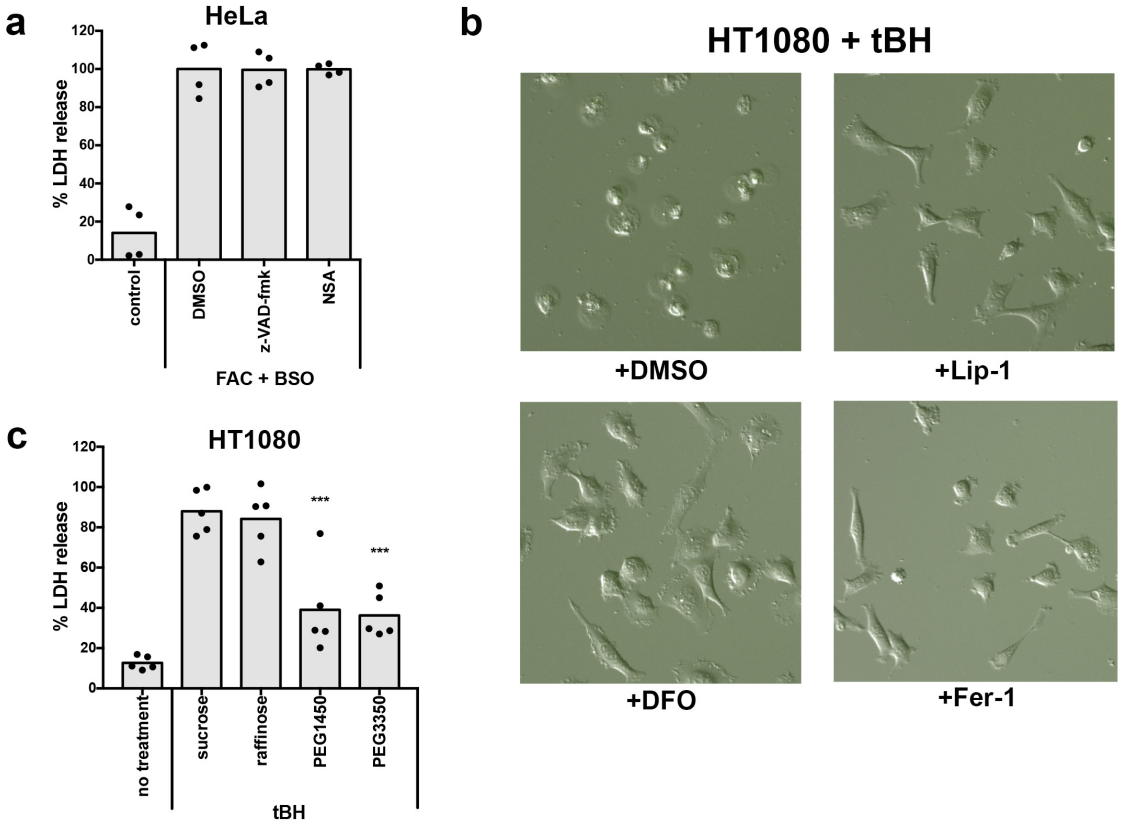

Figure 4.3 Pore formation occurs downstream of lipid peroxidation and is not mediated by caspase activity or MLKL.

(A) Percent LDH released by HeLa cells treated with FAC + BSO and DMSO, 20μM z-VAD-fmk, or 1μM necrosulfonamide (NSA), relative to DMSO control. No statistically significant differences observed by Dunnett's multiple comparisons test.

(B) Images of HT1080 cells treated with 50μM tert-butyl hydroperoxide (tBH) and DMSO or the indicated ferroptosis inhibitors for 12h. The lipophilic antioxidants liproxstatin-1 (Lip-1) and ferrostatin-1 (Fer-1) and the iron chelator deferoxamine (DFO) rescue viability after tBH treatment, indicating that tBH induces ferroptosis in HT1080 cells.

(C) Percent LDH released by HT1080 cells treated with 50μM tBH and 20mM of the indicated osmoprotectants for 12h, relative to tBH in control media without osmoprotectants. Dunnett's multiple comparisons test; ***p=0.0004 for PEG1450, ***p=0.0002 for PEG3350.

The effect of cell rupture inhibition on ferroptosis propagation

As ferroptotic cell rupture could be inhibited using osmoprotectants, we next sought to examine whether cell lysis is required for ferroptosis propagation. When HAP1 cells were treated with FAC and BSO in the presence of the osmoprotectant PEG1450, we observed waves of cell rounding that spread through cell colonies and appeared similar to waves of cell death. Cells that had rounded stopped moving and appeared dead; however, SYTOX uptake was reduced and delayed in the presence of PEG1450, consistent with the inhibition of cell rupture, and could consequently not be used to analyze wave-like behavior in osmoprotected cells. To quantify these waves, we therefore expressed a fluorescent sensor of nuclear calcium (GCaMP6-NLS) in HAP1 cells, reasoning that plasma membrane pore formation might lead to a spike in intracellular calcium levels that could be used as a readout of cell permeabilization. Live imaging of unprotected ferroptotic cells expressing this sensor demonstrated that GCaMP fluorescence indeed increased 15-30 minutes prior to the uptake of SYTOX, and that GCaMP signals spread through cell populations in a wave-like manner, similar to SYTOX and cell rounding (Figure 4.4A). After rupture and the appearance of SYTOX fluorescence the GCaMP signal rapidly disappeared, most likely due to the diffusion of GCaMP protein out of lysed cells. We compared the relative timing of GCaMP and SYTOX fluorescence for individual cells and found a high degree of correlation, indicating that GCaMP signals could be used instead of SYTOX uptake to assess wave-like behavior (Figure 4.4B). When cells were co-treated with PEG1450 to inhibit rupture, wave-like spreading of GCaMP fluorescence still occurred (Figure 4.4C) and persisted much longer,

even after the delayed SYTOX signal had appeared, indicating the protein was retained inside the cell and intracellular calcium levels remained high. We quantitatively examined the spatiotemporal patterns of GCaMP signals, and found them to be significantly non-random in both ruptured and unruptured cells (Figure 4.4D). Furthermore, the Spatial Propagation Index values were similar in the presence and absence of osmoprotectants (Figure 4.4E), demonstrating that cell rupture is not required for ferroptosis propagation in HAP1 cells.

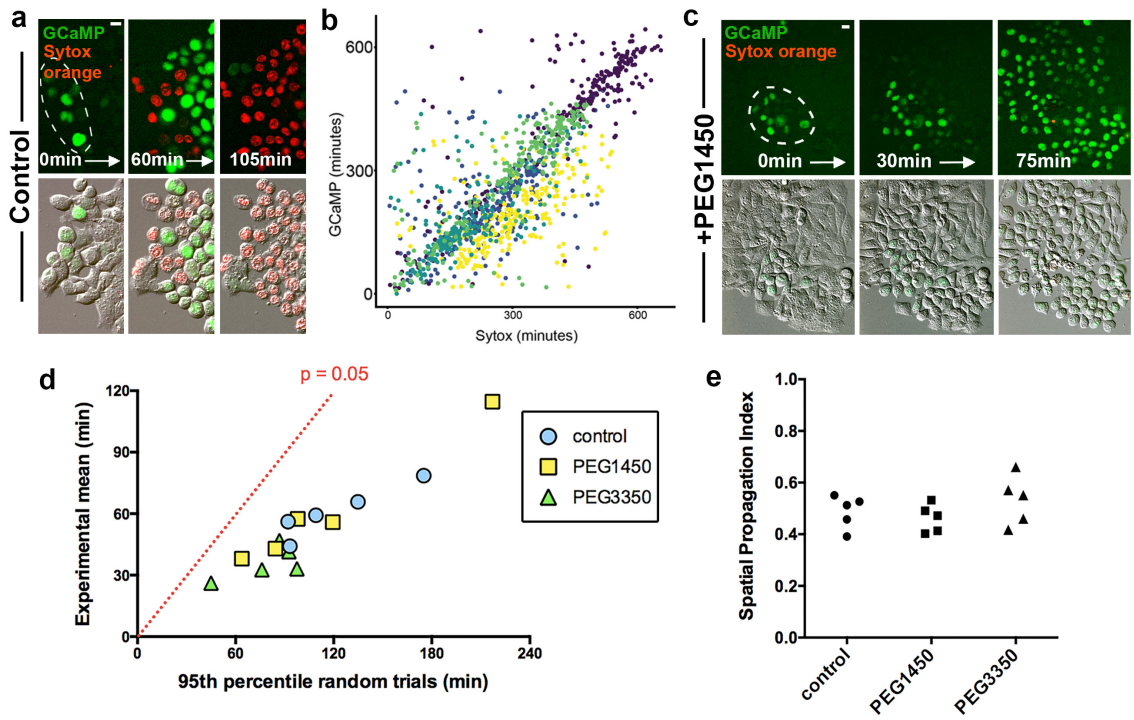

Figure 4.4 Ferroptosis spreading can be read out by calcium influx and does not require cell rupture.
(A) Images show spreading of GCaMP fluorescence (green) prior to cell rupture marked by SYTOX Orange (red) in HAP1 cells treated with FAC and BSO. Dashed circles show origin of death spreading.
(B) Correlation between relative timing of GCaMP fluorescence and SYTOX labeling in HAP1 cells treated with FAC and BSO. Each dot represents a cell and each color represents a different field of view.
(C) Images show spreading of GCaMP fluorescence (green) and SYTOX Orange (red) in HAP1 cells treated with FAC and BSO and PEG1450. Dashed circles show origin of death spreading.
(D) Graph showing $\mu_{exp\Delta t}$ vs. $\mu_{perm95\Delta t}$ of movies of HAP1 cells treated with FAC and BSO and the indicated osmoprotectants, analyzed using GCaMP fluorescence. Dashed line indicates $\mu_{exp\Delta t} = \mu_{perm95\Delta t}$; experimental means below the line are significant with $p<0.05$.
(E) Spatial Propagation Index calculated for experiments shown in panel D. All scale bars = 10μm.
Figure adapted from Riegman *et al.*, 2020.[206]

While treatment with osmoprotectants did not prevent propagation, we wondered whether it could affect wave speed. To test this we used U937 cells, which exhibit long-lived, unidirectional waves of ferroptotic cell death that can be imaged by differential interference contrast (DIC) microscopy even in the absence of SYTOX staining (Figure 4.5A), enabling easy identification of the wave front. Treatment of U937 cells with PEG3350 inhibited cell lysis (Figure 4.5B) yet had no effect on the induction of cell death waves, consistent with our HAP1 data. We then measured the speed of these waves in the presence and absence of PEG3350. Starting from a point at which any smaller, initial areas of death had converged into a larger wave, we measured the distance traveled by the wave front over time to calculate propagation speed. We found ferroptosis waves to be slightly but significantly slower in the presence of PEG3350 (1.66 vs. 1.37 μm/min, see Figure 4.5C), demonstrating that ferroptosis propagation is faster when cells are able to fully lyse.

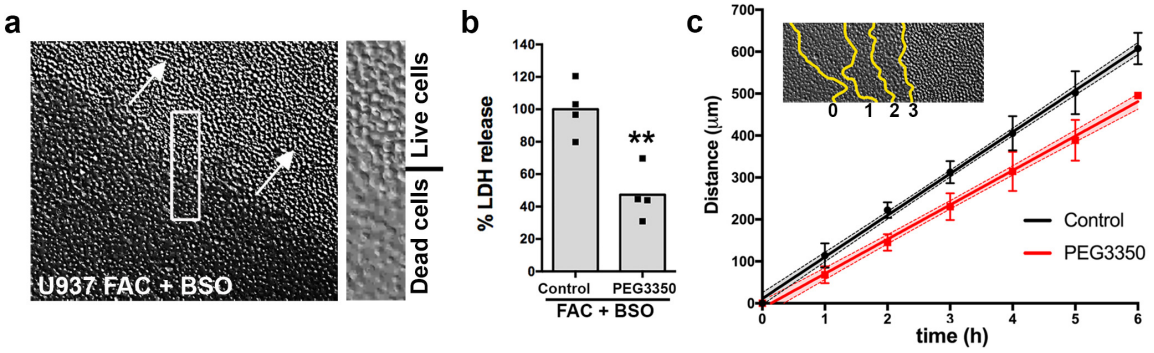

Figure 4.5 PEG3350 slows ferroptosis propagation.
(A) Wave-like spreading of ferroptosis in U937 cells treated with FAC+BSO, imaged by DIC. Arrows indicate direction of wave spreading; inset shows boundary between live and dead cells. Scale bar = 10μm
(B) Percent LDH release in U937 cells treated with FAC+BSO in control and PEG3350-treated conditions. N = 4 independent experiments. **p=0.004 and was obtained using a two-sided t-test.
(C) Wave-like spreading of ferroptosis is slower in the presence of PEG3350. Inset shows a representative example of death progression at each time point indicated by yellow lines. Graph shows distance over time of wave spreading in U937 cells treated with FAC and BSO. Data shown as mean ± SD; line shows linear regression and its 95% confidence interval (shaded regions). Scale bar = 25μm.
Figure adapted from Riegman *et al.*, 2020.[206]

Discussion

In this chapter we show that ferroptosis is an osmotic process that involves cell swelling and calcium influx, and discover that ferroptotic plasma membrane permeabilization is mediated by pore formation, contradicting the prevailing view that ferroptosis is caused by slight increases in membrane permeability due to the destruction of PUFA-containing phospholipids. Based on the fact that sucrose and raffinose do not inhibit ferroptotic lysis, suggesting these molecules are small enough to pass through the pores, whereas PEG1450 and PEG3350 do offer protection, we would estimate the size of ferroptotic pores to be 1 to 2nm in diameter. However, identical results were previously observed in osmoprotectant experiments in pyroptosis,[214] which was later discovered to be mediated by GSDMD. Electron microscopy of GSDMD pores indicated that they were much larger than expected, with an average inner diameter of 10-14nm.[73] This discrepancy has not been conclusively explained, but could be due to the fact that PEGs can aggregate with serum proteins found in cell culture media, potentially forming much larger osmoprotective complexes and leading to an underestimation of pore size. Thus, it is possible that ferroptosis pores are also substantially larger. It is clear, however, that while osmoprotectants may not be able to accurately determine pore size in live cells, they do reliably indicate the existence of pore-like structures in the plasma membrane.

The similarity of the results observed in ferroptosis and pyroptosis is intriguing and raises the possibility that they are mediated by similar proteins. Our results suggest it is unlikely that GSDMD controls ferroptotic pore formation. However, the gasdermin protein family includes five additional members, four of which have a similar structure

to GSDMD, with an N-terminal pore-forming domain linked to an inhibitory C-terminal domain.[73] One of these, GSDME (also known as DFNA5), is known to be cleaved by caspase-3 and has been suggested to form pores during secondary necrosis,[216] cell rupture that occurs when apoptotic cells are allowed to persist instead of undergoing efferocytosis. Whether any of the other gasdermin proteins could be involved in ferroptosis remains to be determined.

The pores formed during ferroptosis need not necessarily be protein-based, however. Lipid peroxidation is known to lead to conformational changes in the plasma membrane, disrupting its normal architecture. Analyses that computationally model the effect of lipid ROS on membrane behavior have suggested that extensive peroxidation may lead to membrane micellization or even the formation of stable water pores.[104,107,108] It should be noted, however, that most of these studies rely on simulated lipid bilayers composed entirely of one type of phospholipid molecule and with peroxidation levels of up to 100%, while peroxidation during ferroptosis is thought to range from 0.1-1% based on lipidomics studies. It is also possible that lipid peroxidation leads to the damage or destruction of hypothetical nanodomains of clustered PUFA-containing phospholipids, thereby generating holes in the plasma membrane.

Pore formation could regulate not only cell death execution, but could also be involved in the propagation of ferroptotic cell death. We show here that inhibition of cell rupture does not prevent wave-like spreading of cell death, demonstrating that propagation occurs upstream of cell lysis. However, wave speed is slightly slower in the presence of osmoprotectants, suggesting that cell rupture accelerates the transmission

of a death-inducing signal between cells. It is possible that the act of lysis generates force or vesicles that allow for more efficient transfer, but as osmoprotectants do not block pore formation, one other possibility is that the signal responsible for ferroptosis is able to diffuse through plasma membrane pores. When rupture is inhibited, diffusion is slowed down, and wave propagation is therefore slower as well. Ferroptotic pore formation could also be involved in the potential release of pro-inflammatory cytokines or damage-associated molecular patterns (DAMPs), which is known to occur during pyroptosis. We previously observed immune activation in response to ferroptosis induction in tumor xenografts. It will be interesting to determine in future studies whether pore formation contributes to cell death propagation or ferroptotic immunogenicity.

CHAPTER 5: Discussion

Summary

In this study we develop an approach for quantifying the population dynamics of cell death, and use it to demonstrate that ferroptosis occurs with different spatiotemporal patterns depending on the method of induction. Several forms of ferroptosis result in highly non-random patterns of death that demonstrate evidence of propagation, unlike TRAIL-induced apoptosis and hydrogen peroxide-induced necrosis, but this is not the case when ferroptosis is triggered by direct inhibition of GPX4. We further find that ferroptotic lysis can be inhibited by osmoprotectants larger than ~2nm in diameter, demonstrating that ferroptosis is an osmotic process mediated by the formation of pores in the plasma membrane. We show that lipid peroxidation is sufficient to induce pore formation but not propagation, and that wave-like spreading of ferroptosis occurs independently of cell rupture.

These results are consistent with a model wherein induction of ferroptosis and subsequent lipid peroxidation leads to the formation of pores in the plasma membrane (Figure 5.1). Ions and small molecules diffuse through these pores along their concentration gradients whereas large molecules are trapped predominantly inside the cell, causing a net influx of solutes into the cell and an increase in cytoplasmic osmolarity. This in turn prompts water influx and cell swelling, eventually leading to membrane rupture and the release of cytoplasmic contents. When ferroptosis is induced by treatments that inhibit glutathione synthesis and/or increase cellular iron levels, ferroptotic cells release a signal that contributes to death in neighboring cells,

thereby causing a domino-like propagation of cell death. This signal is released upstream of cell rupture and requires both iron and lipid peroxidation to spread between cells.

This work thus allows us to distinguish two different types of ferroptosis: cell-autonomous or "single-cell ferroptosis" observed in response to GPX4 inhibition, and propagative or "multicellular ferroptosis" that is induced by treatments that inhibit the generation of glutathione and/or increase cellular iron concentrations. Our finding that there is a ferroptosis pore also contradicts the prevailing view that ferroptosis is caused by the unregulated accumulation of cellular damage. Both of these discoveries further our understanding of the basic biology of ferroptosis and the role it may play in therapy and disease. This chapter will discuss some of the implications of this work and its contributions to the emerging field of cell death population dynamics.

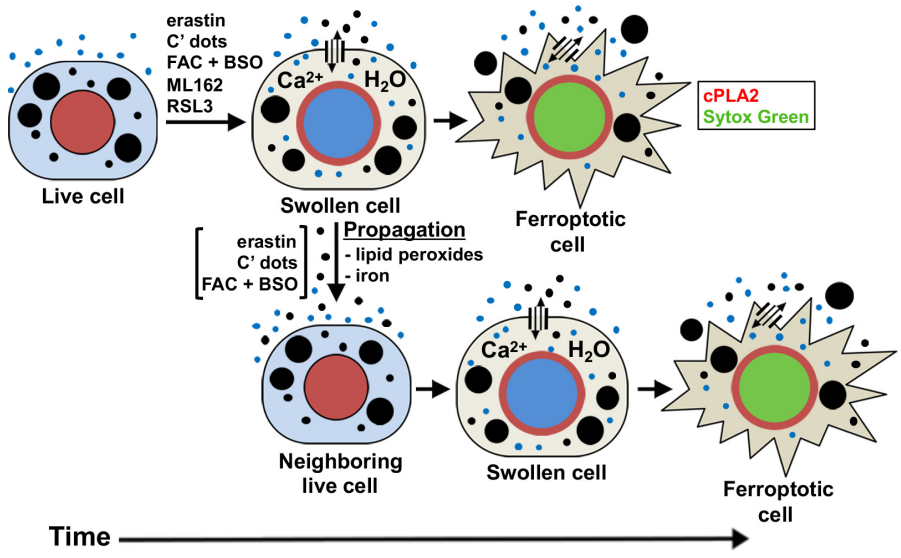

Figure 5.1 Model for osmotic regulation and propagation of ferroptosis.
Ferroptosis involves opening of plasma membrane pores that allow for solute exchange with the external environment, leading to cell swelling and cPLA2 translocation to the nuclear membrane (red). Ferroptotic cells then undergo rupture and death marked by the rapid influx of Sytox Green. When ferroptosis is induced by treatment with erastin, C' dots, or FAC and BSO, but not by treatment with the GPX4 inhibitor ML162, death propagates to neighboring cells in an iron and lipid peroxide-dependent manner, through a signal that is sent independently of cell rupture. Figure adapted from Riegman *et al.*, 2020.[206]

Implications and Future Perspectives

Ferroptosis – Suicide or Sabotage?

As the number of distinct cell death types has expanded over the last twenty years, the morphology-based classification system of yore has given way to a new set of definitions that distinguishes between programmed, regulated, and accidental cell death.[21] Accidental deaths are those caused by extreme and immediate stresses to the cell, such as mechanical damage or exposure to detergents. Regulated cell death, on the other hand, can be prevented or modulated by genetic or pharmacological means, and encompasses two subcategories; cell suicide and cell sabotage.[217,218] Cell suicides, also known as programmed cell death types, are actively controlled by dedicated pro-death machinery and participate in development and homeostasis, thus providing a benefit to the organism. Apoptosis, necroptosis, and pyroptosis are all forms of cellular suicide. By contrast, cell sabotage results from the disruption of essential metabolic processes within the cell. The cell contributes to its own demise by continuing its normal activity in this abnormal context, but there is no involvement of specific death executing proteins. Recognized examples of cell sabotage include parthanatos, mitotic catastrophe, and ferroptosis.

Based on current understanding, ferroptosis appears to be a metabolic vulnerability that is a consequence of the presence of PUFAs in cell membranes. There is no evidence for a dedicated ferroptosis-executing pathway. Indeed, most of the proteins that have been discovered to be involved in ferroptosis, including system x_c^-, GPX4, and FSP1, negatively regulate the death process. The main positive regulator that

has been identified, ACSL4, which contributes to the esterification of PUFAs into phospholipids, has a clear metabolic function that provides other benefits to the cell and is therefore unlikely to be a dedicated death protein. During ferroptosis, the cell participates in its own death through the continuous generation of lipid peroxides as a byproduct of normal metabolism or other enzymatic activities (e.g. lipoxygenases), but this only causes death if the normal process of lipid repair by GPX4 becomes inactivated. Ferroptosis thus has all the symptoms of cell sabotage. Furthermore, *in vivo* ferroptosis seems to mainly occur during pathophysiological processes such as acute kidney injury or stroke, which involve extensive tissue damage and are often lethal. It is unlikely that the occurrence of ferroptosis benefits the organism in some way in these situations.

However, recent evidence has provided some support for the view that ferroptosis may sometimes be induced "intentionally". Several tumor suppressors, including p53 and BAP1, have been shown to be able to engage ferroptosis by repressing the transcription of *SLC7A11*,[126,127] which encodes part of the system x_c^- antiporter. Furthermore, IFNγ secretion by CD8+ T cells may contribute to the anti-tumor immune response, also by downregulating *SLC7A11* expression.[130] The notion that cells may essentially be able to trigger sabotage in a "programmed" manner is an intriguing one, and raises the possibility that some of these forms of death may have been evolutionarily selected for, rather than having inadvertently persisted. What might be the benefit of ferroptosis induction compared to more orderly processes such as apoptosis and pyroptosis is unclear at present, and awaits further investigation. One possibility is the relative simplicity of the ferroptotic pathway.[217] Most forms of

programmed cell death involve a complex choreography of protein-protein interactions that is vulnerable to disruption by selfish actors such as viruses or malignant cells at many points. By contrast, ferroptosis proceeds along a straightforward biochemical pathway: a lack of cysteine leads to glutathione depletion and inactivation of GPX4, allowing the accumulation of lethal levels of lipid peroxides. It is notable that cysteine appears to be unique in that its absence leads to the induction of necrotic death, whereas the withdrawal of other amino acids such as glutamine and leucine tends to trigger apoptosis.[219,220] In the context of tumor suppression, where genetically encoded cell death mechanisms may have already been neutralized, perhaps it is beneficial to have a relatively crude but possibly more robust road to death as a backup mechanism. In this setting the propagative nature of ferroptosis could also be a potential boon, eliminating any surrounding cells that may have also entered the early stages of tumorigenesis.

In this dissertation, I have provided evidence that ferroptosis involves the formation of plasma membrane pores of specific size. Pore formation is a very common mechanism of cell death execution, being known to occur during pyroptosis (GSDMD),[72,73] necroptosis (MLKL),[56] apoptosis (Bax/Bak),[39] secondary necrosis (GSDME),[216] and mitochondrial permeability transition (MPT)-driven necrosis (unknown).[221] Furthermore, many bacteria encode pore-forming toxins that mat be able to lyse host cells.[222] All of these examples involve protein-based pores (although the identity of the MPT pore remains elusive). If a similar dedicated pore-forming protein exists for ferroptosis this could be the first evidence that ferroptosis is more than simply

cell sabotage. However, as it has been hypothesized that lipid peroxidation may be able to lead directly to the formation of a lipid-based pore, this evidence is not sufficient to conclude that ferroptotic death is programmed. Ferroptotic pores could also be formed by proteins with other cellular functions such as pannexin channels that are opened by changes in membrane properties. Ultimately, more work is needed to elucidate the mechanisms underlying pore formation during ferroptosis.

Cell Death Population Dynamics

The emerging field of cell death population dynamics examines how populations of cells respond to different death-inducing stimuli, and how different death events impact the populations in which they occur. As discussed in Chapter 1, population-scale death is seen in a variety of biological systems, but the mechanisms underlying these phenomena are not well characterized. In some instances, these deaths may simply involve the priming of large groups of cells for elimination through e.g. hormone signaling, resulting in synchronous death that involves little to no communication between dying cells. In other cases, there is clear evidence of death propagation, but the mechanism by which this happens is unclear. In addition to propagation, several other population-intrinsic effects of cell death exist. For example, cell competition, in which cells benefit from the deaths of their neighbors rather than being damaged or killed, can be mediated by cell death. Apoptosis can be initiated in developing tissues to eliminate cells that are deemed less fit than their neighbors. These deaths then support the proliferation of neighboring cells, an effect called compensatory proliferation.

Another death mechanism that can mediate competitive interactions in cancer cell populations is entosis, through which cells compete to ingest and kill each other, and in which direct nutrient transfer from loser to winner cells enables compensatory proliferation.[141,223] Thus the types of cell death that occur in stressed tissues and their effects on local cell interactions or the release of secreted factors may dictate distinct population-scale effects.

There has been a recent surge in research on the heterogeneity of cell death responses among isogenic cell populations,[224] especially with a view to investigating the phenomenon of "fractional killing" of cancer cells during chemotherapy. For example, variability in responses to TRAIL was shown to be due to differences in the levels of several pro-apoptotic proteins acting upstream of MOMP.[207] While these differences were non-genetic and only transiently heritable, they were large enough to allow some cells in the clonal population to survive the treatment entirely. Another study determined that the speed and extent of increases in p53 expression following cisplatin treatment decided cell fate, with cell-to-cell variability in p53 dynamics giving rise to fractional killing.[225] Further heterogeneity in cell fate also exists in the choice of cell death pathway. For example, we have shown previously that cell populations experiencing long-term stress (e.g. nutrient starvation) exhibit mixed cell responses involving apoptosis, necrosis and entosis, occurring simultaneously but at different frequencies in the population.[141] Mixed cell death phenotypes are also observed in clinical specimens[151] and during developmental cell death, such as during interdigitation.[226] Meanwhile, other work has focused on the development of methods

to quantify cell death kinetics[227,228] and the application of those methods to study phenotypic heterogeneity and fractional killing in response to a large variety of lethal stimuli.[229]

Here we develop a method that permits the study of not only the kinetics but also the spatial properties of different forms of cell death. We quantitatively show that neighboring cell relationships are stronger during ferroptosis than during other forms of cell death, indicating that this death form has propagative properties. While we do not test it here, this method would also be predicted to work for the study of the opposite phenomenon, where dying cells transmit protective signals to their neighbors and surrounding cells are therefore less likely to die in response to a given stimulus. This method can thus be applied to investigate different types of non-autonomous properties of a variety of different types of cell death. Whether any other forms of regulated necrosis are able to influence neighboring cells remains unclear. Interestingly, pyroptotic cells have been shown to release ASC specks that may then be taken up by neighboring cells.[173,174] Whether this results in propagation of cell death is not known, however. The application of spatiotemporal cell death analyses such as the one described here could help address this question.

Single-Cell vs. Multi-Cellular Ferroptosis

In this dissertation we show that ferroptosis can occur with wave-like spatiotemporal dynamics, but only when induced by treatments that inhibit glutathione synthesis or increase cellular iron levels. Thus we distinguish between propagative and cell-

autonomous ferroptosis, which are both marked by GPX4 inactivation and lipid peroxidation, but only propagative ferroptosis involves the depletion of glutathione. It is unclear at present what accounts for these distinct phenotypes, but given the profoundly different effects these two types of ferroptosis have on their environments there are likely to be significant mechanistic differences between them. In future studies, whether investigating cell death dynamics or the molecular mechanisms of ferroptosis, it will be important to account for this observation.

Ferroptosis has been implicated in cell death occurring during ischemia-reperfusion (I/R) both *in vitro* and *in vivo*, as iron chelators and lipophilic antioxidants were able to reduce tissue damage in experimental models.[119,120,169] Interestingly, I/R often results in the formation of large, continuous zones of necrotic tissue, raising the possibility that propagation of ferroptosis contributes to the manifestation of these diseases. The mechanisms of ferroptosis induction during I/R are still somewhat unclear, but most of the damage is thought to occur during the reperfusion phase, when the return of oxygen- and iron-carrying blood to the tissue generates a burst of ROS formation that results in oxidative damage, including lipid peroxidation.[230] In combination with a temporary depletion of cystine due to ischemia this could lead to a drop in glutathione levels, consistent with the induction of multicellular, propagative ferroptosis.

In discussing mechanisms underlying the propagation of cell death, it may be interesting to also consider what factors could inhibit death spreading, and whether boundaries exist that may be able to limit tissue damage caused by cell death waves. It

is conceivable that metabolic stress in tumors, resulting for example from nutrient deprivation and reduced glutathione synthesis, could render cancer cells more susceptible to ferroptosis than normal cells. In this case normal tissue could present a natural boundary to ferroptosis waves initiated in cancerous lesions, as our results suggest that death is able to spread only to cells that have been sensitized to ferroptosis, most likely through disruption of cellular antioxidant defenses. It is also possible that cells surrounding an expanding region of cell death could upregulate pathways that promote cell survival, as is known to occur in plants, where death spreading in response to pathogen infection is limited by the induction of autophagy as a protective mechanism in adjacent cells.[231] Understanding how death spreading can be inhibited may ultimately prove to be of therapeutic benefit to reduce toxicity to normal tissues during cancer therapy, or for the treatment of degenerative conditions where ferroptosis is thought to play a role in disease pathology, such as stroke or myocardial infarction.

Concluding Remarks

In this dissertation we investigate the spatiotemporal dynamics of ferroptosis, a recently discovered form of necrosis that has been implicated in a variety of human diseases, from cancer to neurodegenerative conditions. Previous studies have suggested that ferroptosis may have the unusual ability to spread between cells, resulting in wave-like patterns of death that can eliminate entire cell populations. This type of propagative activity could play a significant role in disease, but has not yet been systematically investigated and compared to other forms of cell death. Here we develop a computational approach to quantitatively study ferroptotic cell death patterns and use it to make important discoveries about the fundamental biology of ferroptosis. We show that particular forms of ferroptosis have the ability to spread between cells, and uncover some of the mechanisms regulating this process. Our research identifies a new aspect of ferroptosis that may play an important role in the development of degenerative diseases or inform the design of new cancer therapies, and makes a significant contribution to the emerging field of cell death population dynamics by developing a methodology for studying the dynamics and non-autonomous properties of other cell death forms.

We further discover that cell rupture during ferroptosis is mediated by the opening of pores in the plasma membrane, in contrast to the prevailing view that ferroptosis stems from the unregulated accumulation of cellular damage. Similar results were previously observed in pyroptosis, which is now known to be executed by the caspase-dependent formation of Gasdermin D pores. Whether ferroptosis is also

regulated by a protein pore will be an important area for further study, but if so it is possible that ferroptosis may have a more programmed nature than previously thought. Future studies will be needed to provide further insight into the mechanisms and physiological importance of ferroptotic propagation and pore formation, as well as the roles they play in disease.

References

1. Arandjelovic, S. & Ravichandran, K. S. Phagocytosis of apoptotic cells in homeostasis. *Nat. Immunol.* **16**, 907–917 (2015).
2. Jacobson, M. D., Weil, M. & Raff, M. C. Programmed cell death in animal development. *Cell* **88**, 347–354 (1997).
3. Vogt, C. Untersuchungen über die Entwicklungsgeschichte der Geburtshelferkröte (Alytes obstetricans). (1842).
4. Clarke, P. G. H. & Clarke, S. Nineteenth century research on naturally occurring cell death and related phenomena. *Anat. Embryol. (Berl).* **193**, 81–99 (1996).
5. Glücksmann, A. Cell deaths in normal vertebrate ontogeny. *Biol. Rev.* **26**, 59–86 (1951).
6. Lockshin, R. A. & Williams, C. M. Programmed Cell Death-II. Endocrine potentiation of the breakdown of the intersegmental muscles of silkmoths. *J. Insect Physiol.* **10**, 643–649 (1964).
7. Kerr, J. F. R., Wyllie, A. H. & Currie, A. R. Apoptosis: A basic biological phenomenon with wide-ranging implications in tissue kinetics. *Br. J. Cancer* **26**, 239–257 (1972).
8. Sulston, J. E. & Horvitz, H. R. Post-embryonic cell lineages of the nematode, Caenorhabditis elegans. *Dev. Biol.* **56**, 110–156 (1977).
9. Ellis, R. E., Yuan, J. & Horvitz, H. R. Mechanisms and functions of cell death. *Annu. Rev. Cell Biol.* **7**, 663–698 (1991).
10. Trent, C., Tsuing, N. & Horvitz, H. R. Egg-laying defective mutants of the nematode Caenorhabditis elegans. *Genetics* **104**, 619–647 (1983).
11. Ellis, H. M. & Horvitz, H. R. Genetic control of programmed cell death in the nematode C. elegans. *Cell* **44**, 817–829 (1986).
12. Hengartner, M. O., Ellis, R. & Horvitz, H. R. Caenorhabditis elegans gene ced-9 protects cells from programmed cell death. *Nature* **356**, 494–499 (1992).
13. Zou, H., Henzel, W. J., Liu, X., Lutschg, A. & Wang, X. Apaf-1, a human protein homologous to C. elegans CED-4, participates in cytochrome c-dependent activation of caspase-3. *Cell* **90**, 405–413 (1997).
14. Hengartner, M. O. & Horvitz, H. R. C. elegans cell survival gene ced-9 encodes a functional homolog of the mammalian proto-oncogene bcl-2. *Cell* **76**, 665–676 (1994).
15. Yuan, J., Shaham, S., Ledoux, S., Ellis, H. M. & Horvitz, H. R. The C. elegans cell death gene ced-3 encodes a protein similar to mammalian interleukin-1β-converting enzyme. *Cell* **75**, 641–652 (1993).
16. Vaux, D. L., Cory, S. & Adams, J. M. Bcl-2 gene promotes haemopoietic cell survival and cooperates with c-myc to immortalize pre-B cells. *Nature* **335**, 440–442 (1988).
17. Schweichel, J. U. & Merker, H. J. The morphology of various types of cell death in prenatal tissues. *Teratology* **7**, 253–266 (1973).
18. Galluzzi, L. *et al.* Molecular mechanisms of cell death: Recommendations of the

Nomenclature Committee on Cell Death 2018. *Cell Death Differ.* **25**, 486–541 (2018).
19. Holler, N. *et al.* Fas triggers an alternative, caspase-8-independent cell death pathway using the kinase RIP as effector molecule. *Nat. Immunol.* **1**, 489–495 (2000).
20. Brennan, M. A. & Cookson, B. T. Salmonella induces macrophage death by caspase-1-dependent necrosis. *Mol. Microbiol.* **38**, 31–40 (2000).
21. Galluzzi, L. *et al.* Essential versus accessory aspects of cell death: Recommendations of the NCCD 2015. *Cell Death Differ.* **22**, 58–73 (2015).
22. Poon, I. K. H., Lucas, C. D., Rossi, A. G. & Ravichandran, K. S. Apoptotic cell clearance: Basic biology and therapeutic potential. *Nat. Rev. Immunol.* **14**, 166–180 (2014).
23. Yatim, N., Cullen, S. & Albert, M. L. Dying cells actively regulate adaptive immune responses. *Nat. Rev. Immunol.* **17**, 262–275 (2017).
24. Obeid, M. *et al.* Calreticulin exposure dictates the immunogenicity of cancer cell death. *Nat. Med.* **13**, 54–61 (2007).
25. Green, D. R., Ferguson, T., Zitvogel, L. & Kroemer, G. Immunogenic and tolerogenic cell death. *Nat. Rev. Immunol.* **9**, 353–363 (2009).
26. Singh, R., Letai, A. & Sarosiek, K. Regulation of apoptosis in health and disease: the balancing act of BCL-2 family proteins. *Nat. Rev. Mol. Cell Biol.* **20**, 175–193 (2019).
27. Alnemri, E. S. *et al.* Human ICE/CED-3 protease nomenclature. *Cell* **87**, 171 (1996).
28. Shalini, S., Dorstyn, L., Dawar, S. & Kumar, S. Old, new and emerging functions of caspases. *Cell Death Differ.* **22**, 526–539 (2015).
29. Julien, O. & Wells, J. A. Caspases and their substrates. *Cell Death Differ.* **24**, 1380–1389 (2017).
30. Fischer, U., Jänicke, R. U. & Schulze-Osthoff, K. Many cuts to ruin: A comprehensive update of caspase substrates. *Cell Death Differ.* **10**, 76–100 (2003).
31. Aggarwal, B. B., Gupta, S. C. & Kim, J. H. Historical perspectives on tumor necrosis factor and its superfamily: 25 years later, a golden journey. *Blood* **119**, 651–665 (2012).
32. Dickens, L. S., Powley, I. R., Hughes, M. A. & MacFarlane, M. The 'complexities' of life and death: Death receptor signalling platforms. *Exp. Cell Res.* **318**, 1269–1277 (2012).
33. Brenner, D., Blaser, H. & Mak, T. W. Regulation of tumour necrosis factor signalling: Live or let die. *Nature Reviews Immunology* **15**, 362–374 (2015).
34. Barnhart, B. C., Alappat, E. C. & Peter, M. E. The CD95 Type I/Type II model. *Semin. Immunol.* **15**, 185–193 (2003).
35. Jost, P. J. *et al.* XIAP discriminates between type I and type II FAS-induced apoptosis. *Nature* **460**, 1035–1039 (2009).
36. Li, H., Zhu, H., Xu, C. J. & Yuan, J. Cleavage of BID by caspase 8 mediates the mitochondrial damage in the Fas pathway of apoptosis. *Cell* **94**, 491–501 (1998).
37. Llambi, F. *et al.* BOK Is a non-canonical BCL-2 family effector of apoptosis

regulated by ER-associated degradation. *Cell* **165**, 421–433 (2016).
38. Czabotar, P. E., Lessene, G., Strasser, A. & Adams, J. M. Control of apoptosis by the BCL-2 protein family: Implications for physiology and therapy. *Nature Reviews Molecular Cell Biology* **15**, 49–63 (2014).
39. Tait, S. W. G. & Green, D. R. Mitochondria and cell death: Outer membrane permeabilization and beyond. *Nat. Rev. Mol. Cell Biol.* **11**, 621–632 (2010).
40. Aubrey, B. J., Kelly, G. L., Janic, A., Herold, M. J. & Strasser, A. How does p53 induce apoptosis and how does this relate to p53-mediated tumour suppression? *Cell Death and Differentiation* **25**, 104–113 (2018).
41. Chipuk, J. E. & Green, D. R. Dissecting p53-dependent apoptosis. *Cell Death and Differentiation* **13**, 994–1002 (2006).
42. Letai, A. & Kutuk, O. Regulation of Bcl-2 family proteins by posttranslational modifications. *Curr. Mol. Med.* **8**, 102–118 (2008).
43. Zou, H., Li, Y., Liu, X. & Wang, X. An APAf-1 · cytochrome C multimeric complex is a functional apoptosome that activates procaspase-9. *J. Biol. Chem.* **274**, 11549–11556 (1999).
44. Li, P. *et al.* Cytochrome c and dATP-dependent formation of Apaf-1/caspase-9 complex initiates an apoptotic protease cascade. *Cell* **91**, 479–489 (1997).
45. Du, C., Fang, M., Li, Y., Li, L. & Wang, X. Smac, a mitochondrial protein that promotes cytochrome c-dependent caspase activation by eliminating IAP inhibition. *Cell* **102**, 33–42 (2000).
46. Verhagen, A. M. *et al.* Identification of DIABLO, a mammalian protein that promotes apoptosis by binding to and antagonizing IAP proteins. *Cell* **102**, 43–53 (2000).
47. Suzuki, Y. *et al.* A serine protease, HtrA2, is released from the mitochondria and interacts with XIAP, inducing cell death. *Mol. Cell* **8**, 613–621 (2001).
48. Weinlich, R., Oberst, A., Beere, H. M. & Green, D. R. Necroptosis in development, inflammation and disease. *Nat. Rev. Mol. Cell Biol.* **18**, 127–136 (2017).
49. Dondelinger, Y., Hulpiau, P., Saeys, Y., Bertrand, M. J. M. & Vandenabeele, P. An evolutionary perspective on the necroptotic pathway. *Trends Cell Biol.* **26**, 721–732 (2016).
50. Mocarski, E. S., Upton, J. W. & Kaiser, W. J. Viral infection and the evolution of caspase 8-regulated apoptotic and necrotic death pathways. *Nat. Rev. Immunol.* **12**, 79–88 (2012).
51. Vanden Berghe, T., Linkermann, A., Jouan-Lanhouet, S., Walczak, H. & Vandenabeele, P. Regulated necrosis: The expanding network of non-apoptotic cell death pathways. *Nat. Rev. Mol. Cell Biol.* **15**, 135–147 (2014).
52. Cho, Y. S. *et al.* Phosphorylation-driven assembly of the RIP1-RIP3 complex regulates programmed necrosis and virus-induced inflammation. *Cell* **137**, 1112–1123 (2009).
53. He, S. *et al.* Receptor Interacting Protein Kinase-3 determines cellular necrotic response to TNF-α. *Cell* **137**, 1100–1111 (2009).
54. Zhang, D. W. *et al.* RIP3, an energy metabolism regulator that switches TNF-induced cell death from apoptosis to necrosis. *Science* **325**, 332–336 (2009).

55. Sun, L. *et al.* Mixed lineage kinase domain-like protein mediates necrosis signaling downstream of RIP3 kinase. *Cell* **148**, 213–227 (2012).
56. Wang, H. *et al.* Mixed Lineage Kinase Domain-like Protein MLKL causes necrotic membrane disruption upon phosphorylation by RIP3. *Mol. Cell* **54**, 133–146 (2014).
57. Zargarian, S. *et al.* Phosphatidylserine externalization, "necroptotic bodies" release, and phagocytosis during necroptosis. *PLoS Biol.* **15**, e2002711 (2017).
58. Gong, Y. N. *et al.* ESCRT-III acts downstream of MLKL to regulate necroptotic cell death and its consequences. *Cell* **169**, 286–300 (2017).
59. Gutierrez, K. D. *et al.* MLKL activation triggers NLRP3-mediated processing and release of IL-1β independently of Gasdermin-D. *J. Immunol.* **198**, 2156–2164 (2017).
60. Yatim, N. *et al.* RIPK1 and NF-κB signaling in dying cells determines cross-priming of CD8+ T cells. *Science* **350**, 328–334 (2015).
61. Cookson, B. T. & Brennan, M. A. Pro-inflammatory programmed cell death. *Trends Microbiol.* **9**, 113–114 (2001).
62. Boise, L. H. & Collins, C. M. Salmonella-induced cell death: Apoptosis, necrosis or programmed cell death? *Trends in Microbiology* **9**, 64–67 (2001).
63. Broz, P. & Dixit, V. M. Inflammasomes: Mechanism of assembly, regulation and signalling. *Nat. Rev. Immunol.* **16**, 407–420 (2016).
64. Martinon, F., Burns, K. & Tschopp, J. The inflammasome: A molecular platform triggering activation of inflammatory caspases and processing of proIL-β. *Mol. Cell* **10**, 417–426 (2002).
65. Wilson, K. P. *et al.* Structure and mechanism of interleukin-1β converting enzyme. *Nature* **370**, 270–275 (1994).
66. Cerretti, D. P. *et al.* Molecular cloning of the interleukin-1β converting enzyme. *Science* **256**, 97–100 (1992).
67. Thornberry, N. A. *et al.* A novel heterodimeric cysteine protease is required for interleukin-1β processing in monocytes. *Nature* **356**, 768–774 (1992).
68. Gu, Y. *et al.* Activation of interferon-γ inducing factor mediated by interleukin-1β converting enzyme. *Science* **275**, 206–209 (1997).
69. Ghayur, T. *et al.* Caspase-1 processes IFN-γ-inducing factor and regulates LPS-induced IFN-γ production. *Nature* **386**, 619–623 (1997).
70. Shi, J. *et al.* Cleavage of GSDMD by inflammatory caspases determines pyroptotic cell death. *Nature* **526**, 660–665 (2015).
71. Kayagaki, N. *et al.* Caspase-11 cleaves gasdermin D for non-canonical inflammasome signalling. *Nature* **526**, 666–671 (2015).
72. Liu, X. *et al.* Inflammasome-activated gasdermin D causes pyroptosis by forming membrane pores. *Nature* **535**, 153–158 (2016).
73. Ding, J. *et al.* Pore-forming activity and structural autoinhibition of the gasdermin family. *Nature* **535**, 111–116 (2016).
74. Platnich, J. M. & Muruve, D. A. NOD-like receptors and inflammasomes: A review of their canonical and non-canonical signaling pathways. *Arch. Biochem. Biophys.* **670**, 4–14 (2019).

75. Shi, J. *et al.* Inflammatory caspases are innate immune receptors for intracellular LPS. *Nature* **514**, 187–192 (2014).
76. Jorgensen, I., Zhang, Y., Krantz, B. A. & Miao, E. A. Pyroptosis triggers pore-induced intracellular traps (PITs) that capture bacteria and lead to their clearance by efferocytosis. *J. Exp. Med.* **213**, 2113–2128 (2016).
77. Jorgensen, I. & Miao, E. A. Pyroptotic cell death defends against intracellular pathogens. *Immunological Reviews* **265**, 130–142 (2015).
78. Maltez, V. I. *et al.* Inflammasomes coordinate pyroptosis and natural killer cell cytotoxicity to clear infection by a ubiquitous environmental bacterium. *Immunity* **43**, 987–997 (2015).
79. Doitsh, G. *et al.* Cell death by pyroptosis drives CD4 T-cell depletion in HIV-1 infection. *Nature* **505**, 509–514 (2014).
80. Dixon, S. J. *et al.* Ferroptosis: An iron-dependent form of nonapoptotic cell death. *Cell* **149**, 1060–1072 (2012).
81. Yang, W. S. *et al.* Regulation of ferroptotic cancer cell death by GPX4. *Cell* **156**, 317–331 (2014).
82. Thomas, J. P., Geiger, P. G., Maiorino, M., Ursini, F. & Girotti, A. W. Enzymatic reduction of phospholipid and cholesterol hydroperoxides in artificial bilayers and lipoproteins. *Biochim. Biophys. Acta (BBA)/Lipids Lipid Metab.* **1045**, 252–260 (1990).
83. Brigelius-Flohé, R. & Maiorino, M. Glutathione peroxidases. *Biochimica et Biophysica Acta - General Subjects* **1830**, 3289–3303 (2013).
84. Shimada, K. *et al.* Global survey of cell death mechanisms reveals metabolic regulation of ferroptosis. *Nat. Chem. Biol.* **12**, 497–503 (2016).
85. Gaschler, M. M. *et al.* FINO2 initiates ferroptosis through GPX4 inactivation and iron oxidation. *Nat. Chem. Biol.* **14**, 507–515 (2018).
86. Doll, S. *et al.* FSP1 is a glutathione-independent ferroptosis suppressor. *Nature* **575**, 693–698 (2019).
87. Bersuker, K. *et al.* The CoQ oxidoreductase FSP1 acts parallel to GPX4 to inhibit ferroptosis. *Nature* **575**, 688–692 (2019).
88. Shimada, K., Hayano, M., Pagano, N. C. & Stockwell, B. R. Cell-line selectivity improves the predictive power of pharmacogenomic analyses and helps identify NADPH as biomarker for ferroptosis sensitivity. *Cell Chem. Biol.* **23**, 225–235 (2016).
89. Dixon, S. J. *et al.* Human haploid cell genetics reveals roles for lipid metabolism genes in nonapoptotic cell death. *ACS Chem. Biol.* **10**, 1604–1609 (2015).
90. Yang, W. S. *et al.* Peroxidation of polyunsaturated fatty acids by lipoxygenases drives ferroptosis. *Proc. Natl. Acad. Sci. U. S. A.* **113**, E4966-75 (2016).
91. Magtanong, L. *et al.* Exogenous monounsaturated fatty acids promote a ferroptosis-resistant cell state. *Cell Chem. Biol.* **26**, 420–432 (2019).
92. Kagan, V. E. *et al.* Oxidized arachidonic and adrenic PEs navigate cells to ferroptosis. *Nat. Chem. Biol.* **13**, 81–90 (2017).
93. Gao, M. *et al.* Role of mitochondria in ferroptosis. *Mol. Cell* **73**, 354–363 (2019).
94. Torii, S. *et al.* An essential role for functional lysosomes in ferroptosis of cancer

cells. *Biochem. J.* **473**, 769–777 (2016).
95. Seiler, A. *et al.* Glutathione Peroxidase 4 senses and translates oxidative stress into 12/15-lipoxygenase dependent- and AIF-mediated cell death. *Cell Metab.* **8**, 237–248 (2008).
96. Wenzel, S. E. *et al.* PEBP1 wardens ferroptosis by enabling lipoxygenase generation of lipid death signals. *Cell* **171**, 628–641 (2017).
97. Shintoku, R. *et al.* Lipoxygenase-mediated generation of lipid peroxides enhances ferroptosis induced by erastin and RSL3. *Cancer Sci.* **108**, 2187–2194 (2017).
98. Shah, R., Shchepinov, M. S. & Pratt, D. A. Resolving the role of lipoxygenases in the initiation and execution of ferroptosis. *ACS Cent. Sci.* **4**, 387–396 (2018).
99. Zilka, O. *et al.* On the mechanism of cytoprotection by ferrostatin-1 and liproxstatin-1 and the role of lipid peroxidation in ferroptotic cell death. *ACS Cent. Sci.* **3**, 232–243 (2017).
100. Green, D. R. The coming decade of cell death research: five riddles. *Cell* **177**, 1094–1107 (2019).
101. Ayala, A., Muñoz, M. F. & Argüelles, S. Lipid peroxidation: production, metabolism, and signaling mechanisms of malondialdehyde and 4-hydroxy-2-nonenal. *Oxid. Med. Cell. Longev.* **2014**, 1–31 (2014).
102. Chen, Y. *et al.* Quantitative profiling of protein carbonylations in ferroptosis by an aniline-derived probe. *J. Am. Chem. Soc.* **140**, 4712–4720 (2018).
103. Li, X. M., Salomon, R. G., Qin, J. & Hazen, S. L. Conformation of an endogenous ligand in a membrane bilayer for the macrophage scavenger receptor CD36. *Biochemistry* **46**, 5009–5017 (2007).
104. Agmon, E., Solon, J., Bassereau, P. & Stockwell, B. R. Modeling the effects of lipid peroxidation during ferroptosis on membrane properties. *Sci. Rep.* **8**, 5155 (2018).
105. Wong-Ekkabut, J. *et al.* Effect of lipid peroxidation on the properties of lipid bilayers: A molecular dynamics study. *Biophys. J.* **93**, 4225–4236 (2007).
106. Ouchi, Y., Unoura, K. & Nabika, H. Role of oxidized lipids in permeation of H2O2 through a lipid membrane: molecular mechanism of an inhibitor to promoter switch. *Sci. Rep.* **9**, 1–11 (2019).
107. Cwiklik, L. & Jungwirth, P. Massive oxidation of phospholipid membranes leads to pore creation and bilayer disintegration. *Chem. Phys. Lett.* **486**, 99–103 (2010).
108. Boonnoy, P., Jarerattanachat, V., Karttunen, M. & Wong-Ekkabut, J. Bilayer deformation, pores, and micellation induced by oxidized lipids. *J. Phys. Chem. Lett.* **6**, 4884–4888 (2015).
109. Yant, L. J. *et al.* The selenoprotein GPX4 is essential for mouse development and protects from radiation and oxidative damage insults. *Free Radic. Biol. Med.* **34**, 496–502 (2003).
110. Imai, H. *et al.* Early embryonic lethality caused by targeted disruption of the mouse PHGPx gene. *Biochem. Biophys. Res. Commun.* **305**, 278–286 (2003).
111. Friedmann Angeli, J. P. *et al.* Inactivation of the ferroptosis regulator Gpx4 triggers acute renal failure in mice. *Nat. Cell Biol.* **16**, 1180–1191 (2014).
112. Borchert, A. *et al.* The role of phospholipid hydroperoxide glutathione peroxidase isoforms in murine embryogenesis. *J. Biol. Chem.* **281**, 19655–19664 (2006).

113. Smith, A. C. *et al.* Mutations in the enzyme glutathione peroxidase 4 cause Sedaghatian-type spondylometaphyseal dysplasia. *J. Med. Genet.* **51**, 470–474 (2014).
114. Aygun, C. *et al.* Simplified gyral pattern with cerebellar hypoplasia in Sedaghatian type spondylometaphyseal dysplasia: A clinical report and review of the literature. *Am. J. Med. Genet. Part A* **158A**, 1400–1405 (2012).
115. Kerr, B., Smith, V., Patel, R., Ladusans, E. & Sillence, D. O. Spondylometaphyseal dysplasia Sedaghatian type associated with lethal arrhythmia and normal intrauterine growth in three siblings. *Clin. Dysmorphol.* **9**, 167–172 (2000).
116. English, S. J., Gayatri, N., Arthur, R. & Crow, Y. J. Sedaghatian spondylometaphyseal dysplasia with pachygyria and absence of the corpus callosum. *Am. J. Med. Genet. Part A* **140A**, 1854–1858 (2006).
117. Carlson, B. A. *et al.* Glutathione peroxidase 4 and vitamin E cooperatively prevent hepatocellular degeneration. *Redox Biol.* **9**, 22–31 (2016).
118. Matsushita, M. *et al.* T cell lipid peroxidation induces ferroptosis and prevents immunity to infection. *J. Exp. Med.* **212**, 555–568 (2015).
119. Linkermann, A. *et al.* Synchronized renal tubular cell death involves ferroptosis. *Proc. Natl. Acad. Sci. U. S. A.* **111**, 16836–16841 (2014).
120. Gao, M., Monian, P., Quadri, N., Ramasamy, R. & Jiang, X. Glutaminolysis and Transferrin regulate ferroptosis. *Mol. Cell* **59**, 298–308 (2015).
121. Fang, X. *et al.* Ferroptosis as a target for protection against cardiomyopathy. *Proc. Natl. Acad. Sci. U. S. A.* **116**, 2672–2680 (2019).
122. Hanson, L. R. *et al.* Intranasal deferoxamine provides increased brain exposure and significant protection in rat ischemic stroke. *J. Pharmacol. Exp. Ther.* **330**, 679–686 (2009).
123. Peña-Bautista, C., Vento, M., Baquero, M. & Cháfer-Pericás, C. Lipid peroxidation in neurodegeneration. *Clinica Chimica Acta* **497**, 178–188 (2019).
124. Devos, D. *et al.* Targeting chelatable iron as a therapeutic modality in Parkinson's disease. *Antioxidants Redox Signal.* **21**, 195–210 (2014).
125. Do Van, B. *et al.* Ferroptosis, a newly characterized form of cell death in Parkinson's disease that is regulated by PKC. *Neurobiol. Dis.* **94**, 169–178 (2016).
126. Jiang, L. *et al.* Ferroptosis as a p53-mediated activity during tumour suppression. *Nature* **520**, 57–62 (2015).
127. Zhang, Y. *et al.* BAP1 links metabolic regulation of ferroptosis to tumour suppression. *Nat. Cell Biol.* **20**, 1181–1192 (2018).
128. Chu, B. *et al.* ALOX12 is required for p53-mediated tumour suppression through a distinct ferroptosis pathway. *Nat. Cell Biol.* **21**, 579–591 (2019).
129. Tarangelo, A. *et al.* p53 suppresses metabolic stress-induced ferroptosis in cancer cells. *Cell Rep.* **22**, 569–575 (2018).
130. Wang, W. *et al.* CD8+ T cells regulate tumour ferroptosis during cancer immunotherapy. *Nature* **569**, 270–274 (2019).
131. Viswanathan, V. S. *et al.* Dependency of a therapy-resistant state of cancer cells on a lipid peroxidase pathway. *Nature* **547**, 453–457 (2017).
132. Hangauer, M. J. *et al.* Drug-tolerant persister cancer cells are vulnerable to GPX4

inhibition. *Nature* **551**, 247–250 (2017).
133. Miess, H. *et al.* The glutathione redox system is essential to prevent ferroptosis caused by impaired lipid metabolism in clear cell renal cell carcinoma. *Oncogene* **37**, 5435–5450 (2018).
134. Doll, S. *et al.* ACSL4 dictates ferroptosis sensitivity by shaping cellular lipid composition. *Nat. Chem. Biol.* **13**, 91–98 (2017).
135. Trujillo-Alonso, V. *et al.* FDA-approved ferumoxytol displays anti-leukaemia efficacy against cells with low ferroportin levels. *Nat. Nanotechnol.* **14**, 616–622 (2019).
136. Kim, S. E. *et al.* Ultrasmall nanoparticles induce ferroptosis in nutrient-deprived cancer cells and suppress tumour growth. *Nat. Nanotechnol.* **11**, 977–985 (2016).
137. Lee, H. *et al.* Energy-stress-mediated AMPK activation inhibits ferroptosis. *Nat. Cell Biol.* **22**, 225–234 (2020).
138. Riegman, M., Bradbury, M. S. & Overholtzer, M. Population dynamics in cell death: Mechanisms of propagation. *Trends in Cancer* **5**, 558–568 (2019).
139. Pérez-Garijo, A. & Steller, H. Spreading the word: Non-autonomous effects of apoptosis during development, regeneration and disease. *Development* **142**, 3253–3262 (2015).
140. Sun, Q. *et al.* Competition between human cells by entosis. *Cell Res.* **24**, 1299–1310 (2014).
141. Hamann, J. C. *et al.* Entosis Is Induced by Glucose Starvation. *Cell Rep.* **20**, 201–210 (2017).
142. Asally, M. *et al.* Localized cell death focuses mechanical forces during 3D patterning in a biofilm. *Proc. Natl. Acad. Sci. U. S. A.* **109**, 18891–18896 (2012).
143. Levraud, J. P. *et al.* Dictyostelium cell death: Early emergence and demise of highly polarized paddle cells. *J. Cell Biol.* **160**, 1105–1114 (2003).
144. Greenberg, J. T. Programmed cell death: A way of life for plants. *Proc. Natl. Acad. Sci. U. S. A.* **93**, 12094–12097 (1996).
145. Coucouvanis, E. & Martin, G. R. Signals for death and survival: A two-step mechanism for cavitation in the vertebrate embryo. *Cell* **83**, 279–287 (1995).
146. Kimura, S. & Shiota, K. Sequential changes of programmed cell death in developing fetal mouse limbs and its possible roles in limb morphogenesis. *J. Morphol.* **229**, 337–346 (1996).
147. Mailleux, A. A. *et al.* BIM regulates apoptosis during mammary ductal morphogenesis, and its absence reveals alternative cell death mechanisms. *Dev. Cell* **12**, 221–234 (2007).
148. Gabaldón, C., Gómez Ros, L. V., Pedreño, M. A. & Ros Barceló, A. Nitric oxide production by the differentiating xylem of Zinnia elegans. *New Phytol.* **165**, 121–130 (2004).
149. Levine, A., Tenhaken, R., Dixon, R. & Lamb, C. H2O2 from the oxidative burst orchestrates the plant hypersensitive disease resistance response. *Cell* **79**, 583–593 (1994).
150. Zhang, C., Czymmek, K. J. & Shapiro, A. D. Nitric oxide does not trigger early programmed cell death events but may contribute to cell-to-cell signaling

governing progression of the Arabidopsis hypersensitive response. *Mol. Plant-Microbe Interact.* **16**, 962–972 (2003).
151. Elmore, S. A. *et al.* Recommendations from the INHAND Apoptosis/Necrosis Working Group. *Toxicol. Pathol.* **44**, 173–188 (2016).
152. Mesa, K. R. *et al.* Niche-induced cell death and epithelial phagocytosis regulate hair follicle stem cell pool. *Nature* **522**, 94–97 (2015).
153. Juncadella, I. J. *et al.* Apoptotic cell clearance by bronchial epithelial cells critically influences airway inflammation. *Nature* **493**, 547–551 (2013).
154. Monks, J., Smith-Steinhart, C., Kruk, E. R., Fadok, V. A. & Henson, P. M. Epithelial cells remove apoptotic epithelial cells during post-lactation involution of the mouse mammary gland. *Biol. Reprod.* **78**, 586–594 (2008).
155. Link, N. *et al.* A collective form of cell death requires homeodomain interacting protein kinase. *J. Cell Biol.* **178**, 567–574 (2007).
156. Garcia-Hughes, G., Link, N., Ghosh, A. B. & Abrams, J. M. Hid arbitrates collective cell death in the Drosophila wing. *Mech. Dev.* **138**, 349–355 (2015).
157. Pérez-Garijo, A., Fuchs, Y. & Steller, H. Apoptotic cells can induce non-autonomous apoptosis through the TNF pathway. *Elife* **2**, e01004 (2013).
158. Neufeld, T. P. & Baehrecke, E. H. Eating on the fly: Function and regulation of autophagy during cell growth, survival and death in Drosophila. *Autophagy* **4**, 557–562 (2008).
159. Yin, V. P. & Thummel, C. S. A balance between the diap1 death inhibitor and reaper and hid death inducers controls steroid-triggered cell death in Drosophila. *Proc. Natl. Acad. Sci. U. S. A.* **101**, 8022–8027 (2004).
160. Nandy, A. *et al.* The NF-κB factor Relish regulates Atg1 expression and controls autophagy. *Cell Rep.* **25**, 2110–2120 (2018).
161. Berry, D. L. & Baehrecke, E. H. Growth arrest and autophagy are required for salivary gland cell degradation in Drosophila. *Cell* **131**, 1137–1148 (2007).
162. McPhee, C. K., Logan, M. A., Freeman, M. R. & Baehrecke, E. H. Activation of autophagy during cell death requires the engulfment receptor Draper. *Nature* **465**, 1093–1096 (2010).
163. Lin, L. *et al.* Complement-Related regulates autophagy in neighboring cells. *Cell* **170**, 158–171 (2017).
164. Yang, Y., Hou, L., Li, Y., Ni, J. & Liu, L. Neuronal necrosis and spreading death in a Drosophila genetic model. *Cell Death Dis.* **4**, e723 (2013).
165. Wang, Y. *et al.* Neuronal gap junctions are required for NMDA receptor-mediated excitotoxicity: Implications in ischemic stroke. *J. Neurophysiol.* **104**, 3551–3556 (2010).
166. Coburn, C. *et al.* Anthranilate fluorescence marks a calcium-propagated necrotic wave that promotes organismal death in C. elegans. *PLoS Biol.* **11**, e1001613 (2013).
167. Sarhan, M., von Mässenhausen, A., Hugo, C., Oberbauer, R. & Linkermann, A. Immunological consequences of kidney cell death. *Cell Death Dis.* **9**, 1–15 (2018).
168. Skouta, R. *et al.* Ferrostatins inhibit oxidative lipid damage and cell death in diverse disease models. *J. Am. Chem. Soc.* **136**, 4551–4556 (2014).

169. Li, Y. *et al.* Ischemia-induced ACSL4 activation contributes to ferroptosis-mediated tissue injury in intestinal ischemia/reperfusion. *Cell Death Differ.* **26**, 2284–2299 (2019).
170. Magtanong, L. & Dixon, S. J. Ferroptosis and Brain Injury. *Dev. Neurosci.* **40**, 382–395 (2019).
171. DeGregorio-Rocasolano, N., Martí-Sistac, O. & Gasull, T. Deciphering the iron side of stroke: Neurodegeneration at the crossroads between iron dyshomeostasis, excitotoxicity, and ferroptosis. *Front. Neurosci.* **13**, 1–17 (2019).
172. Li, W. *et al.* Ferroptotic cell death and TLR4/Trif signaling initiate neutrophil recruitment after heart transplantation. *J. Clin. Invest.* **129**, 2293–2304 (2019).
173. Franklin, B. S. *et al.* The adaptor ASC has extracellular and 'prionoid' activities that propagate inflammation. *Nat. Immunol.* **15**, 727–737 (2014).
174. Baroja-Mazo, A. *et al.* The NLRP3 inflammasome is released as a particulate danger signal that amplifies the inflammatory response. *Nat. Immunol.* **15**, 738–748 (2014).
175. Väyrynen, S. A. *et al.* Clinical impact and network of determinants of tumour necrosis in colorectal cancer. *Br. J. Cancer* **114**, 1334–1342 (2016).
176. Lipponen, P. Apoptosis in breast cancer: Relationship with other pathological parameters. *Endocrine-Related Cancer* **6**, 13–16 (1999).
177. Moinfar, F., Mannion, C., Man, Y. G. & Tavassoli, F. A. Mammary 'comedo'-DCIS: Apoptosis, oncosis, and necrosis: An electron microscopic examination of 8 cases. *Ultrastruct. Pathol.* **24**, 135–144 (2000).
178. Steinbach, J. P., Wolburg, H., Klumpp, A., Probst, H. & Weller, M. Hypoxia-induced cell death in human malignant glioma cells: Energy deprivation promotes decoupling of mitochondrial cytochrome c release from caspase processing and necrotic cell death. *Cell Death Differ.* **10**, 823–832 (2003).
179. Huang, C. Y., Kuo, W. T., Huang, Y. C., Lee, T. C. & Yu, L. C. H. Resistance to hypoxia-induced necroptosis is conferred by glycolytic pyruvate scavenging of mitochondrial superoxide in colorectal cancer cells. *Cell Death Dis.* **4**, e622 (2013).
180. Zhang, T. *et al.* CaMKII is a RIP3 substrate mediating ischemia- and oxidative stress-induced myocardial necroptosis. *Nat. Med.* **22**, 175–182 (2016).
181. Zhou, W. & Yuan, J. Necroptosis in health and diseases. *Seminars in Cell and Developmental Biology* **35**, 14–23 (2014).
182. Stockwell, B. R. *et al.* Ferroptosis: A Regulated Cell Death Nexus Linking Metabolism, Redox Biology, and Disease. *Cell* **171**, 273–285 (2017).
183. Overholtzer, M. *et al.* A nonapoptotic cell death process, entosis, that occurs by cell-in-cell invasion. *Cell* **131**, 966–979 (2007).
184. Brown, C. W., Amante, J. J. & Mercurio, A. M. Cell clustering mediated by the adhesion protein PVRL4 is necessary for 64 integrin–promoted ferroptosis resistance in matrix-detached cells. *J. Biol. Chem.* **293**, 12741–12748 (2018).
185. Azzam, E. I. & Little, J. B. The radiation-induced bystander effect: Evidence and significance. *Hum. Exp. Toxicol.* **23**, 61–65 (2004).
186. Zhou, H. *et al.* Mechanism of radiation-induced bystander effect: Role of the cyclooxygenase-2 signaling pathway. *Proc. Natl. Acad. Sci. U. S. A.* **102**, 14641–

14646 (2005).
187. Lyng, F. M., Seymour, C. B. & Mothersill, C. Production of a signal by irradiated cells which leads to a response in unirradiated cells characteristic of initiation of apoptosis. *Br. J. Cancer* **83**, 1223–1230 (2000).
188. Belyakov, O. V. *et al.* Biological effects in unirradiated human tissue induced by radiation damage up to 1 mm away. *Proc. Natl. Acad. Sci. U. S. A.* **102**, 14203–14208 (2005).
189. Azzam, E. I., De Toledo, S. M., Gooding, T. & Little, J. B. Intercellular communication is involved in the bystander regulation of gene expression in human cells exposed to very low fluences of alpha particles. *Radiat. Res.* **150**, 497–504 (1998).
190. Azzam, E. I., de Toledo, S. M. & Little, J. B. Direct evidence for the participation of gap junction-mediated intercellular communication in the transmission of damage signals from α-particle irradiated to nonirradiated cells. *Proc. Natl. Acad. Sci. U. S. A.* **98**, 473–478 (2001).
191. Ye, L. F. *et al.* Radiation-induced lipid peroxidation triggers ferroptosis and synergizes with ferroptosis inducers. *ACS Chem. Biol.* **15**, 469–484 (2020).
192. Azzam, E. I., De Toledo, S. M. & Little, J. B. Oxidative metabolism, gap junctions and the ionizing radiation-induced bystander effect. *Oncogene* **22**, 7050–7057 (2003).
193. Narayanan, P. K., Goodwin, E. H. & Lehnert, B. E. α particles initiate biological production of superoxide anions and hydrogen peroxide in human cells. *Cancer Res.* **57**, 3963–3971 (1997).
194. Chai, Y. *et al.* Radiation-induced non-targeted response in vivo: Role of the TGFβ-TGFBR1-COX-2 signalling pathway. *Br. J. Cancer* **108**, 1106–1112 (2013).
195. Roh, J. L., Kim, E. H., Jang, H. J., Park, J. Y. & Shin, D. Induction of ferroptotic cell death for overcoming cisplatin resistance of head and neck cancer. *Cancer Lett.* **381**, 96–103 (2016).
196. Yu, Y. *et al.* The ferroptosis inducer erastin enhances sensitivity of acute myeloid leukemia cells to chemotherapeutic agents. *Mol. Cell. Oncol.* **2**, e1054549 (2015).
197. Chen, L. *et al.* Erastin sensitizes Glioblastoma cells to temozolomide by restraining xCT and cystathionine-γ-lyase function. *Oncol. Rep.* **33**, 1465–1474 (2015).
198. Dixon, S. J. *et al.* Pharmacological inhibition of cystine-glutamate exchange induces endoplasmic reticulum stress and ferroptosis. *Elife* **3**, e02523 (2014).
199. Enyedi, B., Jelcic, M. & Niethammer, P. The cell nucleus serves as a mechanotransducer of tissue damage-induced inflammation. *Cell* **165**, 1160–1170 (2016).
200. Ma, K. *et al.* Control of ultrasmall sub-10 nm ligand-functionalized fluorescent core-shell silica nanoparticle growth in water. *Chem. Mater.* **27**, 4119–4133 (2015).
201. Du, Q. & Gunzburger, M. Grid generation and optimization based on centroidal Voronoi tessellations. *Appl. Math. Comput.* **133**, 591–607 (2002).
202. Iyer, R. & Lehnert, B. E. Factors underlying the cell growth-related bystander responses to α particles. *Cancer Res.* **60**, 1290–1298 (2000).

203. Zou, Y. *et al.* A GPX4-dependent cancer cell state underlies the clear-cell morphology and confers sensitivity to ferroptosis. *Nat. Commun.* **10**, 1–13 (2019).
204. Bailey, H. H. L-S,R-buthionine sulfoximine: Historical development and clinical issues. *Chem. Biol. Interact.* **111–112**, 239–254 (1998).
205. Naguib, Y. M. A. A fluorometric method for measurement of peroxyl radical scavenging activities of lipophilic antioxidants. *Anal. Biochem.* **265**, 290–298 (1998).
206. Riegman, M. *et al.* Ferroptosis occurs through an osmotic mechanism and propagates independently of cell rupture. *Nat. Cell Biol.* **In Press**, (2020).
207. Spencer, S. L., Gaudet, S., Albeck, J. G., Burke, J. M. & Sorger, P. K. Non-genetic origins of cell-to-cell variability in TRAIL-induced apoptosis. *Nature* **459**, 428–432 (2009).
208. Aquilano, K., Baldelli, S. & Ciriolo, M. R. Glutathione: New roles in redox signalling for an old antioxidant. *Front. Pharmacol.* **5**, 196 (2014).
209. Katikaneni, A. *et al.* Lipid peroxidation regulates long-range wound detection through 5-lipoxygenase in zebrafish. *Nat. Cell Biol.* **In Press**, (2020).
210. Kirby, J. E., Vogel, J. P., Andrews, H. L. & Isberg, R. R. Evidence for pore-forming ability by Legionella pneumophila. *Mol. Microbiol.* **27**, 323–336 (1998).
211. Smith, P. T., Huang, M. L. & Kirshenbaum, K. Osmoprotective polymer additives attenuate the membrane pore-forming activity of antimicrobial peptoids. *Biopolymers* **103**, 227–236 (2015).
212. Dacheux, D., Goure, J., Chabert, J., Usson, Y. & Attree, I. Pore-forming activity of type III system-secreted proteins leads to oncosis of Pseudomonas aeruginosa-infected macrophages. *Mol. Microbiol.* **40**, 76–85 (2001).
213. Noronha, F. S. M., Ramalho-Pinto, F. J. & Horta, M. F. Cytolytic activity in the genus Leishmania: involvement of a putative pore-forming protein. *Infect. Immun.* **64**, 3975–3982 (1996).
214. Fink, S. L. & Cookson, B. T. Caspase-1-dependent pore formation during pyroptosis leads to osmotic lysis of infected host macrophages. *J. Immunol.* **202**, 1913–1926 (2006).
215. Wenz, C. *et al.* t-BuOOH induces ferroptosis in human and murine cell lines. *Arch. Toxicol.* **92**, 759–775 (2018).
216. Rogers, C. *et al.* Cleavage of DFNA5 by caspase-3 during apoptosis mediates progression to secondary necrotic/pyroptotic cell death. *Nat. Commun.* **8**, 1–14 (2017).
217. Dixon, S. J. Ferroptosis: bug or feature? *Immunol. Rev.* **277**, 150–157 (2017).
218. Green, D. R. & Victor, B. The pantheon of the fallen: Why are there so many forms of cell death? *Trends in Cell Biology* **22**, 555–556 (2012).
219. Sheen, J. H., Zoncu, R., Kim, D. & Sabatini, D. M. Defective regulation of autophagy upon leucine deprivation reveals a targetable liability of human melanoma cells in vitro and in vivo. *Cancer Cell* **19**, 613–628 (2011).
220. Qing, G. *et al.* ATF4 regulates MYC-mediated neuroblastoma cell death upon glutamine deprivation. *Cancer Cell* **22**, 631–644 (2012).
221. Izzo, V., Bravo-San Pedro, J. M., Sica, V., Kroemer, G. & Galluzzi, L. Mitochondrial

permeability transition: New findings and persisting uncertainties. *Trends Cell Biol.* **26**, 655–667 (2016).
222. Los, F. C. O., Randis, T. M., Aroian, R. V. & Ratner, A. J. Role of pore-forming toxins in bacterial infectious diseases. *Microbiol. Mol. Biol. Rev.* **77**, 173–207 (2013).
223. Hamann, J. C. & Overholtzer, M. Entosis enables a population response to starvation. *Oncotarget* **8**, 57934–57935 (2017).
224. Inde, Z. & Dixon, S. J. The impact of non-genetic heterogeneity on cancer cell death. *Crit. Rev. Biochem. Mol. Biol.* **53**, 99–114 (2018).
225. Paek, A. L., Liu, J. C., Loewer, A., Forrester, W. C. & Lahav, G. Cell-to-cell variation in p53 dynamics leads to fractional killing. *Cell* **165**, 631–642 (2016).
226. Lorda-Diez, C. I., Montero, J. A., Garcia-Porrero, J. A. & Hurle, J. M. Interdigital tissue regression in the developing limb of vertebrates. *Int. J. Dev. Biol.* **59**, 55–62 (2015).
227. Forcina, G. C., Conlon, M., Wells, A., Cao, J. Y. & Dixon, S. J. Systematic quantification of population cell death kinetics in mammalian cells. *Cell Syst.* **4**, 600–610 (2017).
228. Gelles, J. D. *et al.* Single-cell and population-level analyses using real-time kinetic labeling couples proliferation and cell death mechanisms. *Dev. Cell* **51**, 277–291 (2019).
229. Inde, Z., Forcina, G. C., Denton, K. & Dixon, S. J. Kinetic heterogeneity of cancer cell fractional killing. *Cell Rep.* **32**, 107845 (2020).
230. Kalogeris, T., Baines, C. P., Krenz, M. & Korthuis, R. J. Cell Biology of Ischemia/Reperfusion Injury. in *International Review of Cell and Molecular Biology* **298**, 229–317 (Elsevier Inc., 2012).
231. Liu, Y. *et al.* Autophagy regulates programmed cell death during the plant innate immune response. *Cell* **121**, 567–577 (2005).